Quantifying regional pectoralis major fatigue and its influence on performance of activities of daily living

by

Bhillie Luciani

A thesis

presented to the University of Waterloo

in fulfillment of the

thesis requirement for the degree of

Master of Science

in

Kinesiology

Waterloo, Ontario, Canada 2020

Author's Declaration

I hereby declare that I am the sole author of this thesis. This is a true copy of the thesis, including any required final revisions, as accepted by my examiners.

I understand that my thesis may be made electronically available to the public.

Abstract

Extensive research reports on healthy shoulder function in the context of motion and muscular activity. However, less is known regarding how the shoulder complex and in particular its muscular components respond to disruptions, including musculoskeletal disorders, iatrogenic damage, or fatigue. The pectoralis major is a multipennate fan-shaped muscle, composed of three regions, and contributes to many upper extremity actions such as internal rotation, adduction, and horizontal adduction. Despite contentions that the pectoralis major may not be necessary for normal shoulder function, when damaged, shoulder function changes. The objective of this study was to examine differential fatigue in the pectoralis major as well as the effects of pectoralis major fatigue on shoulder muscle activation and shoulder kinematics in the context of daily activities.

Twenty, young healthy male participants performed baseline activities of daily living, then performed a fatiguing protocol targeting the pectoralis major. Following the fatigue protocol, participants performed the same activities of daily living at 0, 1, 3, 7, and 15-minutes post-fatigue. Electromyography (EMG) was collected from the three regions of the pectoralis major and surrounding shoulder musculature of the dominant upper extremity were collected to assess muscle contributions to the activities of daily living (mean EMG). Kinematics of the dominant upper extremity were also collected to identify changes to joint angle range of motion changes (torso, thoracohumeral, and elbow). Fatigue was quantified in the three regions of the pectoralis major in order to determine differential fatigue. Fatigue, EMG, and kinematic data from post-fatigue time points were compared to pre-fatigue.

All participants experienced fatigue in the pectoralis major as a result of the fatiguing protocol. More specifically, differential fatigue occurred between regions of the pectoralis major,

with participants fatiguing in one, two, or all three regions. Further, changes in kinematics and muscle activity during the activities of daily living occurred, indicating changes in muscle activation patterns and joint angle ranges of motion due to fatigue. Joint angle ranges of motion changed (~6˚) as a result of the fatigue protocol, while there were small changes (less than 2% maximum voluntary contraction) in muscle activity. Overall, this thesis suggests that the pectoralis major muscle is complex and focused investigation of its regional contributions is necessary to understand how the muscle variously contributes to shoulder function. These initial findings can inform future research on the pectoralis major while informing on the utility of fatigue as a muscle knock-out or knock-down model.

Acknowledgements

This thesis would not have been possible without the support, advice, and encouragement from many, many individuals. First, my supervisor, Dr. Clark Dickerson, who decided it was a good idea to encourage a Hawaii girl to spend time in the Waterloo winters. Thank you for your continued support, dedication, and pep talks throughout my degree as well as convincing me the shoulder is the coolest thing that we, as humans, have got going on.

Thank you to my committee members, Dr. Jack Callaghan and Dr. Steve Fischer. Your input on this project was invaluable and pushed me to be a better researcher and I am very grateful for your time and feedback.

A huge thank you to those directly involved with this project. In particular, Jacklyn Kurt for being by my side during every collection, helping me keep my head on straight, reminding me to take calibration trials, and occasionally braiding my hair. This truly would not have been possible without your help. To Rachel Whittaker, thank you for pushing me to think real hard about the questions I was trying to answer, letting me pester you with a million questions, as well as teaching me that MATLAB isn't as smart as you think it is. Thank you to the DIESEL team Alicia, Jackie, Alan, Alison, Dan, and Tea for always being around for a coffee, go on a snack hunt, have a chat, be a shoulder to cry on, or provide comedic relief.

There was a lot of behind the scenes during my time here in Waterloo. Thank you to Craig, Trevor, and Lowell for reviving my personal computer after the Great Crash of 2018. Thank you to Jeff Rice for instrumenting a pulley system and a "shower curtain" so I could successfully complete my thesis.

To all of my friends who have been by my side for the past two and a half years, thank you a million times over – you all mean the world to me. To Laura Healey, "my one friend", the Great Canadian Baker, thank you so much for determining we had to be friends before even meeting each other. I'm not sure if I would have made it through 612 or this degree without you, our late-night bakes, getting mistaken for each other, braid4braid, or moving each other in and out of our respective 3 apartments apiece. It has truly been an honor. To Gary Mangan, sorry but also very not sorry for derailing your productivity more often than not and for stealing your food during the time we shared an office. To Mamiko Noguchi, how the heck am I going to survive without your pep talks?! Thank you both so much for your life and research advice. To the 613 Killaz, keep killin'.

Last, but definitely not least, thank you to my outrageously convoluted family. Mom and Bob, Dad and Momi, Sarah, Malia, Romero, the Reisers, and the Clarry-Sohriakoff-Rudds, thank you for supporting me throughout this wild, wild journey. I'm not able to come up with something that isn't generically cheesy, but I'm so glad you all are in my corner.

TABLE OF CONTENTS

LIST OF FIGURES

LIST OF TABLES

LIST OF ABBREVIATIONS

AC………………………………………………………………Acromioclavicular

ADL………………………………………………………...Activities of Daily Living

EMG……………………………………………………………Electromyography

GCS……………………………………………………..Global Coordinate System

GH…………………………………………………………...Glenohumeral

iEMG……………………………………………………...Integrated Electromyography

LCS……………………………………………………………Local Coordinate System

MdPF………………………………………………………….Median Power Frequency

MPF……………………………………………………….Mean Power Frequency

MMG……………………………………………………Mechanomyography

MPF……………………………………………………..Mean Power Frequency

MVC……………………………………………….Maximum Voluntary Contraction

ROM……………………………………………………....Range of Motion

RPE……………………………………………………..Rate of Perceived Exertion

RPF……………………………………………………....Rate of Perceived Fatigue

SC………………………………………………………Sternoclavicular

sEMG……………………………………………………..Surface Electromyography

SMG……………………………………………………Sonomyography

VAS……………………………………………………...Visual Analogue Scale

1.0 INTRODUCTION

While the human shoulder includes a complex musculoskeletal arrangement that allows for an unparalleled mobility and instability compared to other body joint regions, knowledge is expanding on how the shoulder complex responds to disruptions. The many muscles allow for precise manual actions performed by positioning the glenoid and maintaining a stable base for the arm. Typical shoulder function has been extensively studied in the context of motion and muscular activity; however, less is known regarding how the system, and its muscular components, respond to disruptions to function, such as musculoskeletal disorders or fatigue.

The pectoralis major crosses all three joints of the shoulder complex (acromioclavicular, sternoclavicular, and glenohumeral) and contributes to many shoulder and upper extremity actions. It is a flat, fan-shaped muscle located on the anterior wall of the chest and includes three different functional regions. The clavicular region supports shoulder flexion, horizontal adduction, and internal rotation (Carrino et al., 2000; Fung et al., 2009; Leonardis, Desmet, & Lipps, 2017; Paton & Brown, 1994; Stegnik-Jansen, Buford Jr., Patterson, & Gould, 2011), the sternocostal region acts in adduction, horizontal adduction, and shoulder flexion (Leonardis et al., 2017; Paton & Brown, 1994; Stegnik-Jansen et al., 2011), and the abdominal region facilitates adduction, particularly at 90° of abduction, and extension against a flexor force (Paton & Brown, 1994). While its primary functions and architectural properties are known, claims exist that the muscle is not necessary for typical shoulder function (Marmor, Bechtol, & Hall, 1961; Wolfe, Wickiewicz, & Cavanaugh, 1992).

Despite contentions that the pectoralis major may not be necessary for normal shoulder function, when the muscle is damaged, shoulder function changes. This is evident in breast cancer survivors, as treatments cause structural damage, decreases in muscular activity, atrophy,

and muscle dysfunction (Brookham, Cudlip, & Dickerson, 2018b; Brookham & Dickerson, 2016; Stegnik-Jansen et al., 2011), which manifests as decreases in strength and range of motion, and altered kinematic strategies (Brookham, Cudlip, & Dickerson, 2018a; Brookham & Dickerson, 2016; Chopp-Hurley, Brookham, & Dickerson, 2016). Further, the pectoralis major is one of many muscles that may continue to show signs of dysfunction after breast cancer treatments are completed (Lipps, Sachdev, & Strauss, 2017; Shamley et al., 2007; Stegnik-Jansen et al., 2011).

The activation patterns of muscles and the kinematic strategies associated with individual muscle activations provide an understanding of normal and impaired function. Selective knockout of specific muscles (by fatigue or nerve block) can provide insights into a muscle's role in an activity and the consequences associated with an impaired system (McCully, Suprak, Kosek, & Karduna, 2006, 2007; Umehara et al., 2018). In the context of the shoulder, many muscles lie deep to bone and other muscles, making direct assessment difficult. Although research exists focused on the rotator cuff and other shoulder musculature with regards to function, injury, and impairment, little details behavior of the pectoralis major. This is increasingly important concerning specific patient populations, such as breast cancer survivors, in which impairment of the pectoralis major may substantially impact quality of life. The proposed study used a fatigue protocol to target the three regions of the pectoralis major as a means to attempt to quantify the muscle's role in shoulder and arm function.

1.1 Research Objectives

The purpose was to examine the effects of pectoralis major fatigue on shoulder muscle activation and shoulder kinematics in the context of commonly performed, clinically relevant tasks. A secondary purpose was to examine the effect of a targeted pectoralis major fatigue protocol on the different regions of the pectoralis major.

Specifically,

1) Does pectoralis major fatigue induce compensatory muscular activation during various activities of daily living?

2) Does pectoralis major fatigue induce compensatory kinematic changes during various activities of daily living?

3) Is the presence of fatigue different across regions of the pectoralis major?

1.2 Hypotheses

The related hypotheses are:

1) Fatigue of the pectoralis major will result in compensatory activation of surrounding shoulder musculature, as evidenced by modified activation in specific muscles, and these compensations will be task dependant. More specifically:

   a. There will be an increase in posterior deltoid, latissimus dorsi, and upper trapezius muscle activity during the scratch activity of daily living.

   b. There will be an increase in anterior, middle, and posterior deltoid muscle activity during the shower curtain pull activity of daily living.

   c. There will be an increase in anterior deltoid, middle deltoid, and upper trapezius muscle activity during the reach to shelf activity of daily living.

These hypotheses are inferred from the ADLs that each muscle contributes to and in light of results from Brookham et al. (2018a), which reported increased upper trapezius muscle activity during ADLs on the affected side of breast cancer survivors.

2) Fatigue of the pectoralis major will result in compensatory trunk, thoracohumeral, and elbow kinematics, which will depend on the ADL. More specifically:

   a. There will be an increase in trunk extension range of motion and a decrease in thoracohumeral plane of elevation range of motion during the scratch activity of daily living.

   b. There will be a decrease in throacohumeral elevation range of motion during the shower curtain pull activity of daily living.

   c. There will be an increase in trunk flexion range of motion and decrease in thoracohumeral elevation range of motion during the reach to shelf activity of daily living.

3) The targeted fatigue protocol in this study will induce fatigue primarily in the clavicular and sternocostal regions of the pectoralis major. This hypothesis is based on research that outlines the actions of each region. The tasks of the fatigue protocol involve both horizontal adduction and internal rotation, which are known to recruit both the clavicular and sternocostal regions of the pectoralis major (Leonardis et al., 2017; Paton & Brown, 1994; Rockwood Jr., 2009; Stegnik-Jansen et al., 2011). Relative to the two other regions, there will not be any fatigue present in the abdominal region, as the tasks in the fatigue protocol do not involve extension or adduction. While horizontal adduction is action of the abdominal region, the sternocostal region is believed to contribute more to this movement (Paton & Brown, 1994).

1.3 Importance of This Research

This work enhances knowledge of the pectoralis major and its contributions to shoulder function. Additionally, the findings enable greater clinical understanding of shoulder and arm function in both diagnosis and rehabilitation from dysfunction. While this research does not directly examine breast cancer survivors or other pathological cohorts, it can provide insight into the effects of pectoralis major disability on other aspects of shoulder function. For instance, the pectoralis major is physically and mechanically affected by various treatments for breast cancer and as the prevalence of breast cancer continues to rise in the United States and Canada, it is important to understand the general role of pectoralis major in shoulder function to improve quality of life of breast cancer survivors. This thesis quantified muscle activation and kinematics pre- and post- fatigue protocol in a controlled laboratory setting with healthy young adults. This could potentially translate into delineating potential mechanisms of pectoralis morbidity driven consequences for breast cancer survivors.

2.0 LITERATURE REVIEW

2.1 The Shoulder Complex

The bones of the clavicle, sternum, humerus, and scapula variously articulate with one another to form the shoulder complex (Figure 1), which allows a large range of motion coupled with a high degree of instability (Veeger & van der Helm, 2007). The anatomical form of these three bones and joints helps determine function (Lieber & Fridén, 2000; Schenkman & Rugo De Cartaya, 1987), and it is through these three bones and their joints that shoulder movement is coordinated (Ebaugh, McClure, & Karduna, 2006; Tsai, Mcclure, & Karduna, 2003). The range of motion that the shoulder is capable of necessitates a variety of muscle activations, as changes in posture will result in changes in muscle length, lines of action, and force-producing capability. Further, the ligamentous structures, muscle lengths, injury history, and activity history also will modulate an individual's mobility, flexibility, and force generation capabilities. While the main functions of the shoulder complex are to position the glenoid for maximum mobility while providing a stable base for arm support, the mobility and stability of the joint complicate easy characterization, provoking study of shoulder mechanics.
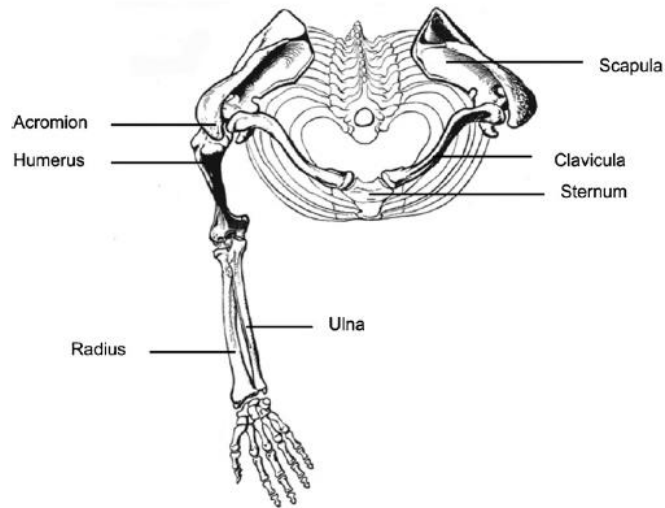
Figure 1. The shoulder complex from a superior view (Veeger & van der Helm, 2007).

The shoulder complex is a kinematic chain, meaning that a force generated or applied at one element will ultimately influence another (Inman, Saunders, & Abbott, 1944; Veeger & van der Helm, 2007). The sternum, also known as the breastbone, is the base of the kinematic chain. The manubrial portion of the sternum is where the S-shaped clavicle articulates to form the sternoclavicular (SC) joint, which is the only connection between the upper limb and thorax (Rockwood Jr., 2009; Schenkman & Rugo De Cartaya, 1987). While there is little intrinsic stability in this joint, it is compensated for by the ligamentous structures around it. The anterior and posterior sternoclavicular ligaments prevent rotation of the clavicle during depression, while the anterior and posterior costoclavicular ligaments limit protraction and retraction (Rockwood Jr., 2009). The clavicle itself functions as a muscle attachment site to control and support the neck as well as dividing mechanical demand by driving support to the scapula.

The only articulation between the clavicle and the scapula is the acromioclavicular (AC) joint, which like the SC joint, has a complex ligamentous structure, which limits motion at the joint. The acromioclavicular ligaments contribute to anteroposterior stability, while the coracoclavicular ligaments contribute to vertical stability (Rockwood Jr., 2009). The scapula is a

sheet of bone that sits on the posterior ribcage and serves as a bony attachment for several muscles, several of which control scapular movement. The scapulothoracic "joint", which is the non-bony articulation between the scapula and the thorax that contributes to shoulder complex integrity (Schenkman & Rugo De Cartaya, 1987) is usually maintained by periscapular muscles. The periscapular muscles, such as serratus anterior and levator scapulae, attach the scapula to the thorax and act to maintain scapular position, while the scapulohumeral muscles, such as the rotator cuff, coracobrachialis and deltoid, attach to the humerus for movement.

The articulation between the scapula and the humerus is the glenohumeral (GH) joint. Just as the femoral head sits in the acetabulum of the pelvis, the sphere-like head of the humerus interfaces with the glenoid of the scapula, though it is much less stable than the hip due to the small contact surface resulting from the shapes of both the humeral head and glenoid. This small contact surface allows for large ranges of motion in six degrees of freedom (Veeger & van der Helm, 2007), although GH motion is difficult to quantify since movement is accompanied by rotations and translations. While the ligaments and surrounding musculature contribute to glenohumeral stability by directing the force of the humeral head toward the center of the glenoid (Rockwood Jr., 2009).

Many muscles are considered "shoulder musculature" and can be classified as those that cross the shoulder to insert on the humerus or elbow, muscles that originate on the trunk and insert on the scapula or clavicle, and muscles that originate on the trunk and insert on the humerus (Inman et al., 1944). Through the kinematic chain of the shoulder, these muscles contribute to scapulohumeral rhythm, the coordinated movement of the humerus and scapula (Schenkman & Rugo De Cartaya, 1987), which involves all joints of the shoulder complex (Inman et al., 1944). While all shoulder musculature contribute to movement and stability of the

shoulder, the pectoralis major crosses all three joints of the shoulder, yet little is known about its effects on each of those joints, which will be explored in the next section.

2.2 Pectoralis Major

2.2.1 Gross Anatomy

Located on the anterior wall of the thorax, the pectoralis major is a large, fan-shaped muscle, reported as having three regions: clavicular, sternocostal, and abdominal (Fung et al., 2009; Wolfe et al., 1992). The clavicular region originates on the medial half of the clavicle, the sternocostal region originates on the anterior surface of the manubrium, sternum, and costal cartilages of ribs 1-6, and the abdominal region originates on the abdominal aponeurosis of the external oblique (Fung et al., 2009; Petilon, Carr, Sekiya, & Unger, 2005; Rockwood Jr., 2009; Stegnik-Jansen et al., 2011; Wolfe et al., 1992). All portions insert on the lateral lip of the intertubercular groove of the humerus (Wolfe et al., 1992), with the abdominal region inserting superoposteriorly and the clavicular region inserting inferoanteriorly (Figure 2) (Ashley, 1952; Fung et al., 2009; Petilon et al., 2005; Rockwood Jr., 2009; Stegnik-Jansen et al., 2011).
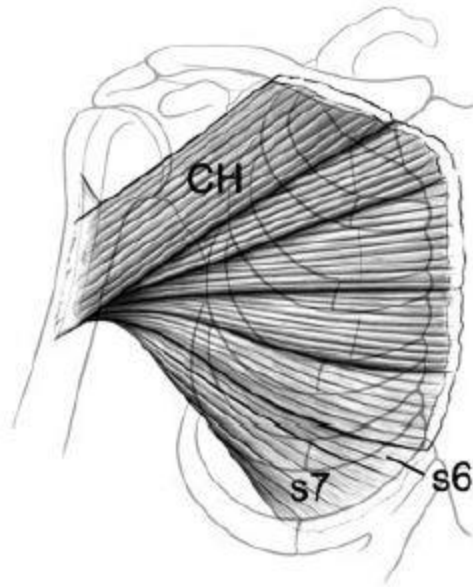
Figure 2. The pectoralis major and its regions. CH indicates the clavicular head, or region, of the muscle, s6 and s7 indicate the abdominal region of the muscle, and the unlabeled portions indicate the sternocostal region of the muscle (Fung et al., 2009).

Blood supply to the pectoralis major comes from the pectoral branch of the thoracoacromial artery (Petilon et al., 2005). However, a review of the clavicular region of the pectoralis major (Barberini, 2014) found that the clavicular region of the muscle is supplied by the deltoid branch of the thoracoacromial artery, while the sternocostal region of the muscle is supplied by pectoral branch of the thoracoacromial artery. Further, it has also been reported that the abdominal region of the muscle has an independent blood supply (Manktelow, McKee, & Vettese, 1980), branching from the axillary artery, sharing a common trunk with the lateral thoracic artery (Sato & Takafuji, 1992). The muscle has been reported to be innervated by two different nerve supplies – the medial and lateral pectoral nerves that branch off of the brachial plexus (Barberini, 2014; Petilon et al., 2005). The medial pectoral nerve innervates the lateral portion of the sternocostal region, while the lateral pectoral nerve innervates the medial portion of the sternocostal and clavicular regions. These independent neural and vascular elements

indicate that the different regions of the pectoralis major likely function independently, as will be explored in subsequent sections of this thesis.

2.2.2 Architectural Properties

Architectural differences are reported for each region of the pectoralis major (Fung et al., 2009; Langenderfer, Jerabek, Thangamani, Kuhn, & Hughes, 2004; Wolfe et al., 1992) as well as the ability to independently control each region (Brown, Wickham, McAndrew, & Huang, 2007; Paton & Brown, 1994). Thus, the individual regions of the pectoralis major could plausibly be treated as different muscles.

The three regions of the pectoralis major (clavicular, middle sternal, and inferior sternal) can exert moments differentially, having distinct lines of action (Ackland & Pandy, 2009). Although the data was based on a single-specimen model, abduction and flexion in the scapular plane resulted in lines of action greater than 180° (measured counter clockwise from x-axis) for the clavicular and middle sternal regions and a line of action less than 180° for the inferior sternal region, creating the potential for a superior and inferior shear force, respectively (Figure 3). Abduction and flexion in the transverse plane resulted in lines of action less than 180° for all three regions, indicating anterior shear force action.
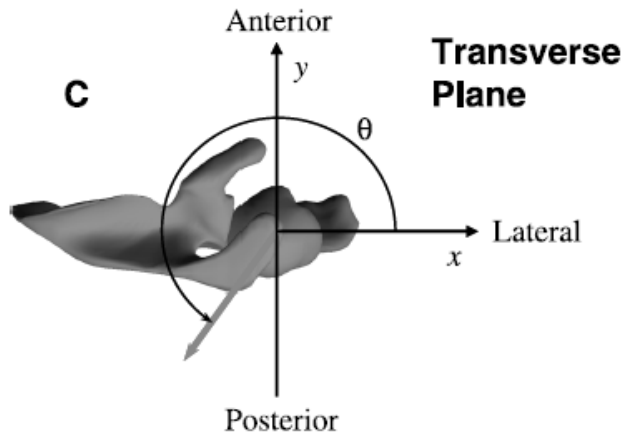
Figure 3. The plane in which shoulder muscle lines of action were defined (Ackland & Pendy, 2009). Directions of all muscle force vectors were measured in the counterclockwise direction starting from the x-axis. The lines of action were defined as creating superior ($\theta > 180°$) or inferior ($\theta < 180°$) shear force at the glenohumeral joint.

In the pectoralis major, there is a progressive increase of fiber length from superior to inferior regions (Carrino et al., 2000; Fung et al., 2009). Although one study found the longest fibers occur in the central portion of the sternocostal region (Fung et al., 2009), this still supports the findings of Wolfe et al. (1992), which state the longest fibers come from the sternocostal and abdominal regions.

The broad, fan shape and multiple regions of the pectoralis major present difficulty in reporting muscle fiber length and pennation angle. The reported mean fiber length of both regions of the pectoralis major is 16.1 ± 1.1 cm, while the lengths of the clavicular and sternocostal regions are 15 ± 0.8 cm and 16.4 ± 1.2 cm, respectively (Fung et al., 2009). Pennation angle was measured at both the medial and lateral portions of the fiber regions of both the clavicular and sternocostal regions. Medially, the mean pennation angle of both regions is $24.8 \pm 2.5°$, while the pennation angles of the clavicular and sternocostal regions are $31.2 \pm 2.4°$ and $22.9 \pm 3.8°$, respectively (Fung et al., 2009). Laterally, the mean pennation angle of both regions is $22.7 \pm 3.5°$, while the pennation angles of the clavicular and sternocostal regions are

12

29.4 ± 6.9° and 20.6 ± 2.7°, respectively (Fung et al., 2009). Langenderfer et al. (2004) also defined the pectoralis major as having two regions and identified the clavicular region as having shorter fiber length. However, Langenderfer et al. (2004) found that the pennation angle of the clavicular region is smaller. Further, it has also been found that the clavicular region's tendon is shorter, the physiological cross-sectional area is smaller, and optimal muscle length is shorter than the sternocostal region (Langenderfer et al., 2004). These differences in fiber properties may allow for different shortening velocities within the pectoralis major, which can maximize power over shortening velocities (Wolfe et al., 1992).

2.2.3 Muscle Action

The pectoralis major is involved in many actions, all of which depend on the posture of the humerus relative to the thorax (Rockwood Jr., 2009). It is commonly stated that the pectoralis major functions as a humeral adductor, a humeral flexor, a humeral internal rotator, and a horizontal adductor (Aarimaa, Rantanen, Heikkila, Helttula, & Orava, 2004; Carrino et al., 2000; Inman et al., 1944; Leonardis et al., 2017; Paton & Brown, 1994; Stegnik-Jansen et al., 2011; Wolfe et al., 1992). Less commonly, the pectoralis major is suggested to function in extension against a flexor force (Paton & Brown, 1994; Stegnik-Jansen et al., 2011).

Many studies have also differentiated the functions of the three regions of the pectoralis major, although monitoring the abdominal region is less common. The clavicular region acts as a flexor and internal rotator (Carrino et al., 2000; Leonardis et al., 2017; Stegnik-Jansen et al., 2011), while the sternocostal region acts as an adductor, a horizontal adductor, and an extender against resistance in flexion (Leonardis et al., 2017; Paton & Brown, 1994; Stegnik-Jansen et al., 2011). The abdominal region acts as a humeral adductor, extender, and horizontal adductor (Brown et al., 2007; Paton & Brown, 1994).

13

Brown et al. (2007) further classified the different regions of the pectoralis major found in Paton & Brown (1994) as prime movers, synergists, or antagonists. They defined a prime mover as a segment with an agonist moment arm that activates first during a task. A synergist was defined as a segment with an agonist moment arm that activates significantly later than the prime mover. An antagonist was defined as a segment with an antagonist moment arm that activates with the prime mover. They monitored the activity of muscle regions of the pectoralis major, latissimus dorsi, and the deltoids – all of which may have independent control – in adduction, flexion, and extension using surface electromyography. Brown et al. (2007) found that in adduction, the sternocostal and abdominal regions of the pectoralis major acted as a synergists with the latissimus dorsi during adduction, while the clavicular region activated later at a lower intensity. During flexion, the clavicular region of the pectoralis major acted as a primary mover alongside the anterior deltoid, while the sternocostal region acted as a synergist. In extension, the upper portion of the sternocostal region acted as an antagonist, acting at the same time as the prime movers. These results contradict Wolfe et al. (1992), which indicated that the primary action of the pectoralis major is adduction, with internal rotation and flexion as secondary actions.

In addition to humeral adduction, humeral flexion, humeral internal rotation, and horizontal adduction, the pectoralis major's actions have also been quantified while exerting hand forces in different positions (McDonald, Brenneman, Cudlip, & Dickerson, 2014; McDonald, Picco, Belbeck, Chow, & Dickerson, 2012; Nadon, Vidt, Chow, & Dickerson, 2016). Two hand forces that elicited the most muscle activity in the clavicular region of the pectoralis major were pulling horizontally with the right arm, starting from a hand position to the left of the body, directly in front of the body, and at the height of the head (McDonald et al., 2012) and

14

downward exertions starting from a hand position to the left of the body, slightly in front of the body, and slightly below the umbilicus (Nadon et al., 2016). Similarly, the two hand forces that elicited the most muscle activity in the sternocostal region of the pectoralis major were pulling horizontally with the right arm, starting from a hand position to the left of the body, directly in front of the body, slightly above the umbilicus (McDonald et al., 2012) and pressing left from a hand position slightly to the left of the body, an arms length away from the body, and slightly below the umbilicus (McDonald et al., 2014). These findings are consistent with past studies on the sternocostal region (Leonardis et al., 2017; Paton & Brown, 1994; Stegnik-Jansen et al., 2011), as a pressing action involves horizontal adduction. However, there is no information on how the abdominal region activates with regards to any of these hand force positions.

2.2.4 Coactivators

For each of the actions of the pectoralis major, there are different muscles that coactivate, depending on the starting position of the humerus. These coactivation patterns are inferred from either anatomic action or electromyographic assessments. The latissimus dorsi coactivates with the pectoralis major during internal rotation (Brookham & Dickerson, 2016) and adduction (Brown et al., 2007). Ekholm et al. (1978) reported latissimus dorsi coactivation with the pectoralis major while pulling down and across the body, diagonally. The anterior deltoid coactivates during humeral flexion (Brown et al., 2007; Rockwood Jr., 2009) and horizontal adduction (Rockwood Jr., 2009). During internal rotation, the subscapularis coactivates with the pectoralis major (Brookham & Dickerson, 2016; McDonald, 2017). In extension, posterior deltoid coactivates with the pectoralis major (Ekholm, Arborelius, Hillered, & Ortqvist, 1978; Rockwood Jr., 2009), although extension is not commonly referenced as a task that highly involves the pectoralis major.

15

As stated in section 2.2.3, activation patterns of shoulder musculature depend on the position and capable range of motion of the shoulder. While coactivation patterns are commonly noted based on anatomic muscle action, little electromyographic data exists with regards to the pectoralis major and its coactivators. The activation patterns stated above are generalized, and it is likely the activation pattern strategies vary between individuals.

2.3 Muscle Fatigue

2.3.1 Definitions of Fatigue

The concept of fatigue has been researched since at least 1901 (Gandevia, 2001) and is usually regarded as extreme tiredness after mental or physical exertion. Indicators of fatigue include a decrease in performance and an increase in mental work (Enoka & Stuart, 1992; Gandevia, 2001). According to Cifrek et al. (2009), there are two types of fatigue that develop at the same time (Tarata, 2003): central and peripheral. Central fatigue has been defined as a decrease in higher order response to excitation, sometimes before the endurance limit is reached (Al-Mulla, Sepulveda, & Colley, 2011; Cifrek, Medved, Tonković, & Ostojić, 2009; Gandevia, 2001; Moritani, Muro, & Nagata, 1986; Potvin & Fuglevand, 2017; Tarata, 2003). In other words, the body is less willing to produce a maximum force. Peripheral fatigue, also known as localized muscle fatigue, has been defined as the inability to meet an increased energy demand at or distal to the neuromuscular junction, or the impairment of cross-bridge cycling (Al-Mulla et al., 2011; Gandevia, 2001; Potvin & Fuglevand, 2017; Tarata, 2003). Most of what is measured, with regards to fatigue, is peripheral fatigue, although Barry & Enoka (2007) state that there is not a clear distinction between central and peripheral fatigue.

Muscular fatigue is often defined as the failure to exert more force or power (Al-Mulla et al., 2011; Barry & Enoka, 2007; Enoka & Duchateau, 2008; Gandevia, 2001; Potvin & Fuglevand, 2017) or failure to continue working at a given intensity (Gandevia, 2001). Muscular fatigue is also suggested as a protective strategy to prevent damage (Gentil, Oliveira, De Araujo Rocha Junior, Do Carmo, & Bottaro, 2007). While fatigue is commonly defined with regards to a specific time point, it actually begins at the onset of any exercise and varies in degree until the exercise bout is completed (Al-Mulla et al., 2011; Barry & Enoka, 2007; Gandevia, 2001). Further, muscular fatigue is not due to a singular mechanism, rather it is the combination of many physiological and psychological processes (Barry & Enoka, 2007; Enoka & Stuart, 1992).

2.3.2 Fatigue by Electrical Stimulation

When investigating fatigue, a researcher can implement a protocol designed to induce fatigue via different exercises targeting the muscle or muscles in question, otherwise known as voluntary fatigue. If a single muscle is targeted by a fatigue protocol, issues may arise if the muscle cannot be isolated, leading to the fatigue of surrounding musculature, which could confound results. To improve muscle isolation, researchers have electrically stimulated the muscles to induce fatigue (De Luca & Merletti, 1988; Huffenus & Forestier, 2006; Koh & Grabiner, 1992; Merletti & Lo Conte, 1995; Umehara et al., 2018; Vanderthommen et al., 2003). The use of electrical stimulation is appealing, as the elicited signals are cleaner and less variable, as shown in Figure 3 (Merletti & Lo Conte, 1995; Merletti, Knaflitz, De Luca, 1990). However, electrical stimulation may not be able to fully isolate a muscle or group of muscles and result in unintentional activation of surrounding musculature (Gandevia, 2001).
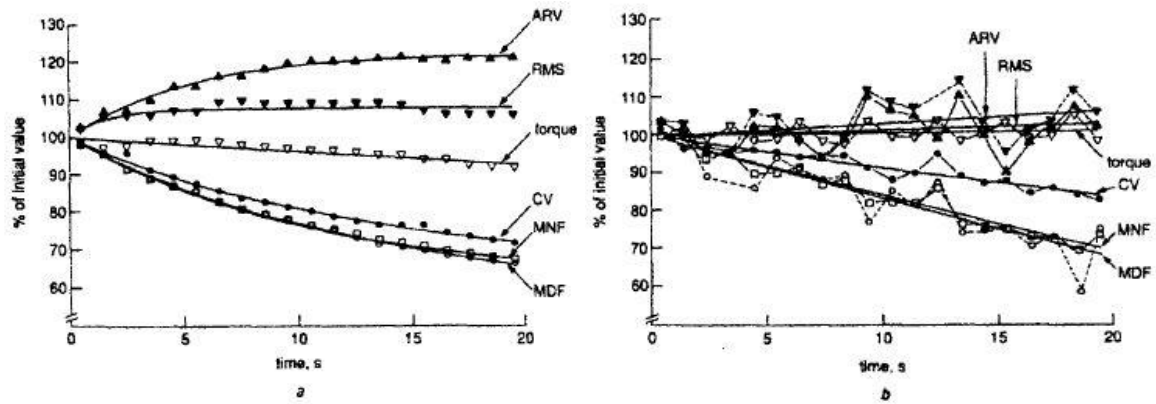
Figure 4. Average rectified value (ARV), root mean square (RMS), torque, conduction velocity (CV), mean frequency (MNF), and median frequency (MDF) during an (a) electrically stimulated contraction and a (b) voluntary contraction at 80% maximum voluntary contraction (Merletti et al., 1990).

Although electrical stimulation of a muscle has been able to produce EMG signals that are similar in frequency content and amplitude (Koh & Grabiner, 1992; Merletti & Lo Conte, 1995) as well as able to induce greater fatigue in a muscle (Merletti et al., 1990), it may result in an unrealistic recruitment of muscle fibers and stimulate other cutaneous pathways that influence the signal (Solomonow et al., 1994). Electrical stimulation leads to recruitment of motor units from large to small, opposite to that of Henneman's Size Principle, during voluntary contractions (Farina, Blanchietti, Pozzo, & Merletti, 2004; Koh & Grabiner, 1992; Merletti & Lo Conte, 1995; Vanderthommen et al., 2003). While electrical stimulation has been shown to lead to greater metabolic fatigue due to higher energy demands (Merletti et al., 1990; Vanderthommen et al., 2003), stimulation artifact shows up in the obtained EMG signal (Koh & Grabiner, 1992; Merletti & Lo Conte, 1995), the whole muscle may not be stimulated (Merletti & Lo Conte, 1995), kinematic strategies may not change (Huffenus & Forestier, 2006), and there may be a potential increase in endurance causing a need for longer fatigue protocols (Umehara et al., 2018). Further, the frequency of electrical stimulation may have to be individualized based on the tolerance of the subject, which indicates that the maximum muscle excitation elicited by

18

stimulation may not be a true maximum (Gandevia, 2001; Solomonow et al., 1994) The results of these studies demonstrate that while electrically stimulated muscle activation and voluntary muscle activation can both effectively fatigue a muscle, they are not equivalent (Merletti & Lo Conte, 1995).

2.3.3 Methodology

Information gained via muscle fatigue can be useful for performance and injury prevention measures in sport and the workplace. Fatigue is often estimated via subjective measures, such as a visual increase in muscle tremors or self-declared reports of discomfort, difficulty, or the desire to abandon the task (Chaffin, 1974). Although these measures may provide insights to mental fatigue states, they are clinically limited in assessing muscular fatigue. With continued advances in technology, more objective fatigue assessments emerged; commonly, these measures are obtained via electromyography (EMG), but are also obtainable through other methods such as mechanomyography, sonomyography, and perceived ratings.

2.3.3.1 Electromyography

EMG measures the electrical signals generated by active muscles and are attractive to researchers, as the signals, when properly collected and processed, can relate to the amount of force measured about a joint (De Luca, 1997; Hagberg, 1981). These signals come from action potentials that are transported by the active fibers through a volume conductor's electrical potential field (De Luca & Merletti, 1988), which are then picked up by electrodes either within the muscle itself or on the skin's surface. Using this instrumentation, many approaches can be used in post-processing to determine the fatigued state of a muscle either in the time domain or the frequency domain.

2.3.3.2 Sonomyography

Sonomyography uses ultrasound technology to detect real-time changes in muscle architecture during contraction, such as pennation angle, muscle fiber length, and cross-sectional area, and has been investigated as an alternative measure of muscle activity (Hodges, Pengel, Herbert, & Gandevia, 2003; Shi, Chang, & Zheng, 2010). Leiber & Friden (2000) state that architectural form is an indication of function, which commends SMG as a viable option to infer muscle activation properties. Past studies reported that SMG could be used with EMG to acquire additional information about a muscle during fatigue (Huang, Zheng, Chen, He, & Shi, 2007; Shi et al., 2010; Zheng, Chan, Shi, Chen, & Huang, 2006). Using ultrasound eliminates crosstalk, it is less invasive and encumbering, and provides a more localized assessment than EMG. Huang et al. (2007) found that SMG and sEMG could be synchronized to provide a more robust assessment of muscle activity, however a limitation with using both methods concurrently is that the ultrasound probe cannot obtain images where the EMG electrode is placed synchronously. Further, while SMG may be able to garner muscle activity information about deep muscles, it can only be used for low level contractions at or under 30% maximum voluntary contraction (MVC), as Hodges et al. (2003) found that there were notable changes in muscle architecture up to 30% MVC, but little to no change at stronger contractions.

2.3.3.3 Mechanomyography

Mechanomyography signals are the mechanical changes of a muscle detected as sound waves or mechanical oscillations (Al-Mulla et al., 2011; Guo, Zheng, Huang, & Chen, 2008). A little more versatile than EMG, MMG can be obtained with many different forms of instrumentation such as microphones, goniometers, piezoelectric contact sensors, lasers, or accelerometers. However, each comes with limitations. When collecting with microphones, the

signal may be subject to noise artifact from external mechanical noise due to the amplification needed to detect the waves generated by the muscles (Al-Mulla et al., 2011; Guo et al., 2008) While goniometers are not subject to mechanical noise, they may not accurately be able to detect fatigue about a joint, as individuals can have differing kinematic strategies when performing a task (McCully et al., 2006, 2007; McDonald, 2017). MMG signals obtained via accelerometers are considered the most reliable, as they are not affected by environmental electrical noise and are inexpensive, although they are more subject to drift and tissue filtering, as they cannot be placed directly on the muscle belly. Tarata (2003) states that different kinds of muscular mechanical vibrations exist: muscle contractions, muscular tremor, and artifact, all of which can be distinguished from each other, as they occur in different frequency ranges. MMG has been used to quantify fatigue in muscles, although the signal characteristics of both EMG and MMG are different, MMG has a lower frequency content (Orizio, Gobbo, Diemont, Esposito, & Veicsteinas, 2003; Tarata, 2003) as well as unchanged amplitude characteristics in response to fatiguing contractions above 65% MVC (Orizio et al., 2003).

2.3.4 Determination of Fatigue

During post-processing of biophysical signals, fatigue can be detected via different methods, all of which can provide different information about the mechanisms of fatigue. These detection methods include EMG time and frequency domains as well as mental fatigue.

2.3.4.1 EMG Amplitude

One way of detecting fatigue is by analyzing the signal amplitude during sustained isometric contractions. Typically, an increase in signal amplitude while maintaining a constant isometric force, over time indicates muscular fatigue (Gandevia, 2001; Moritani et al., 1986). This indicates that more muscle activity is required to perform the work required of the muscle

and is due to the increase in motor unit recruitment to compensate for a decrease in firing rate of already active motor units (Winter, 2009). Historically, calculating the rate of zero crossings or counting spikes of an EMG signal amplitude was used to evaluate fatigue, both of which contain similar information to a spectral analysis (Cifrek et al., 2009). However, both measures depend on the signal to noise ratio and are not commonly used for fatigue analysis. More commonly, root mean square (RMS) or average rectified value (ARV) are used as smoothing techniques for an EMG signal and to evaluate fatigue in the time domain. The RMS of a signal is equivalent to the power in a signal, while the ARV is the average area under the curve over time, both of which provide insights to muscular contributions and efforts. While EMG amplitude methods provide insights to fatigue, they are rarely used on their own as indicators, and are instead often used in conjunction with spectral fatigue evaluation methods.

2.3.4.2 EMG Frequency Spectrum

As discussed in the previous section, an increase in EMG amplitude can be an indicator of fatigue, though a stronger indication of fatigue is an increase in EMG amplitude coupled with a decrease in its frequency spectrum (Hagberg, 1981; Moritani et al., 1986). Compression of the spectrum, or a shift toward lower frequencies, is usually evaluated with mean or median power frequency (MPF, MdPF). According to Winter (2009), the decrease in EMG frequency spectrum is due to lower conduction velocities of action potentials as a result of metabolite accumulation (Moritani et al., 1986), dropout of fast motor units, and synchronous firing of motor units.

The MPF gives the mean value of the frequency spectrum of a signal, while the MdPF gives the frequency value at which the frequency spectrum of a signal is divided in half. While both MPF and MdPF provide similar insights at contractions above 20% (Öberg, Sandsjö, & Roland Kadefors, 1994; Winter, 2009; Yung, Mathiassen, & Wells, 2012), MdPF is less

susceptible to noise and error (Clancy, Bertolina, Merletti, & Farina, 2008; Ebaugh et al., 2006). Regardless of which frequency spectral analysis is chosen, a baseline measure is required while at rest in the position of the contraction to enable comparisons, in which a decrease in MPF or MdPF greater than 8% indicates that a muscle has been fatigued (Öberg, Sandsjö, & Kadefors, 1990). However, frequency spectrum measures do not contain any temporal information, which is another reason why amplitude measures are used to complement frequency spectrum measures (Cifrek et al., 2009).

2.3.4.3 Perceived Ratings

Fatigue is not likely due to one singular mechanism and influences both physical and mental capabilities (McDonald, 2017; Micklewright, St Clair Gibson, Gladwell, & Al Salman, 2017), emphasizing the importance of perceived ratings of exertion or fatigue. Prior to using more objective measures of fatigue, ratings of "discomfort" or a "desire to abandon the task" were used to evaluate fatigue during a task (Chaffin, 1974). These ratings are commonly obtained by using Borg's rating of perceived exertion (RPE) and category ratio scales (Borg, 1990) as well as visual analogue scales (VAS), and are advantageous when describing how subjective feelings tie into physical exertion. While perceived ratings are subjective, they are multifaceted and are dependent on not only psychological factors, but participant characteristics, physical load, and task parameters (Dickerson et al., 2006; Dickerson et al., 2007), whereas the indicators of fatigue obtained from EMG are localized to a specific muscle or muscle group. Although perceived ratings can be used on their own to understand the accumulation of fatigue, when used with physiological measures (such as spectral or amplitude indicators obtained from EMG), perceived ratings can be used to gain information about an individual's psychological

state and can indicate the amount of physical strain an individual is experiencing (Borg, 1990; Hagberg, 1981).

Although Borg's scales are valid and used frequently, Micklewright et al. (2009) distinguishes exertion and fatigue from one another, defining exertion as how hard a task is and fatigue as the decreased ability to cope with physical and/or mental stressors. Another distinction made between exertion and fatigue defines perceived exertion as the sensation one feels during exercise, while perceived fatigue is defined as the sensation one feels post-exertion (Tseng, Gajewski, & Kluding, 2010). Thus, using an RPE scale to rate fatigue is not appropriate. Perceived exertion should drop as soon as an activity concludes, while perceived fatigue may persist, although perceived ratings of fatigue can be used to monitor recovery (Micklewright et al., 2017).

The VAS is another rating scale used to measure a continuous characteristic that is not easily detected (Gould et al., 2001), often used in clinical settings to rate pain (Dauphin et al., 1999). Due to the fact that fatigue is a continuous perception that does not make discrete jumps in classification as Borg and Micklewright's scales suggest, a VAS could be appropriate to use when rating fatigue. In the case of pain ratings, the VAS is commonly a 100-millimeter line and starts at "none" and ends in "extreme pain," in which participants mark where on the continuum they feel represents their current state. While the VAS is sensitive to small changes, it is more appropriate to use when looking at changes within individual as opposed to across individuals (Gould, Kelly, Goldstone, & Gammon, 2001). Additionally, when the VAS is properly calibrated to a benchmark, such as load or maximum voluntary exertion, the classification of perceived effort is more meaningful.

2.3.5 Signal Factors Influencing Fatigue

Although EMG is a common and easily obtained signal to assess fatigue with, care should be taken when collecting and interpreting the data, as there are multiple factors that can influence the signal. When collecting signals, researchers should control as many factors as possible related to data collection. Electrode properties, such as inter-electrode distance, distance between the electrode and the muscle, and electrode placement all influence measured EMG signals (Al-Mulla et al., 2011; De Luca, 1997; De Luca, 1979; Moritani et al., 1986), consequently influencing the obtained signal, rested or fatigued. Researchers should take steps to ensure participants are healthy, do not smoke, and do not drink or consume caffeine the day before the collection, as it will help maintain fatigued signals that are comparable between participants (Al-Mulla et al., 2011). Wust et al. (2010) assessed the muscle strength of the quadriceps in smokers and non-smokers, finding that while force-generating capacity was similar between the groups, smokers fatigued significantly faster. In a double-blind experiment, Lopes et al. (1983) administered caffeine or placebo to subjects before voluntary and electrically stimulated contractions of the adductor pollicis muscle. In instances of low frequency stimulation, ingestion of caffeine resulted in an increase in tension. Additionally, while not statistically significant, endurance times slightly increased when caffeine was consumed.

Researchers should be cautious when deciding who to recruit, as population characteristics, such as age and sex, also alter fatigue initiation and progression (Al-Mulla et al., 2011; Enoka & Duchateau, 2008). Baudry et al. (2007) reported significantly higher declines in peak torque during concentric (50.2%) and eccentric (42.1%) contractions of the tibialis anterior post-fatigue in older adults. Additionally, in low-force fatiguing contractions of the elbow flexor muscles, older adults experienced an increase in muscle activity due to activation of a greater

portion of the motor unit pool (Yoon, De-Lap, Griffith, & Hunter, 2008). In addition to aging effects on fatigue, men are generally more fatigable than women (Al-Mulla et al., 2011; Enoka & Duchateau, 2008). Several studies indicate that women can sustain submaximal contractions longer than men (Clark, Collier, Manini, & Ploutz-Snyder, 2005; Hicks, Kent-Braun, & Ditor, 2001; Hunter, Butler, Todd, Gandevia, & Taylor, 2006). Further, Demura et al. (2008), reported that males experienced higher subjective sensations of muscular fatigue at contractions of 40-60% MVC.

These ostensibly controllable factors are complemented by other confounding signal factors. It has been reported that fiber type influences the fatigability of a muscle (Al-Mulla et al., 2011; De Luca, 1997), with type II muscles fatiguing faster, indicated by a decrease in surface EMG RMS amplitude (Moritani et al., 1986). While muscle fiber type can, in theory, be controlled if a muscle's fiber composition is known, it has also been shown that different muscles are composed of different proportions of fiber types. Thus, attributing specific muscular fatigue to a single fiber type is unrealistic (Enoka & Duchateau, 2008). In addition to fiber type, other physiological properties of muscle such as fiber diameter, blood flow, and accumulation of metabolic by-products influence the EMG signal by a decrease in the external force produced, as well as a decrease in spectral indicators of fatigue (Al-Mulla et al., 2011; De Luca, 1997; Moritani et al., 1986).

2.4 Fatigue Response

2.4.1 Upper Extremity Fatigue Response

Under rested conditions, there is a supposed linear relationship between EMG and muscle force, as described by the equation $F_m = F(v) * F(l) * a * (\rho * PCSA) + Fp(l)$, where F_m is the predicted for the of the muscle, $F(v)$ is the normalized force-velocity relationship, $F(l)$ is the normalized force-length relationship, a is the normalized activation of the muscle obtained from EMG, ρ is the specific tension of a muscle, $PCSA$ is the physiological cross-sectional area of the muscle, and $Fp(l)$ is the passive force-length relationship. This is often used to predict muscle forces; however, when using data obtained from a fatigued muscle, the equation often over predicts muscle force, shifting the EMG-force curve to the left, becoming non-linear, indicating an influence of fatigue on the relationship between EMG signals and muscle force (Dideriksen, Farina, & Enoka, 2010).

In a given muscle, during a given task, fatigue can be dependent on mechanisms such as motivation, pattern of muscle activation, or the nature of an activity (intensity, duration, continuous, or intermittent) (Barry & Enoka, 2007; Enoka & Stuart, 1992). However, no mechanism in particular can be singled out as causing fatigue, as the mechanisms can vary between tasks or even as a task progresses (Barry & Enoka, 2007; Enoka & Stuart, 1992). Under fatigue, EMG signals may appear to rotate within and between muscles with periods of coactivation (Gandevia, 2001) or be accompanied by an increase in activity in a neighboring muscle (Joshi, Thigpen, Bunn, Karas, & Padua, 2011; McCully et al., 2007), which will vary between individuals and the specific task. Fatigue will also manifest itself in different kinematic strategies, as there are different fatigue rates for each muscle in individuals (Tse, McDonald, &

Keir, 2016). Further, in submaximal functional tasks, fatigue may not be the cause for task failure, as performance can be maintained while fatigued (Enoka & Duchateau, 2008).

In both non-fatigued and fatigued states, there is a typical recruitment order of scapular musculature during arm elevation in the scapular plane (Mendez-Rebolledo et al., 2018). During both high and low velocity, non-fatigued elevation, the middle trapezius, lower trapezius, and serratus anterior activated before the anterior deltoid, while the upper trapezius was the last to activate, supporting similar findings that the trapezius group activates after the deltoid group (Cools et al., 2002). During fatigued elevation, the upper trapezius was activated first (Mendez-Rebolledo et al., 2018); however, earlier work showed that while muscle latency slows for both the trapezius and deltoid, there is no significant change in order of activation (Cools et al., 2002). Mendez-Rebolledo et al. (2018) attributed the activation pattern pre- and post-fatigue as an anticipatory postural adjustment and postulate that the activations could possibly lead to a diagnosis of shoulder dysfunction. Similarly, Cools et al. (2002) theorized that the delay in muscle onset time due to fatigue could lead to an alteration in scapular kinematics, which could then lead to overuse injuries.

Global and targeted fatigue in the upper extremity have been reported in muscles such as the serratus anterior, the anterior deltoid, the rotator cuff muscle group, and shoulder musculature involved in arm elevation (Borstad, Szucs, & Navalgund, 2009; Chopp, Fischer, & Dickerson, 2011; Dickerson, Meszaros, Cudlip, Chopp-Hurley, & Langenderfer, 2015; Ebaugh et al., 2006; Joshi et al., 2011; Mulla, McDonald, & Keir, 2018; Noguchi, Chopp, Borgs, & Dickerson, 2013; Tse et al., 2016; Umehara et al., 2018; R. L. Whittaker, La Delfa, & Dickerson, 2018). In each of these studies, fatigue altered both muscle activation and kinematics, though Tse et al. (2016) showed that task performance was maintained even after a fatigue protocol. In response to

fatigue, kinematic effects were often small in magnitude (~4-6°) (Borstad et al., 2009; Mulla et al., 2018; Noguchi et al., 2013), or occurred at multiple segments and joints (Joshi et al., 2011; Tsai et al., 2003; Tse et al., 2016). Likewise, in the presence of fatigue, muscle activity observed using EMG has shown increases in amplitude (Borstad et al., 2009; Chopp et al., 2011; Dickerson et al., 2015; Joshi et al., 2011; Mulla et al., 2018; Noguchi et al., 2013) or shifts in the power spectrum (Chopp-Hurley, Langenderfer, & Dickerson, 2016; Chopp et al., 2011; Dickerson et al., 2015; Ebaugh et al., 2006; Noguchi et al., 2013; R. L. Whittaker et al., 2018). Additionally, fatigue response is variable between individuals (Chopp-Hurley & Dickerson, 2015; Chopp-Hurley, Langenderfer, et al., 2016; Dickerson et al., 2015; Tse et al., 2016) and within individuals (Mulla et al., 2018), as there is no one specific muscle activation or kinematic pattern that occurs in response to upper extremity fatigue. In instances of targeted fatigue, the surrounding musculature has also fatigued via myoelectric indicators, despite selecting exercises that attempt to selectively fatigue a single muscle or group of muscles (Borstad et al., 2009; Chopp-Hurley & Dickerson, 2015; Noguchi et al., 2013). These results indicate postural compensations accompanying altering muscle activities to either preserve task performance by increasing muscle activities to maintain force production (Joshi et al., 2011; R. L. Whittaker et al., 2018). This may also indicate injury prevention, as fatigue can aggravate muscular imbalances (Tsai et al., 2003), as postural compensations could be used as an offloading strategy to reduce the demand on fatigued muscles (Tse et al., 2016; R. L. Whittaker et al., 2018).

Although unrelated to fatigue, McCully et al. (2006 & 2007) found that when the suprascapular nerve was disabled, both kinematics and muscle activation were affected. Changes in muscle activation were small (McCully et al., 2007), while there were marked changes in scapular rotation and glenohumeral motion (McCully et al., 2006). When compared with rotator

cuff tears and fatigue models, the scapular kinematic patterns of all three models (rotator cuff tear, fatigue, and suprascapular block) were comparable, as they all resulted in an increase in upward rotation of the scapula. To further support this statement, it has been shown that fatigue mimics injury or muscle dysfunction (Chopp-Hurley & Dickerson, 2015; Tsai et al., 2003). This suggests a common compensatory mechanism in each model, which could potentially be applied to other injuries in different regions of the body.

2.4.2 Fatigue Recovery

Just as fatigue onset begins immediately as an activity starts, recovery from fatigue begins as soon as the activity terminates. Frey Law et al. (2012) developed an optimization model to predict muscle fatigue onset and recover, finding that fatiguing of a muscle of interest occurs 10-15 times faster than recovery. However, their model used endurance time as an indicator of fatigue, was based off of isometric data, and used constant values for both fatigue and recovery during high and low intensity tasks. In contrast, there is evidence that suggests that recovery from fatigue depends on the duration, intensity, and nature of the task (Yung et al., 2012). Further, McDonald et al. (2016) reported that immediately following the fatigue protocol, strength and perceived effort increased. Throughout the post-fatigue trials, both muscle activity and kinematics changed over time, with a few muscles recovering from fatigue and others maintaining their fatigued state or developing fatigue. By the end of the post-fatigue trials, both strength and perceived effort returned to baseline levels, although spectral indicators of fatigue persisted.

2.5 Literature Review Summary

The pectoralis major is involved in a multitude of humeral movements, though there has been little exploration with regards to how the muscle contributes to overall shoulder function or how the muscle responds to disruption. Previous research indicated that voluntary fatigue, measured with EMG and motion capture, can be used as a proxy for shoulder musculoskeletal disorders (i.e. subacromial impingement syndrome; rotator cuff tears), inducing changes in muscle activity and movement patterns that are similar to specific injuries. A relationship between targeted voluntary pectoralis major fatigue and shoulder responses may provide a more specific understanding of how the muscle contributes to shoulder function with and without the presence of a disruption.

3.0 METHODOLOGY

3.1 Participants

Twenty healthy, university-aged adult males were recruited for this study, as the

pectoralis major is more easily accessible for superficial muscular recordings. An initial *a priori*

power analysis determined a minimum sample of 16 participants were required to detect

significant differences using a one-way repeated measures ANOVA ($\alpha = 0.05$, 1-$\beta = 0.85$) using

previous means and standard deviations from Tse et al. (2016). This sample size is larger than

previous fatigue studies, which range from 10-15 participants (Mulla et al., 2018; Noguchi et al.,

2013; Tse et al., 2016; Yung et al., 2012). Participants were excluded from this study if they had

any upper extremity, neck, or back injuries in the last year, any shoulder surgery in the past 6

months, or if they were chronic smokers (Wüst et al., 2010). Participant demographics are

presented in Table 1. Informed consent was obtained before data collection, following approval

of the protocol by the University of Waterloo Office of Research Ethics Committee (ORE#:

40388). Upon recruitment, all participants were instructed to avoid upper extremity and trunk

exercise, alcohol consumption, and caffeine consumption 24 hours prior to the experimental

protocol (Lopes et al., 1983; Yung et al., 2012). This was to prevent potential prior fatigue or

known confounding variables.

Table 1: Participant demographics (mean ± SD). L indicates left-hand dominant, while R
indicates right-hand dominant, with regards to handedness

	Age (years)	Height (cm)	Weight (kg)	Handedness
n = 20	25.8 ± 3.95	177.4 ± 8.37	79.56 ± 10.08	4L, 16R

3.2 Instrumentation

3.2.1 Surface Electromyography

Surface electromyography was collected from sites overlying seven upper extremity muscles, including the three areas of the pectoralis major (clavicular, sternocostal, and abdominal), on the dominant arm using the Noraxon T2000 telemetered system (Noraxon, Arizona, USA). The sEMG was recorded at 1500 Hz within the Vicon Nexus 1.8.5 program (VICON, Oxford, UK). Noraxon bipolar Ag-AgCl dual surface electrodes (Noraxon, Arizona, USA) were placed with a 2 cm inter-electrode distance over the belly of each muscle, parallel to the direction of the muscle fibers. The seven muscles monitored were the pectoralis major (clavicular region, upper sternal region, abdominal region), the anterior, middle, and posterior deltoids, upper trapezius, latissimus dorsi, and infraspinatus. Before electrode placement, the skin was shaved, abraded with gel (NuPrep, Weaver and Company, Colorado, USA), and swabbed with alcohol to reduce skin impedance. Electrode placement is outlined in Table 2. Once the electrodes were placed, a quiet trial was recorded to obtain baseline muscle activity. After, participants performed muscle-specific isometric maximum voluntary contractions (MVCs) based on the recommendations of Cram & Kasman (1998) and Fung et al. (2009) (Table 4). The EMG signals were bandpass filtered and differentially amplified between 10-500 Hz (common mode rejection ratio > 100 dB at 60 Hz, input impedance 100 MΩ). The signals were converted from analog to digital at 1500 Hz with a 16-bit A/D card with a range of ±10 Volts.
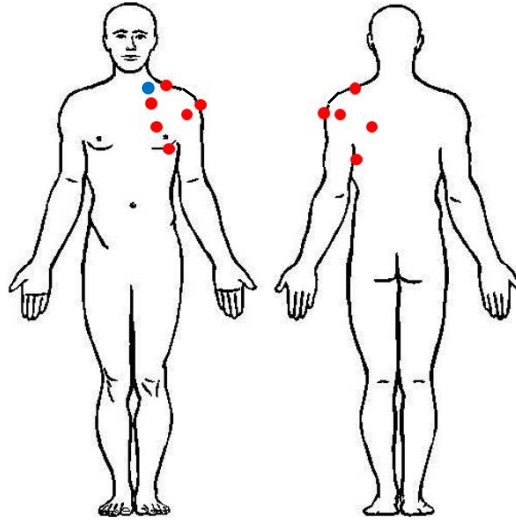
Figure 5. Surface EMG electrode placements. The blue dot indicates the ground electrode placement on the clavicle.

Table 2: A description of electrode placements in this experiment based on Cram & Kasman (1998), Fung et al. (2009), and pilot data. * denotes electrode placement suggested by Fung et al. (2009).

Muscle	Placement
Pectoralis Major (Clavicular)	2 cm below the clavicle, halfway between the sternoclavicular joint and coracoid process, at an oblique angle toward the clavicle
Pectoralis Major (Sternocostal)	6 cm above the nipple, 2 cm medial to the axillary fold, parallel to the muscle fibers
Pectoralis Major (Abdominal)*	Between ribs 4-6, at the midpoint of the clavicle, directed toward the axillary fold
Anterior Deltoid	4 cm below the clavicle on the anterior aspect of the arm, at an oblique angle pointing toward the deltoid tuberosity
Middle Deltoid	3 cm below the acromion on the lateral aspect of the arm, midway between the deltoid tuberosity and acromion process
Posterior Deltoid	2 cm below the lateral surface of the acromion, at an oblique angle pointing toward the deltoid tuberosity
Upper Trapezius	2 cm lateral to the midpoint between the C7 spinous process and the posterior portion of the acromion process along the line of the trapezius
Infraspinatus	4 cm below the scapular spine, over the lateral portion of the infrascapular fossa
Latissimus Dorsi	4 cm below the inferior angle of the scapula, parallel to the lateral border of the scapula at an oblique angle

3.2.2 Motion Capture

Three-dimensional kinematic data of the dominant upper limb and torso was collected at 60 Hz using a 13-camera VICON MX20 passive optoelectronic motion capture system (VICON, Colorado, USA). The collection space was calibrated prior to the participants' arrival. The global origin was set so that the movements of participants occurred in positive axes throughout the experiment, while the global coordinate system was set to ISB standards (Wu & Cavanaugh, 1995), where +Y was directed up, +X was directed forward, and +Z was to the right of the origin, defined by the right-hand rule.

A total of 23 reflective markers were placed on the dominant arm and the torso over bony landmarks following ISB recommendations (Table 3, Figure 6) (Wu et al., 2005). In addition to the individual markers, upper arm, forearm, chest, and back clusters containing 3 markers each were attached to facilitate reconstruction if trials that had marker dropout. A 5-second static calibration trial was performed before starting dynamic activity, where the participant stood in a "T pose". This trial was used to develop an anatomical calibration matrix, which described the position of anatomical landmarks of the trunk and upper extremity within the respective cluster coordinate systems.

Table 3: Vicon marker placement based on recommendations made by Wu et al. (2005).

Body Segment	Anatomical Landmark
Thorax	Xiphoid Process (XP)
	Suprasternal Notch (SS)
	Chest Cluster (Chest1, Chest2, Chest3)
	Spine of Cervical Vertebrae 7 (C7)
	Spine of Thoracic Vertebrae 8 (T8)
	Back Cluster (Back1, Back2, Back3)
	Acromion Process (AP)
Humerus	Upper Arm Cluster (UA1, UA2, UA3)
	Medial Epicondyle (ME)
	Lateral Epicondyle (LE)
Forearm	Forearm Cluster (FA1, FA2, FA3)
	Radial Styloid Process (RS)
	Ulnar Styloid Process (US)
Hand	2nd Metacarpal Joint (MCP2)
	5th Metacarpal Joint (MCP5)
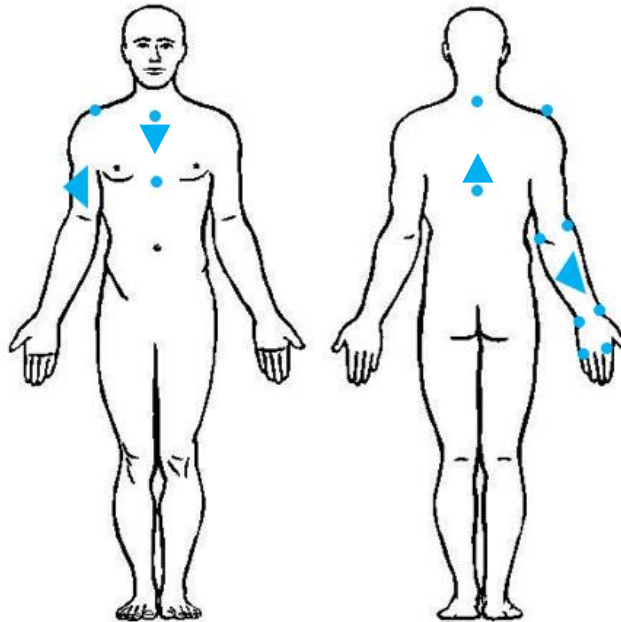
Figure 6. VICON marker placement on the anterior and posterior dominant upper extremity and torso. Each blue circle indicates a marker and each triangle indicates a marker cluster.

3.2.3 Ratings of Perceived Exertion/Fatigue

Participants provided both a rating of perceived exertion (RPE) (Figure 7a) and a rating of perceived fatigue (RPF) (Figure 7b), using modified Borg CR-10 scales (Borg, 1990). When providing both RPE and RPF, participants verbally indicated their level of exertion with visual reminders of each scale, providing a rating between 0 and 10, and were instructed that they were not restricted to whole numbers and may choose any value between those bounds. Additionally, participants were reminded that these scales were restricted to the pectoralis major region and not the whole body. These scales were used to monitor changes in muscle fatigue as the participant progressed through the fatigue protocol, as the scales were used to determine task completion. An RPE rating of 8/10 for three consecutive cycles was used to determine the point of task completion.

Score	Level of exertion			RPF Scale		
0	No exertion at all	**(a)**	**Completely Rested**	0	No fatigue at all	**(b)**
0.5	Very, very slight (just noticeable)			0.5	Very light fatigue	
1	Very slight			1	Light fatigue	
2	Slight			2	Fairly fatigued	
3	Moderate			3	Moderately fatigued	
4	Somewhat severe			4	Fatigued	
5	Severe		**50% Rested**	5	Very fatigued	
6				6		
7	Very severe			7	Nearly exhausted	
8				8		
9	Very, very severe (almost maximal)			9		
10	Maximal		**Completely Fatigued**	10	Absolutely exhausted	

Figure 7. (a) Borg's CR-10 rating of perceived exertion taken from Borg, 1990 and (b) Borg's rating of perceived fatigue scale

3.2.4 Strength Measures

Maximum voluntary internal rotation strength was quantified throughout the experimental protocol in the form of external hand force in order to measure potential strength

decrements associated with fatigue. A D-handle was attached to a 6-degree of freedom force

transducer (MC3A, AMTI, Watertown, Massachusetts). The force cube was positioned to ensure

participants produced force along the Z-axis, while the X- and Y-axes forces were minimized.

Strength measures coincided with the MVC trials and were sampled for 5 seconds at 1500 Hz.

3.3 Experimental Protocol

Participants spent approximately 3.5 hours in the lab, during which they performed muscle-specific maximum voluntary contractions (MVCs), task-specific MVCs, a series of pre-fatigued activities of daily living (ADL), a fatigue protocol, and post-fatigue ADLs. The general study protocol is outlined in Figure 8.
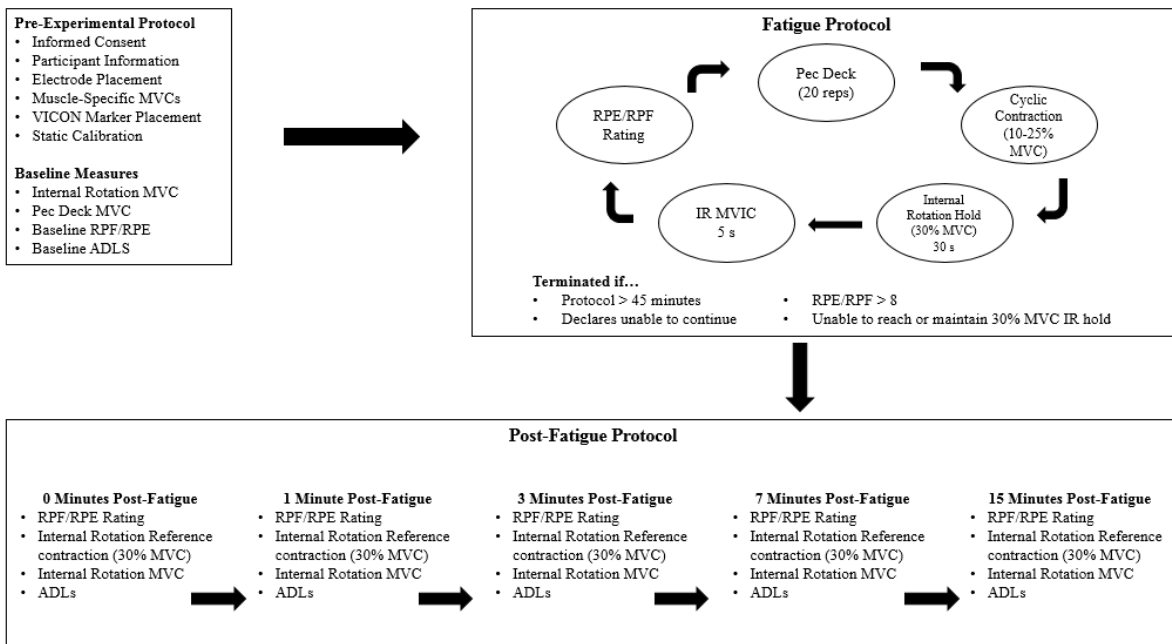
Figure 8. A general overview of experimental collection protocol. First, instrumentation with sEMG and VICON markers and baseline measures were performed. During this time, participants were familiarized with the fatigue protocol tasks, the RPE/RPF scales, and the ADLs. Following baseline measures, participants completed a fatigue protocol involving the Pec Deck (40% MVC), a cyclic internal rotation contraction (10-25% MVC) lasting 2 minutes, an isometric internal rotation hold (30% MVC), followed by an internal rotation maximum contraction. RPE and RPF were obtained following each cycle of the fatigue protocol. If the termination criteria were met, the participant moved on the post-fatigue measures. Otherwise, they continued to cycle through the fatigue protocol until they met termination criteria.

3.3.1 Collection Protocol

Before starting experimental data collection, participants reviewed the information consent form, provided written informed consent. Age, height, and weight were taken during this

time. Following this, participants had EMG electrodes placed over the shoulder musculature of

the dominant arm. After electrode placement, participants performed two, 5 second muscle-

specific MVCs for each muscle (Table 4). There was a two-minute rest period between each

exertion to avoid fatigue.

Table 4: A description of MVC postures for the 7 muscles in this experiment based on Cram & Kasman (1998) and Daniels & Worthingham (1986).

Muscle	MVC Posture
Pectoralis Major (Clavicular)	Lying supine, shoulder is abducted to 60 degrees, while the elbow is flexed to 90 degrees with the hand pointing at the ceiling. Participant will bring their arm through horizontal adduction against resistance provided by the researcher.
Pectoralis Major (Sternocostal)	Lying supine, shoulder is abducted to 90 degrees, while the elbow is flexed to 90 degrees with the hand pointing at the ceiling. Participant will bring their arm through horizontal adduction against resistance provided by the researcher.
Pectoralis Major (Abdominal)	Lying supine, shoulder is abducted to 90 degrees, while the elbow is flexed to 90 degrees with the hand pointing at the ceiling. Participant will bring their arm through horizontal adduction against resistance provided by the researcher.
Anterior Deltoid	Seated, the shoulder flexed forward to 90 degrees, elbow fully extended, and thumb pointing up. Participant will continue shoulder flexion against resistance provided by the researcher.
Middle Deltoid	Seated, the shoulder abducted to 90 degrees, elbow fully extended, and thumb pointing forward. Participant will continue shoulder adduction against resistance provided by the researcher.
Posterior Deltoid	Seated, the shoulder abducted to 90 degrees, elbow fully extended, and thumb pointing backward. Participant will continue shoulder adduction against resistance provided by the researcher.
Upper Trapezius	Lying prone, shoulder abducted to 90 degrees, elbow fully extended, and thumb pointing down toward the floor. Participant will continue shoulder abduction against resistance provided by the researcher.
Infraspinatus	Lying on the opposite side of the arm being investigated, arm at side, and elbow flexed to 90 degrees. Participant will externally rotate against resistance provided by the researcher.
Latissimus Dorsi	Seated, the participant will abduct their arm to 90° and flex their elbow to 90°. From this position, the participant will adduct their arm against resistance provided by the researcher.

After the muscle-specific MVCs, participants performed two task-specific MVCs for

both internal rotation of the humerus and horizontal adduction in the apprehension position to

determine exertion percentages for the fatigue protocol. The mean of the two trials was used as

the maximum to scale the fatiguing protocol tasks. Descriptions of each task are provided in

Table 5. Prior to collecting the strength data, participants were familiarized with the perceived

rating scales and baseline RPF and RPE (Borg, 1990) values that were to be recorded.

Table 5: Description of fatigue protocol tasks designed to target the pectoralis major. *denotes posture based off of Gentil et al. (2007)

Task	Task Posture
Internal Rotation	Squeezing a foam block in between the elbow and trunk, elbow flexed to 90 degrees, forearm neutral. Internally rotate, generating external hand force against resistance.
Horizontal Adduction from Apprehension*	Shoulder abducted to 90 degrees; elbow flexed to 90 degrees. Horizontally adduct against resistance.

Following the MVCs, reflective markers were placed on the participant and a 5-second

static calibration trial was taken. After at least 2 minutes of rest following the MVCs,

participants were asked for a baseline RPF and RPE value. Next, the participant performed one

trial of each ADL (Brookham et al., 2018a, 2018b; Maciukiewicz, 2017; McDonald et al., 2012)

(Table 5). The ADLs that suggest the involvement of props used physical props, as simulated

tasks do not accurately replicate movements (Taylor, Kedgley, Humphries, & Shaheen, 2018).

Table 6: Description of activities of daily living based off of Brookham et al. (2018), Brookham et al. (2018a), and Maciukiewicz (2017). * indicates ADLs based off of Brookham et al. (2018) and Brookham et al., (2018a). § indicates ADLs based on the findings of McDonald et al. (2012). † indicates ADLs based off of Maciukiewicz (2017)

ADL	Description
Back scratch*	Starting with their hands at their sides while standing, the participant will reach behind their back and up to attempt to touch the inferior angle of the contralateral scapula
Shower curtain pull§	Starting with their hands at their sides while standing, the participant will reach across their body to pull a shower curtain closed, release it, and then pull the shower curtain back open
Reach to shelf (shoulder height)†	In a seated position, start with arms at sides. Participant will grasp a weighted object, lift it to the shelf at shoulder height, release it, and then return it to resting position. This is completed with a bottle weighing 2 kg.

Once these baseline measures were completed, the participant completed a 45-minute

fatigue protocol (Figure 8). The protocol involved 20 repetitions of horizontal adduction from the

apprehension position (also known as the "pec deck" exercise) at 40% MVC. Participants were

instructed to keep time to a metronome (1 Hz frequency) while performing the repetitions.

Immediately following the pec deck exercise, participants completed a cyclical internal rotation

contraction from 10-25% MVC for 2 minutes. Following the cyclic contraction, participants

completed an internal rotation isometric hold, scaled to 30% MVC, for 30 seconds. Immediately

after the 30% hold, participants performed a maximum internal rotation contraction for 5

seconds. Participants continued to cycle through these three blocks for 45 minutes, or until they

declared that they were unable to continue the tasks anymore. After every internal rotation

isometric hold, a 5-second period was allotted to participants to report RPE and RPF on Borg's

scales before moving back to the pec deck to begin another cycle of the protocol. The fatigue

protocol was terminated when at least one of the following criteria were met: 1) completing the

45 minutes, 2) verbal indication they were no longer able to continue, 3) inability to reach and

maintain internal rotation at 30% MVC for 30 seconds, or 4) a rating of perceived discomfort or

fatigue greater than or equal to 8 out of 10 for three consecutive cycles.

As soon as the fatigue protocol was terminated, participants performed an internal

rotation MVC followed by the same ADLs assessed pre-fatigue. At 1, 3, 7, and 15 minutes post-

fatigue, participants completed the internal rotation MVC, 30% MVC reference contraction, and

ADLs again, giving an RPF/RPE rating at the end of each (Figure 8).

3.4 Data Analysis

3.4.1 Electromyography Processing

The surface EMG signals during the muscle-specific MVCs, the baseline measures, the internal rotation reference contractions, and the post-fatigue measures were processed identically to facilitate comparisons.

3.4.1.1 Amplitude

The raw sEMG data were processed in a customized MATLAB 2017a program (Mathworks, Inc., Massachusetts, USA). First, the raw signals were averaged in order to remove the DC bias. Next, the quiet trial was averaged in order to remove the DC bias from the quiet signal. The quiet trial was processed, averaged, and removed. Next, the sEMG signals were highpass filtered using a dual pass, 2nd order Butterworth filter with a 30 Hz cut off to remove heart rate contamination and other noise from the signal (Drake & Callaghan, 2006).

To normalize the sEMG signals to each individual, the middle 3 seconds of each MVC trial were used to calculate an average RMS (375 sample window, 300 sample overlap) to represent the maximum activity for each MVC trial. The peak RMS value of the sEMG signal was extracted for each muscle across the two muscle-specific MVC trials and used to represent the maximum activation for the muscle of interest. The normalized values are subsequently reported as percent maximum voluntary contraction (%MVC).

For the static reference contractions, mean EMG (375 sample window, 300 sample overlap) was calculated to quantify muscular contribution from all collected muscles. The EMG signals collected during the ADLs were cropped based on synced kinematic data, outlined in the

43

next section. An RMS (375 sample window, 300 sample overlap) was performed on the dynamic EMG collected during each of the ADLs, from which the mean EMG amplitude wasextracted.

3.4.1.2 Mean Power Frequency (MPF)

All muscles were assessed with mean power frequency (MPF) analysis. The raw sEMG signal collected at baseline and post-fatigue measures, during the internal rotation reference contractions, were processed to obtain MPF values. Raw data were bandpass filtered using a dual pass 2nd order Butterworth filter from 30-500 Hz to remove heart rate contamination and noise, as with the sEMG amplitude analysis (Drake & Callaghan, 2006). The data from the reference contractions, lasting 5-seconds, were divided into 0.5-second intervals (750 data points), resulting in 10 intervals per static reference contraction. These intervals were padded with zeros to create an interval of 1500 data points to obtain a 1 Hz frequency resolution of each interval. The reference contractions and their subsequent intervals were analyzed with a Fast Fourier Transform (FFT) and the MPF was calculated as the frequency that is the sum of the power spectral density at each frequency divided by the spectral moment (Equation 1).

$$MPF = \frac{\sum_{f=30}^{f?} PSD(f) \times f}{Ptotal} \qquad (1)$$

Following the FFT performed on each interval, all 10 intervals from each reference task were averaged in order to quantify the MPF for each reference task as a single number.

The MPF values obtained from the reference contractions during the fatigue protocol and post-fatigue protocol. These values were used as an indicator of fatigue in the upper extremity muscles collected, as decreases in MPF greater than 8% indicate that a muscle is fatigued (Öberg et al., 1990). To determine the presence of fatigue, the MPF values from all reference contractions were calculated with Equation 1 and used to discern changes that were 8% or greater.
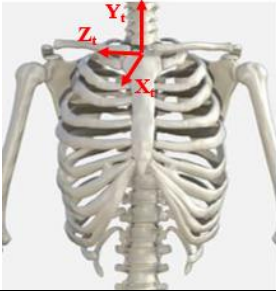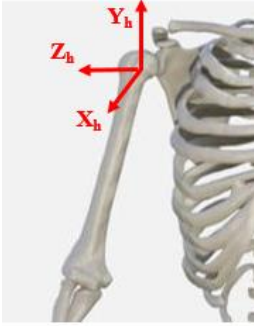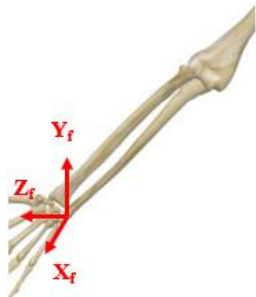
44

3.4.2 Motion Capture Processing

Kinematic data was collected during the pre-fatigue measures and immediately after the fatigue protocol during post-fatigue measures. These data were used to determine initiation and completion of the ADL trials in order to parse out the sEMG for the movements.

Raw kinematic data were visually inspected and labeled or re-labeled when necessary in Vicon Nexus 1.8.5 (Vicon, Oxford, UK). Missing markers were gap-filled using the same software. The kinematic data was filtered with a dual pass, 2nd order, low-pass Butterworth filter with a cutoff frequency of 4 Hz (Whittaker, 2017) to remove high frequency noise content, as human motion falls between 0-6 Hz (Winter, 2009).

The static calibration trial was used to develop an anatomical rotation matrix, which described the position of anatomical landmarks of the trunk and upper extremity within the respective cluster coordinate systems (Winter, 2009). This was done, as the position data from the clusters is less sensitive to skin motion artifact when compared to anatomical markers. Therefore, the position data of the clusters was used to compute joint angles. The local coordinate systems (LCS) computed during the calibration trial were calculated via the anatomical markers for the torso, humerus, and forearm, as per ISB recommendations (Wu et al., 2005) (Table 7) as well as for the clusters on the forearm, humerus, upper arm, and back. The segment rotation matrices between the anatomical and cluster axis systems (Winter refers to this as "M to A matrices") were computed the segment cluster (forearm, humerus, chest or back) relative to that same segment axis system. The relationship between the cluster and anatomical axis systems were assumed to remain constant during the repetitive task.

Table 7: Local coordinate systems of each segment, based off of ISB standards (Wu et al., 2005)

Body Segment	Origin	Local Coordinate System
Thorax	IJ	Y_t: Line connecting the midpoint between XP and T8 and the midpoint between IJ and C7, pointing up Z_t: Line perpendicular to the plane formed by IJ, C7, and midpoint between XP and T8, pointing right X_t: Common line perpendicular to Z_t and Y_t axes, pointing forward
Humerus	GH	Y_h: Line connecting GH and the midpoint of LE and ME, pointing to GH X_h: Line perpendicular to the plane formed by LE, ME, and GH, pointing forward Z_h: Common line perpendicular to Y_h and Z_h axes, pointing right
Forearm	US	Y_f: Line connecting the US and the midpoint between LE and ME, pointing proximally X_f: Line perpendicular to the plane through US, RS, and the midpoint between LE and ME, pointing forward Z_f: Common line perpendicular to X_f and Y_f axes, pointing right

During each ADL trial, glenohumeral, elbow, and wrist joint centers were calculated according to ISB recommendations (Wu et al., 2005) using the positional data collected. The filtered data was used to identify the initiation and termination of each ADL in order to crop the EMG data. The initiation of each ADL was defined as the time point at which the acceleration of the wrist center in the Y+ direction was no longer zero. The termination of each ADL was defined as the time point at which the acceleration of the wrist center in the Y+ was once again zero.

The joint angles were computed for torso to global, thoracohumeral (humerus to torso), and elbow (forearm to humerus) from positional data as follows. First, a time-varying rotation matrix between the global coordinate system (GCS) and the cluster LCS (Winter refers to this as "G to M matrix") was calculated using the position data from the clusters on the humerus, forearm, and chest. Next, a rotation matrix between the GCS and the anatomical coordinate system (Winter refers to this as "G to A matrix") was calculated for each body segment. This was done by finding the product of the time-varying "G to M matrix" and the constant "M to A matrix" for the humeral, forearm, and chest clusters. Using the LCS of each segment, rotation matrices were calculated between the distal LCS with respect to the proximal LCS to extract joint angles. This was done by multiplying the transpose of the distal LCS (transpose of "G to A" matrix = "A to G" matrix) by the proximal LCS ("G to A" matrix). This resulted in direction cosine matrices from which the recommended rotation sequences for each joint angle were calculated (Table 8) using a custom MATLAB 2017a program (Mathworks, Inc., Massachusetts, USA).

For the thorax and elbow, the ZXY rotation sequence (Equation 3) was used. Carrying angle in the elbow was calculated, but not analyzed, as it is the passive response to elbow flexion/extension (Wu et al., 2005). Thoracohumeral flexion/extension, horizontal adduction/abduction, and internal rotation were calculated with the YXY' rotation sequence (Equation 4) for the curtain ADL, as participants were more likely to flex their humerus above 90° and ISB recommendations by Wu et al. (2005) suggest that gimbal lock occurs at 0° and 180°. The XZY rotation sequence (Equation 5) was used for the scratch and shelf ADLs to calculate flexion/extension, horizontal adduction/abduction, and axial rotation, as this gimbal

47

lock occurs between -90° and 90° of horizontal adduction (Phadke, Braman, LaPrade, & Ludewig, 2011) and participants performed the ADLs within this range.

Following angle extraction, the range of motion (ROM) of each ADL was calculated by subtracting the minimum from the maximum for comparison with earlier reported angles (Brookham et al., 2018a; Hall, Middlebrook, & Dickerson, 2011; Vidt et al., 2016). For only the torso angles, the difference from pre-fatigue to post-fatigue was calculated by subtracting the pre-fatigue ROM from the ROM of each post-fatigue time point, as not every participant was facing the same direction as the calibration trial when they performed the tasks.

$$\begin{bmatrix} \cos(\gamma)\cos(\alpha) - \sin(\gamma)\sin(\beta)\sin(\alpha) & \cos(\gamma)\sin(\alpha) + \sin(\gamma)\sin(\beta)\cos(\alpha) & -\sin(\gamma)\cos(\beta) \\ -\cos(\beta)\sin(\alpha) & \cos(\beta)\cos(\alpha) & \sin(\beta) \\ \sin(\gamma)\cos(\alpha) + \cos(\gamma)\sin(\beta)\sin(\alpha) & \sin(\gamma)\sin(\alpha) - \cos(\gamma)\sin(\beta)\cos(\alpha) & \cos(\gamma)\cos(\beta) \end{bmatrix} \quad (2)$$

$$\begin{bmatrix} \cos(\gamma)\cos(\alpha) - \sin(\gamma)\cos(\beta)\sin(\alpha) & \sin(\gamma)\sin(\beta) & -\cos(\gamma)\sin(\alpha) - \sin(\gamma)\cos(\beta)\cos(\alpha) \\ \sin(\alpha)\sin(\beta) & \cos(\beta) & \cos(\alpha)\sin(\beta) \\ \sin(\gamma)\cos(\alpha) + \cos(\gamma)\cos(\beta)\sin(\alpha) & -\cos(\gamma)\sin(\beta) & -\sin(\gamma)\sin(\alpha) + \cos(\gamma)\cos(\beta)\cos(\alpha) \end{bmatrix} \quad (3)$$

$$\begin{bmatrix} \cos(\gamma)\cos(\alpha) & \cos(\gamma)\sin(\alpha)\cos(\beta) + \sin(\gamma)\sin(\beta) & \cos(\gamma)\sin(\alpha)\sin(\beta) - \sin(\gamma)\cos(\beta) \\ -\sin(\alpha) & \cos(\beta)\cos(\alpha) & \cos(\alpha)\sin(\beta) \\ \sin(\gamma)\cos(\alpha) & \sin(\gamma)\sin(\alpha)\cos(\beta) - \cos(\gamma)\sin(\beta) & \sin(\gamma)\sin(\alpha)\sin(\beta) + \cos(\gamma)\cos(\beta) \end{bmatrix} \quad (4)$$

Table 8: Joint coordinate systems and the Euler rotation sequence descriptions as well as clinically relevant interpretations based off of ISB recommendations (Wu et al., 2005). * indicates the rotation will not be analyzed in this thesis.

Joint	Rotation and Clinical Interpretations
Thorax to Global	Rotation sequence: Z-X-Y **e1:** Z-axis of the global coordinate system; flexion (-); extension (+) **e3:** Axis coincident with Y-axis of thorax coordinate system; left axial rotation (+); right axial rotation (-) **e2:** Axis perpendicular to e1 and e3 (rotated X-axis of the thorax); right lateral flexion (+); left lateral flexion (-)
Thoracohumeral (Shelf ADL)	Rotation sequence: Y-X-Y' e**1:** Axis coincident with the Y-axis of the thorax coordinate system; plane of elevation where 0° is abduction and 90° is forward flexion **e3:** Axial rotation around Y-axis of the humerus; internal rotation (+); external rotation (-) **e2:** Axis coincident with the X-axis of the humerus coordinate system; GH elevation (-)
Thoracohumeral (Curtain and Scratch ADLs)	Rotation sequence: X-Z-Y e**1:** Axis fixed to the thorax and coincindent with the X-axis of the thorax system; elevation (+); depression (-) **e3:** Axial rotation around Y-axis of the humerus; internal rotation (+); external rotation (-) **e2:** Common axis perpendicular to e1 and e3 (the rotated Z-axis of the humerus; horizontal flexion (+); horizontal extension (-)
Elbow	Rotation sequence: Z-X-Y **e1:** Axis coincident with the Z-axis of the humerus coordinate system; flexion (+); hyperextension (-) **e3:** Axis coincident with the Y axis of the forearm coordinate system; pronation (+); supination (-) **e2*:** Common axis perpendicular to e1 and e3; carrying angle

3.4.3 Statistical Analyses

All statistical analyses were performed using SPSS version 25.0 (IBM, Armonk, NY).

Prior to testing each hypothesis, a Shapiro-Wilk test was run on each dataset to determine

normality. Statistical outliers were removed if the dataset was determined to be not normal. For

each dataset, this occurred 0-5 times.

One-way repeated measures analysis of variance (ANOVAs) were used to test the effect

of fatigue state (pre- and post-fatigue) on compensatory muscular activation (mean EMG

amplitude in other monitored muscles) and kinematics (joint angle ROM, minimums, and

maximums). To assess compensatory muscle activation (research question 1), six one-way within participants repeated measures ANOVAs ($\alpha = 0.05$) were used to detect differences in the anterior, middle, and posterior deltoids, latissimus dorsi, infraspinatus, and upper trapezius of the dominant arm pre- and post-fatigue (Table 9). To assess kinematic changes (research question 2), five one-way within participants repeated measures ANOVAs were ($\alpha = 0.05$) were used to detect differences in range of motion for the elbow and thoracohumeral rotations (Table 9). A one-way within participants repeated measures ANOVA assessed the torso to global rotation ROM differences from pre-fatigue to post-fatigue (Table 9). In the case of violation of sphericity, a Greenhouse-Geisser correction was used. Post hoc Tukey HSD were calculated on the mean differences that were determined to have main effects for research questions 1 and 2. Statistical significance was set at $P = 0.05$.

To examine the presence of fatigue across the three regions of the pectoralis major and whether or not there was differential fatigue between the regions (research question 3), the internal rotation reference contractions were used. This was determined using the traditional definition of fatigue: an increase in amplitude coupled with a decrease in MdPF. Counts were totaled for each region for both an increase in amplitude and a decrease in MdPF.

Table 9. Statistical tests and their variables

Statistical Test	Task	Independent Variables	Dependent Variables
One-way ANOVA	Activities of Daily Living Kinematics	Pre-fatigue * Post-fatigue (0, 1, 3, 7, and 15-minutes post-fatigue)	Torso to global pre-/post- differences
			Thoracohumeral ROM
			Elbow ROM
			Thoracohumeral minimums and maximums
			Elbow minimums and maximums
One-way ANOVA	Activities of Daily Living EMG	Pre-fatigue * Post-fatigue (0, 1, 3, 7, and 15-minutes post-fatigue)	Anterior Deltoid mean EMG
			Middle Deltoid mean EMG
			Posterior Deltoid mean EMG
			Upper Trapezius mean EMG
			Infraspinatus mean EMG
			Latissimus Dorsi mean EMG

4.0 RESULTS

4.1 General Post-Fatigue Responses

All participants completed at least 3 rounds of the fatigue protocol. On average, time to fatigue took 1460 ± 556.2 seconds for participants. In baseline measures, participants reported an RPE of 0.25 ± 0.62 and an RPF of 0.65 ± 0.91 (Figure 9). Immediately following the fatigue protocol, participants reported an RPE of 8.55 ± 1.61 and an RPF of 8.6 ± 0.93. These values decreased for both ratings over time following fatigue, though RPF ratings were slightly higher than RPE ratings for all time points following the fatigue protocol (Table 10).
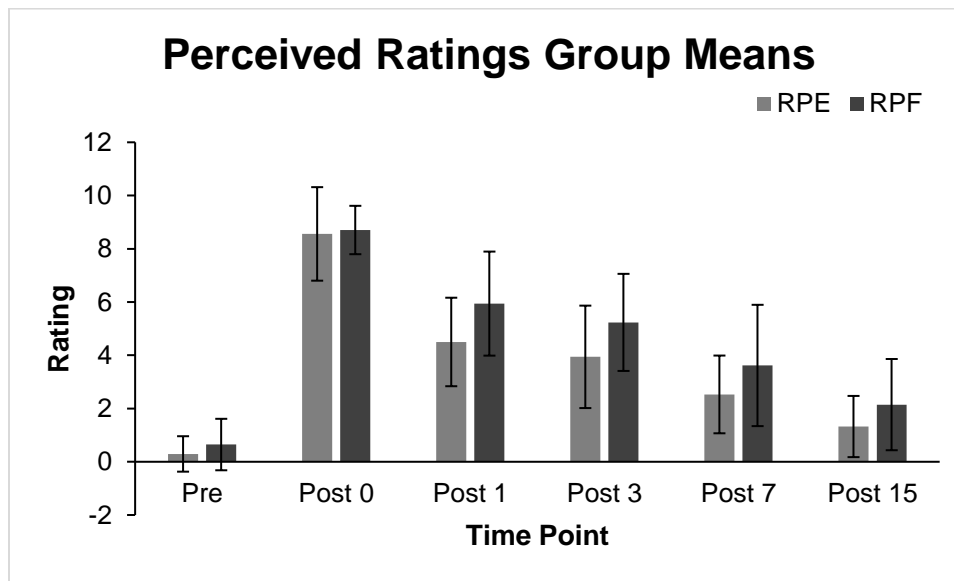

Figure 9. A visual representation of the Pre- vs Post-Fatigue RPE and RPF group means. Lighter gray bars indicate RPE ratings, while darker gray bars indicate RPF ratings. Error bars represent standard deviation.

Table 10: Group RPE and RPF ratings. Mean (SD).

	Pre-Fatigue		Post 0		Post 1		Post 3		Post 7		Post 15	
	RPE	**RPF**	**RPE**	**RPF**	**RPE**	**RPF**	**RPE**	**RPF**	**RPE**	**RPF**	**RPE**	**RPF**
Mean (SD)	0.29 (0.66)	0.64 (0.97)	8.56 (1.75)	8.71 (0.97)	4.50 (1.66)	5.94 (1.95)	3.94 (1.92)	5.23 (1.82)	2.53 (1.46)	3.62 (2.28)	1.32 (1.15)	2.15 (1.71)

A one-way within subjects repeated measures ANOVA assessed fatigue progression and recovery using the internal rotation strength measures pre-fatigue and all time points post-fatigue. One participant's strength values were determined to be statistical outliers for all time points and the data was removed from analysis. There was a main effect of fatigue on internal rotation strength ($F(2.579,38.692.615) = 8.988$; $p = 0.000$) (Figure 10). The 0-, 1-minutes post-fatigue internal rotation MVC values were all significantly different when compared to pre-fatigue ($p = 0.001$, $p = 0.001$), where there was a 15.2% reduction in internal rotation strength immediately following the fatigue protocol. This was followed by a recovery of strength for all time points afterwards (Table 11).
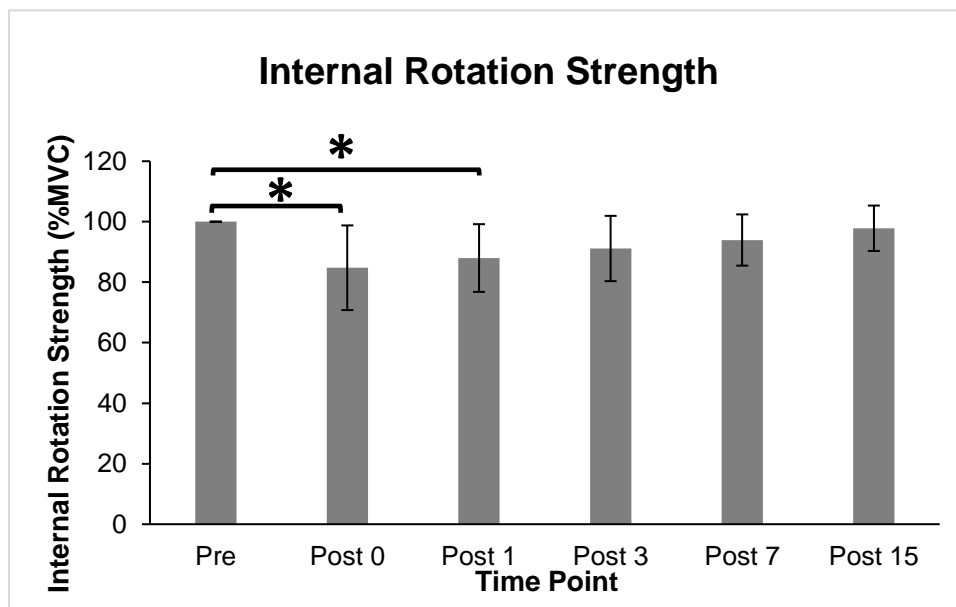

Figure 10. Internal rotation strength measures pre- and post-fatigue showing an initial decrease in strength immediately following the fatigue protocol followed by a recovery close to pre-fatigue values. Error bars represent standard error. * indicates significance at $P < 0.05$.

Table 11: Internal rotation strength and % decrease group means and standard deviations. Shaded values indicate significant differences of $p < 0.01$ when compared to pre-fatigue values. Pre refers to pre-fatigue, while Post 0, 1, 3, 7, and 15 refer to each time point post-fatigue.

	Pre (N)	Post 0 (N)	Post 1 (N)	Post 3 (N)	Post 7 (N)	Post 15 (N)
Mean (SD)	181.4 (47.1)	152.6 (46.4)	157.7 (38.8)	164.0 (44.7)	169.4 (42.1)	175.9 (42.4)
Mean % Decrease from Pre	-	15.2%	12.0%	8.9%	6.0%	2.2%

4.2 Pectoralis Major Fatigue

For the purposes of this thesis, fatigue was defined as an increase in amplitude coupled with an 8% or greater decrease in MPF. Three participants failed to fatigue in any region by this definition and were subsequently removed from further analysis. In total, 9 participants fatigued in the clavicular region, 6 participants fatigued in the sternocostal region, and 9 participants fatigued in the abdominal region (Table 12). Further, there were 2 participants that fatigued in both the sternocostal and abdominal regions, 1 participant that fatigued in both the clavicular and abdominal regions, and 2 participant that fatigued in all three regions. There was also fatigue present in the surrounding shoulder musculature in at least a few participants. Appendix C contains specific fatigue details for surrounding shoulder musculature in individual participants, including total counts.

Table 12. Fatigue presence in the three regions of the pectoralis major during the internal rotation reference contractions. 'X' indicates an MdPF decrease of 8% or greater. Grey shaded boxes indicate an increase in mean EMG amplitude. A grey shaded box with an 'X' indicates an increase in RMS amplitude and a decrease in MdPF, representative of fatigue in the muscle.

Participant	Clavicular Region	Sternocostal Region	Abdominal Region	# of Regions Fatigued
1	X			1
2	X	X	X	3
3		X		1
4	X			1
5			X	1
6	X			1
7	X	X	X	3
8			X	1
9		X	X	2
10	X		X	2
11				0
12		X		1
13				0
14			X	1
15				0
16	X			1
17	X	X	X	3
18	X			1
19		X	X	2
20	X			1
Total Participants Fatigued	**9**	**6**	**9**	**Mean = 1.2**

4.3 Changes in Kinematics

Several joint angle rotation ROMs changed following the fatiguing protocol, though this varied by ADL. General ROM responses for each ADL are described first, followed by specific ROMs. Significant differences for ROM data are reported here, but full data for all ROMs are available in Appendix B.

4.3.1 Kinematics Summary

Joint angle differences for each rotation were calculated for each ADL to discern whether there were any trends in compensation, if at all. During the Curtain ADL, most joint angle ROMs

decreased with respect to their pre-fatigue ROM (Figure 11). Thoracohumeral rotation ROMs all

had the largest changes and decreased from pre-fatigue to post-fatigue and by 15-minutes post-

fatigue, although each rotation trended back toward pre-fatigue ROMs, the ROM values were

still lower than pre-fatigue. At the elbow, flexion ROM did not initially change by much, but

after 0-minutes post-fatigue, continued to decrease through 15-minutes post-fatigue. On the other

hand, elbow pronation ROM did not change very much from pre-fatigue to post-fatigue,

increasing and decreasing from pre-fatigue by about 1-3 degrees. Thorax rotation ROMs

experienced small changes with regards to pre-fatigue, as thorax extension decreased very

slightly during post-fatigue measures. Right lateral bending and axial rotation of the thorax

increased following the fatigue protocol and then continued to decrease, settling back around
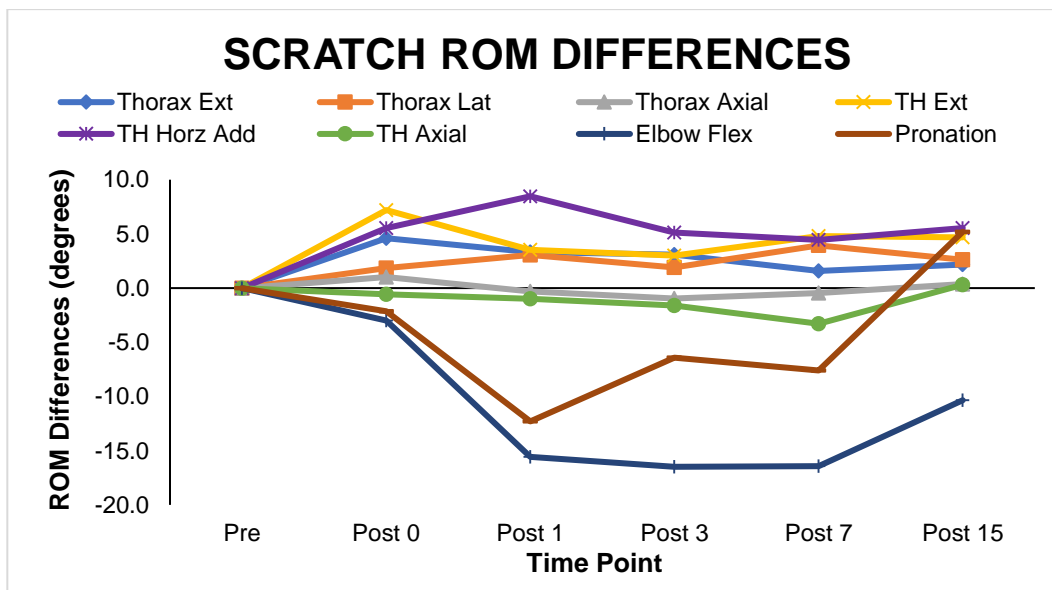
pre-fatigue ROMs.
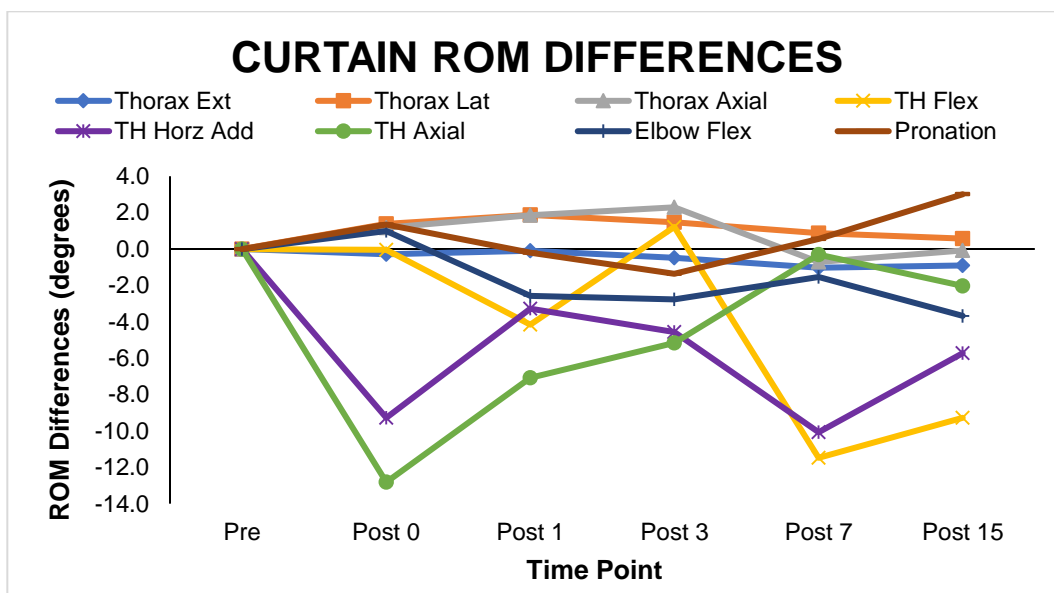
Figure 11. Differences in ROM for the Curtain ADL from pre- to post-fatigue for all joint angle
rotations. Negative values indicate a decrease in ROM. Thorax ext, thorax lat, and thorax axial
refer to the extension, right lateral bending, and axial rotation of the thorax. TH flex, TH horz ad,
and TH axial refer to the flexion, horizontal adduction, and axial rotation of the humerus with
respect to the thorax. Elbow flex and pronation refer to flexion and pronation at the elbow.

During the Scratch ADL, most joint angle ROMs increased with respect to their pre-fatigue ROM (Figure 12). The largest differences in ROM occurred at the elbow, with elbow flexion and pronation decreasing pre-fatigue to post-fatigue, however, after 1-minute post-fatigue, these differences in ROM trended back toward pre-fatigue values. Thoracohumeral rotation ROMs increased from pre-fatigue, although thoracohumeral axial rotation ROMs remained very similar to thoracohumeral axial rotation pre-fatigue. The ROMs of thoracohumeral flexion decreased over the course of post-fatigue measures, while thoracohumeral horizontal adduction increased. Finally, thorax rotation ROMs all increased post-fatigue, though all changes in ROM remained lower than 5 degrees.
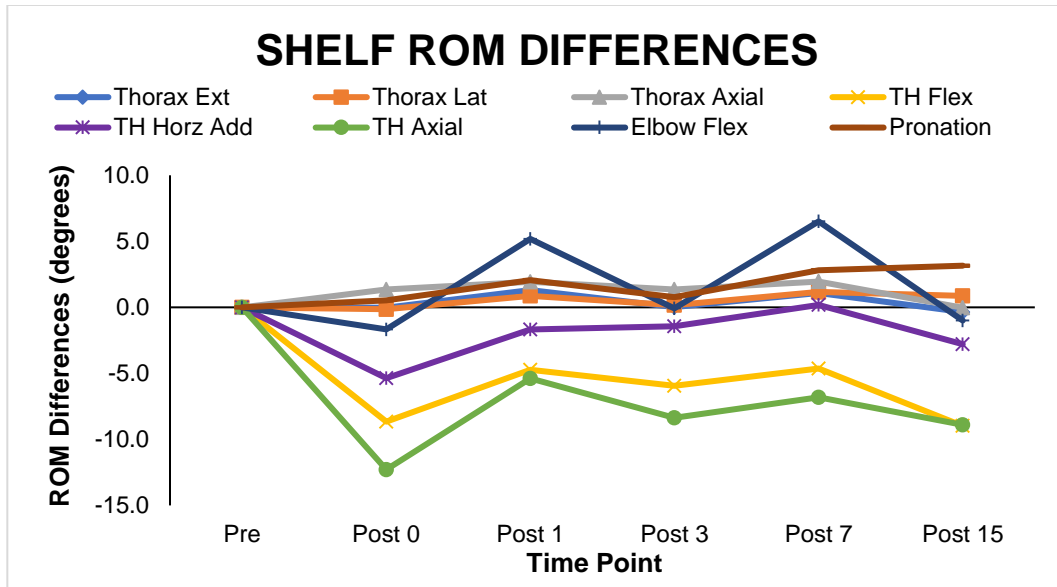

Figure 12. Differences in ROM for the Scratch ADL from pre- to post-fatigue for all joint angle rotations. Negative values indicate a decrease in ROM. Thorax ext, thorax lat, and thorax axial refer to the extension, right lateral bending, and axial rotation of the thorax. TH ext, TH horz ad, and TH axial refer to the extension, horizontal adduction, and axial rotation of the humerus with respect to the thorax. Elbow flex and pronation refer to flexion and pronation at the elbow.

During the Shelf ADL, thoracohumeral rotation ROMs decreased with respect to pre-fatigue, while elbow rotation ROMs increased (Figure 13). The largest differences with respect to pre-fatigue ROMs occurred at each of the thoracohumeral rotation ROMs. All three rotations

decreased in ROM post-fatigue and then trended back toward pre-fatigue ROMs, although all ROMs remained smaller than pre-fatigue ROMs at 15-minutes post-fatigue. Elbow pronation ROMs increased post-fatigue, although elbow flexion underwent an initial decrease in ROM immediately following the fatigue protocol. At 15-minutes post-fatigue, elbow flexion ROM decreased back toward pre-fatigue ROM, however, elbow pronation remained elevated. Thorax rotation ROMs all increased very slightly following the fatigue protocol, however, they remained very close to pre-fatigue ROMs.

Figure 13. Differences in ROM for the Shelf ADL from pre- to post-fatigue for all joint angle rotations. Negative values indicate a decrease in ROM. Thorax ext, thorax lat, and thorax axial refer to the extension, right lateral bending, and axial rotation of the thorax. TH flex, TH horz ad, and TH axial refer to the flexion, horizontal adduction, and axial rotation of the humerus with respect to the thorax. Elbow flex and pronation refer to flexion and pronation at the elbow.

4.3.2 Curtain ADL

4.3.2.1 Thorax Lateral Bending

There was a main effect of fatigue state on thorax lateral bending differences in ROM during the Curtain ADL ($F_{(5, 55, 12)} = 6.677$, $p = 0.0009$ (Figure 14). There was an increase in

thorax right lateral bending differences from baseline to immediately post-fatigue. Following 0-minutes post-fatigue, there was a continued decrease in right lateral bending differences. By 15-minutes post-fatigue, the lateral bending differences decrease past baseline differences. This resulted in significant decreases in right lateral bending ROM from 0-minutes post-fatigue to 15-minutes post-fatigue (2.1° decrease; $p = 0.019$).
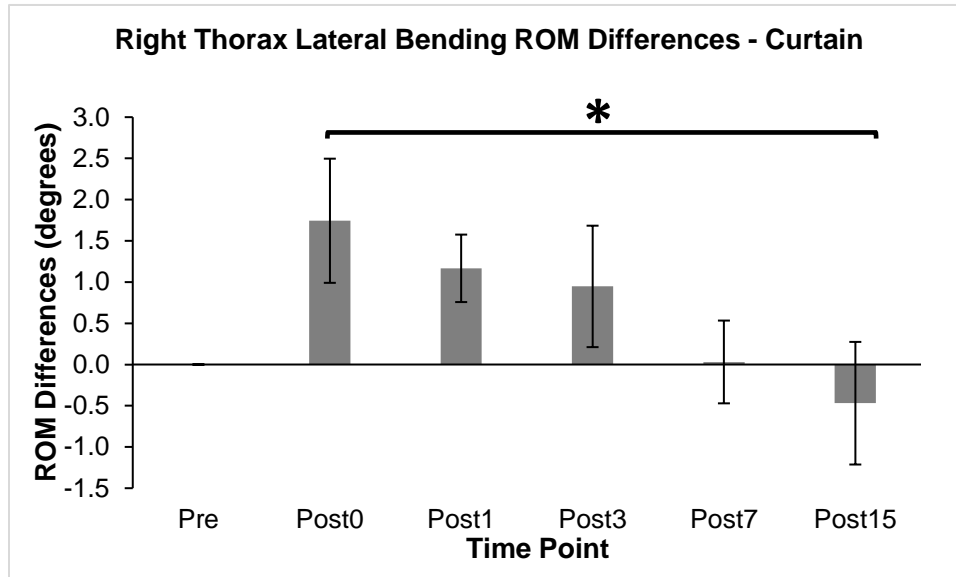

Figure 14. Right lateral bending differences in thorax ROM for the Curtain ADL pre- and post-fatigue. Positive values indicate an increase from pre-fatigue measures. Error bars indicate standard error. * indicates significance at $P < 0.05$.

4.3.2.2 Thoracohumeral Plane of Elevation

There was a main effect of fatigue state on thoracohumeral plane of elevation ROM during the Curtain ADL ($F(5, 65, 14) = 2.393$, $p = 0.047$) (Figure 15). From pre-fatigue to immediately post-fatigue, there was a 6° decrease in thoracohumeral horizontal adduction, though not significant ($p = 0.058$). Overall, the trend from pre-fatigue to post-fatigue was a decrease in thoracohumeral horizontal adduction, however, the largest decreases occurred between pre-fatigue and 7-minutes post-fatigue (11.2°; $p = 0.003$).
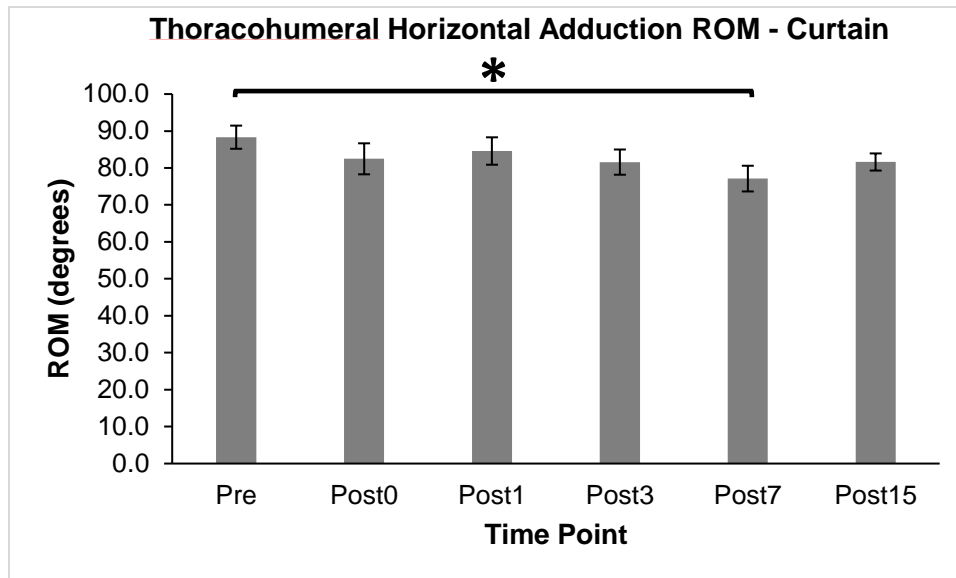
Figure 15. Thoracohumeral plane of elevation ROM for the Curtain ADL pre- and post-fatigue. Error bars indicate standard error. * indicates significance at $P < 0.05$.

4.3.2.3 Shifts in Joint Angle Minimums and Maximums

After investigating the effects of fatigue on joint angle minimums and maximums, there were no differences in joint angle minimums or maximums pre-fatigue to post-fatigue for the Curtain ADL.

4.3.3 Scratch ADL

4.3.3.1 Thorax Extension

There was a main effect of fatigue state on thorax extension differences ROM during the Scratch ADL (F(5, 70, 175= 3.363, $p = 0.009$) (Figure 16). There was an increase in thorax extension differences in ROM immediately following the fatigue protocol (2.9° increase; $p = 0.003$). The general trend after 0-minutes post-fatigue was a continued increase in ROM differences through 1- and 3-minutes post-fatigue (3° increase; $p = 0.003$; 3.2° increase; $p = 0.014$). Through the thorax extension ROM differences began to decrease at 7-minutes post-fatigue, the differences were still significant when compared to baseline values (1.5° increase; p

60

= 0.025). At 15-minutes post-fatigue, thorax extension differences in ROM increased again, when compared to baseline values (2.4° increase; $p = 0.003$).
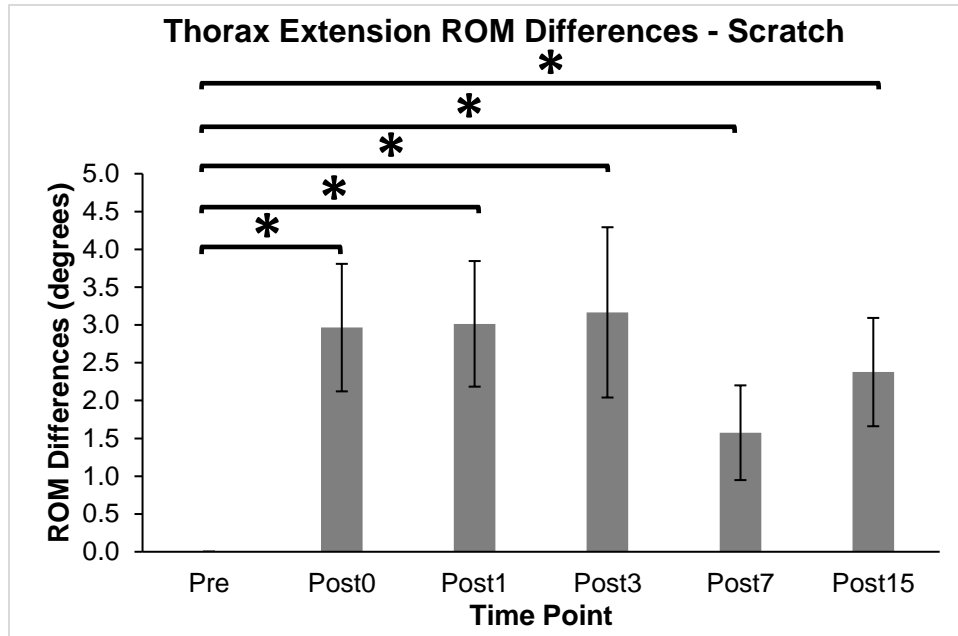

Figure 16. Thorax extension differences in ROM for the Scratch ADL pre- and post-fatigue. Positive values indicate an increase from pre-fatigue measures. Error bars indicate standard error. * indicates significance at $P < 0.05$.

4.3.3.2 Thorax Lateral Bending

There was a main effect of fatigue state on thorax lateral bending differences in ROM during the Scratch ADL ($F(5, 70, 15) = 4.351$, $p = 0.023$) (Figure 17). There was an increase in right thorax lateral bending differences from baseline to all time points except 3-minutes post-fatigue. Pre-fatigue to 1-minute post-fatigue, there was a 2.6 degree increase in lateral bending differences ($p = 0.005$). Pre-fatigue to 3-minutes post-fatigue, there was a 1.5 degree increase in lateral bending differences, though this was not significant ($p = 0.081$). The largest increase in lateral bending differences from pre-fatigue to post-fatigue occurred at 7-minutes post-fatigue (3.4° increase; $p = 0.002$). Finally, from pre-fatigue to 15-minutes post-fatigue, there was a 2.2 degree increase in lateral bending differences ($p = 0.008$). Additionally, there was also a

61

significant increase from 0-minutes post-fatigue to 7-minutes post-fatigue (2.2° increase; $p = 0.032$).
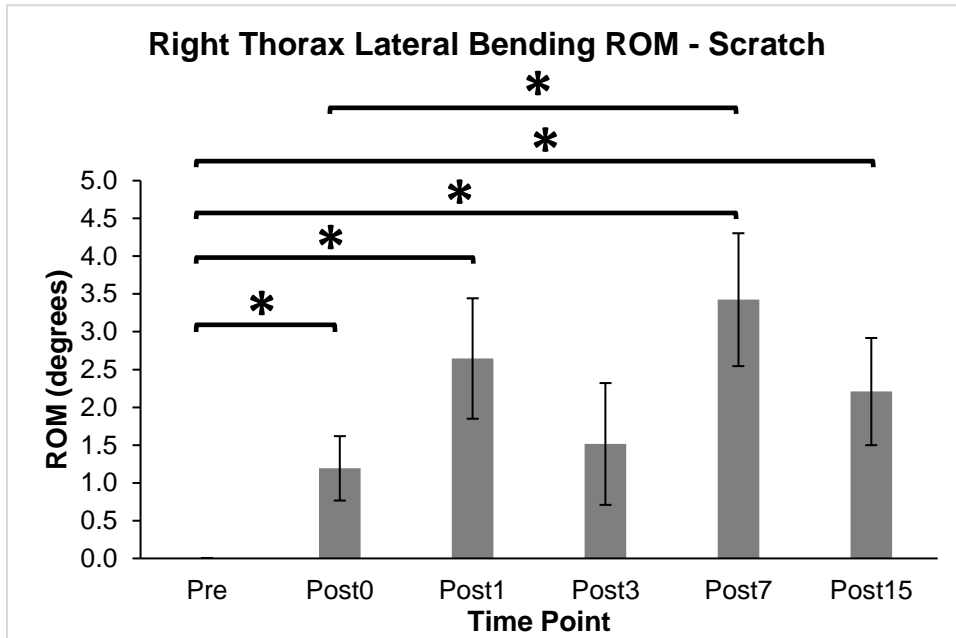

Figure 17. Right lateral bending differences in thorax ROM for the Scratch ADL pre- and post-fatigue. Positive values indicate an increase from pre-fatigue measures. Error bars indicate standard error. * indicates significance at $P < 0.05$.

4.3.3.3 Thoracohumeral Plane of Elevation

There was a main effect of fatigue state on thoracohumeral plane of elevation ROM during the Scratch ADL ($F(5, 70, 15) = 3.594$, $p = 0.030$) (Figure 18). There was an increase in horizontal adduction ROM from pre-fatigue to 1-minute post-fatigue (8.6° increase; $p = 0.006$). While all time points post-fatigue resulted in greater horizontal adduction compared to pre-fatigue, the differences between pre-fatigue and 0-minutes, 3-minutes, 7-minutes, and 15-minutes post-fatigue resulted in the lowest magnitude of differences.
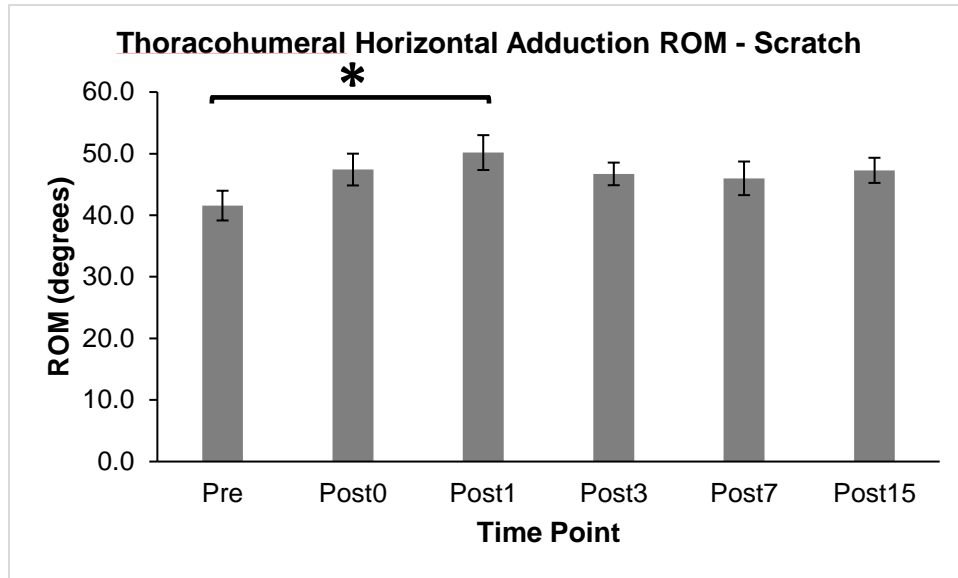
Figure 18. Thoracohumeral plane of elevation ROM for the Scratch ADL pre- and post-fatigue. Error bars indicate standard error. * indicates significance at $P < 0.05$.

4.3.3.4 Shift in Joint Angle Minimums and Maximums

After investigating the effects of fatigue on joint angle minimums and maximums, there was a main effect of fatigue state on maximum thorax extension angles during the Scratch ADL ($F(5, 65, 14) = 9.598$, $p = 0.000$) (Figure 19). There was an increase in maximum thorax extension from pre-fatigue to all time points post-fatigue, except 7-minutes post-fatigue. The largest differences occurred between pre-fatigue and 0- (4.1° increase; $p = 0.000$), 1- (3.4° increase; $p = 0.003$), and 3-minutes post-fatigue (2.7° increase; $p = 0.003$). From pre-fatigue to 15-minutes post-fatigue, there was an increase in thorax extension of 2.6 degrees ($p = 0.001$). Additionally, there was also a significant decrease in thorax extension angle from 0-minutes post-fatigue to 7-minutes post-fatigue (2.2° decrease; $p = 0.001$)
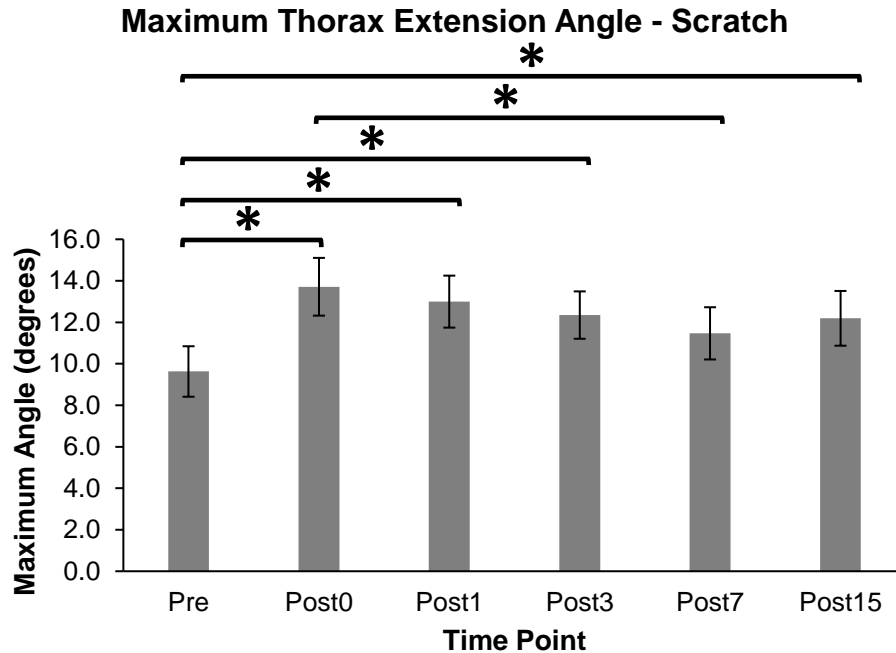
63

Figure 19. Maximum thorax extension angles for the Scratch ADL pre- and post-fatigue. Error bars indicate standard error. * indicates significance at $P < 0.05$.

4.3.4 Shelf ADL

4.3.4.1 Thoracohumeral Axial Rotation

There was a main effect of fatigue state on thoracohumeral axial rotation ROM during the Shelf ADL ($F(5, 80, 17) = 4.093$, $p = 0.016$) (Figure 20). There was a decrease in internal rotation ROM from pre-fatigue to immediately post-fatigue ($12.3°$; $p = 0.009$). The trend from pre-fatigue to post-fatigue was a decrease in internal rotation across all time points, however, the largest decrease outside of the one that occurred at 0-minutes post-fatigue, the decrease from baseline to 3-minutes post-fatigue was the next largest ($8.4°$; $p = 0.043$).
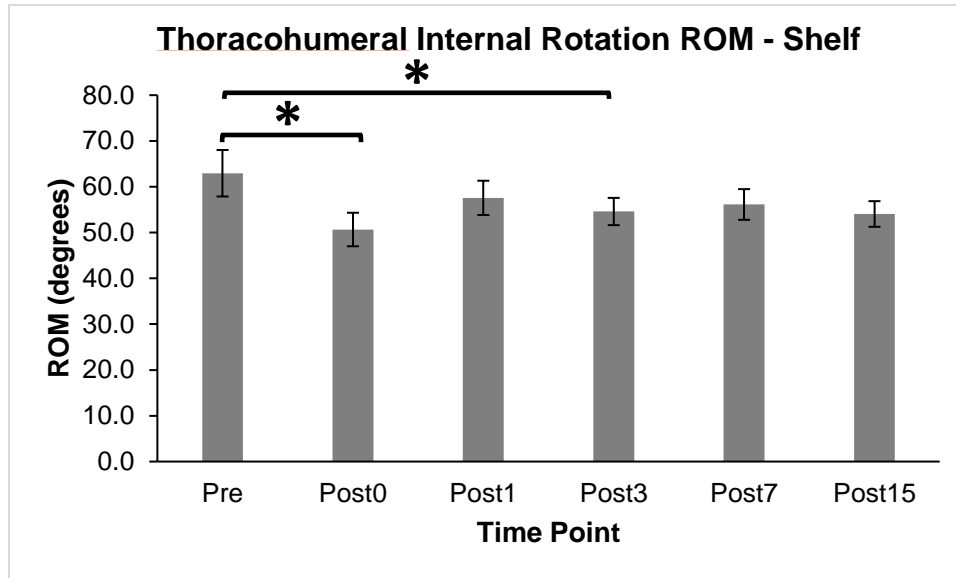
Figure 20. Thoracohumeral internal rotation ROM for the Curtain ADL pre- and post-fatigue. Error bars indicate standard error. * indicates significance at $P < 0.05$.

4.3.4.5 Shift in Joint Angle Minimums and Maximums

After investigating the effects of fatigue on joint angle minimums and maximums, there were no differences in joint angle minimums or maximums pre-fatigue to post-fatigue for the Shelf ADL.

4.4 Changes in Muscular Activity

Several muscles were activated differently following the fatiguing protocol, though this varied by ADL. General muscular activation patterns for each ADL are described first, followed by specific muscle activations. Significant differences for mean and median RMS data are reported here, but full data for all muscles are available in Appendix C.

4.4.1 Muscular Activity Summary

During the Curtain ADL, the region of the pectoralis major most involved in the movement is the clavicular region of the pectoralis major (Figures 21), increasing in contribution over post-fatigue time points past pre-fatigue contributions. The muscle that appears to

contribute the most to this movement, however, appears to be the anterior deltoid, increasing in

contribution 0-minutes post-fatigue, followed by a decrease in contribution through 7-minutes

post-fatigue, and a final increase in contribution at 15-minutes post-fatigue.
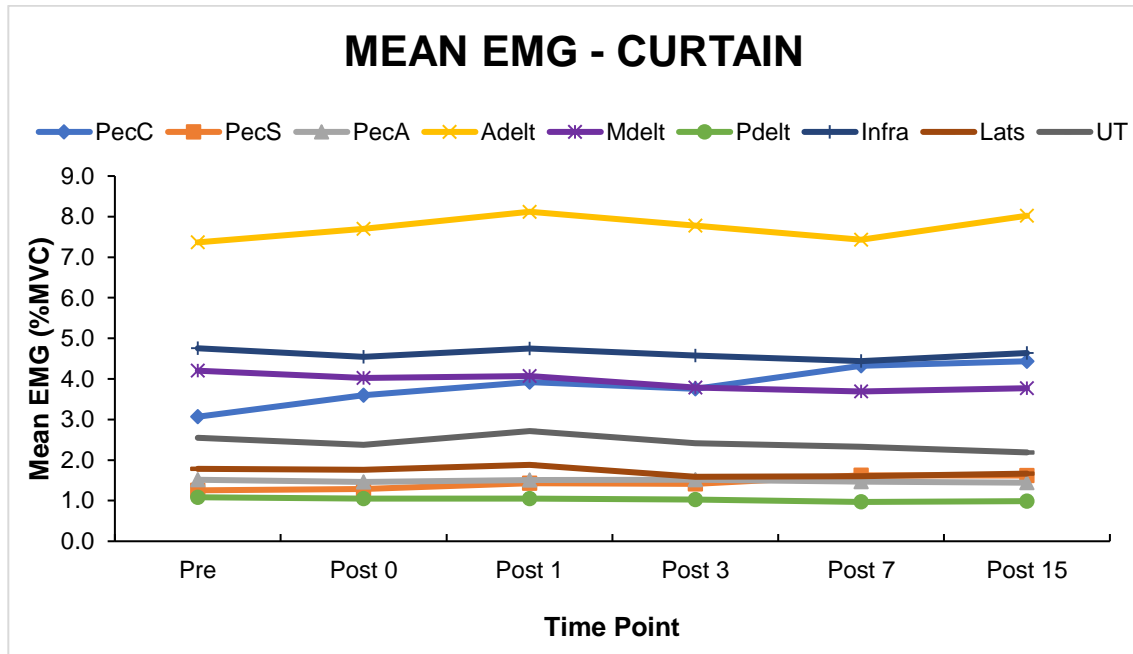

Figure 21. Mean EMG for the Curtain ADL pre- and post-fatigue for all muscles collected.
PecC, PecS, and PecA refer to the 3 regions of the pectoralis major. Adelt, Mdelt, and Pdelt refer
to the anterior, middle, and posterior deltoids. Infra, Lats, and UT refer to infraspinatus,
latissimus dorsi, and upper trapezius, respectively.

During the Scratch ADL, the region of the pectoralis major that is most involved is the

abdominal region of the pectoralis major (Figure 22). Evaluating the abdominal pectoralis major

using mean EMG, there is an initial increase in contribution and then a decrease in contribution

following 3-minutes post-fatigue. The muscle that appears to contribute the most to this

movement appears to be the latissimus dorsi, increasing in contribution from pre-fatigue to post-

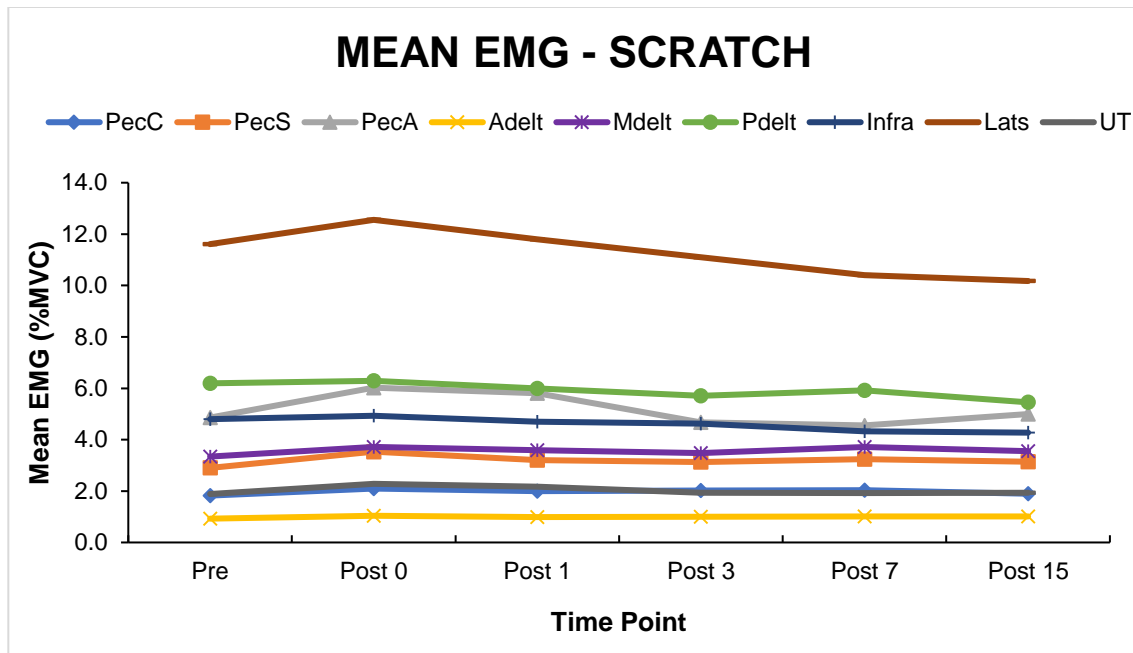fatigue, followed by a decreasing trend over time.

Figure 22. Mean EMG for the Scratch ADL pre- and post-fatigue for all muscles collected. PecC, PecS, and PecA refer to the 3 regions of the pectoralis major. Adelt, Mdelt, and Pdelt refer to the anterior, middle, and posterior deltoids. Infra, Lats, and UT refer to infraspinatus, latissimus dorsi, and upper trapezius, respectively.

During the Shelf ADL, the region of the pectoralis major most involved in the movement is the abdominal pectoralis major (Figures 23), although all regions of the pectoralis major were the least involved in this movement, maintaining about the same activation level across all time points. Mean EMG data show that anterior deltoid, middle deltoid, infraspinatus, and upper trapezius are contributing the most to this movement. These muscles increased in their contributions from pre-fatigue to 0-minutes post-fatigue, followed by a decrease in contribution from 0-minutes to 1-minute post-fatigue. The anterior deltoid continued to decrease through 3-minutes post-fatigue, while the infraspinatus remained about the same through 15-minutes post-fatigue. The middle deltoid and upper trapezius both decreased following 1-minute post-fatigue, though at 7-minutes post-fatigue, the middle deltoid increased, and the upper trapezius decreased. The anterior and middle deltoids both decreased in contribution from 3-minutes to 7-minutes post-fatigue and then increased from 7-minutes to 15-minutes post-fatigue.
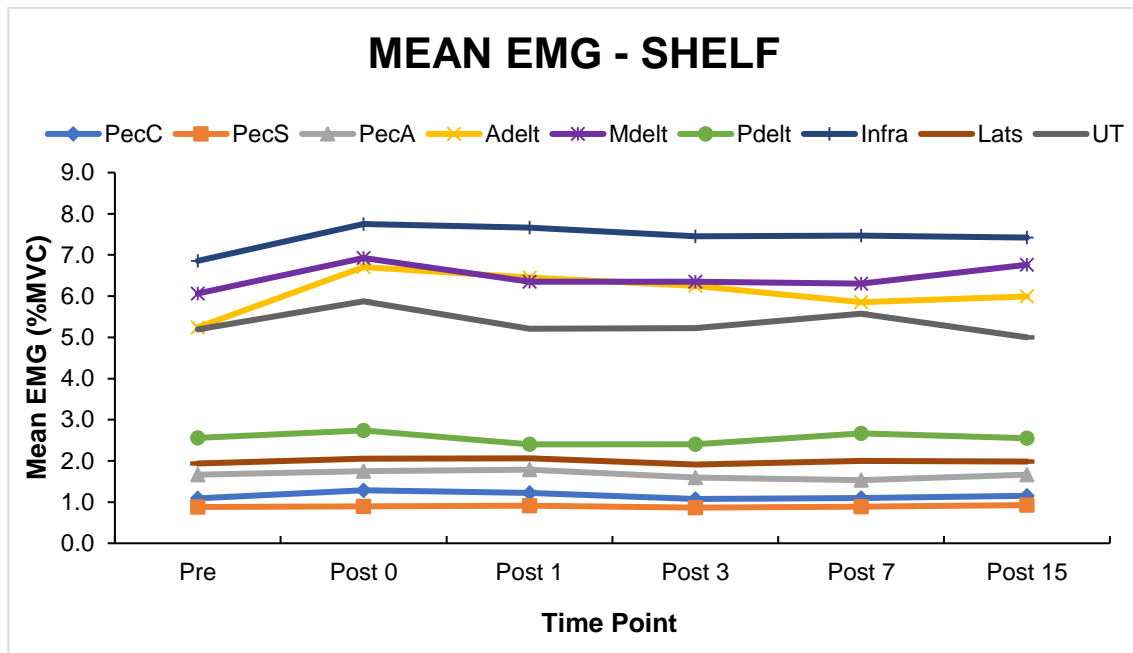
Figure 23. Mean EMG for the Shelf ADL pre- and post-fatigue for all muscles collected. PecC, PecS, and PecA refer to the 3 regions of the pectoralis major. Adelt, Mdelt, and Pdelt refer to the anterior, middle, and posterior deltoids. Infra, Lats, and UT refer to infraspinatus, latissimus dorsi, and upper trapezius, respectively.

4.4.2 Curtain ADL

After investigating the effects of fatigue on surrounding shoulder musculature activity, there were no differences in mean EMG pre-fatigue to post-fatigue for the Curtain ADL.

4.4.3 Scratch ADL

After investigating the effects of fatigue on surrounding shoulder musculature activity, there were no differences in mean EMG pre-fatigue to post-fatigue for the Scratch ADL.

4.4.4 Shelf ADL

4.4.4.1 Anterior Deltoid

There was a main effect of fatigue state on anterior deltoid mean EMG activation during the Shelf ADL ($F(5,80, 14) = 4.514$, $p = 0.001$) (Figure 24). The largest differences in mean EMG pre-fatigue to post-fatigue occurred from pre-fatigue to immediately post-fatigue with an increase in mean EMG amplitude of 1.5 %MVC ($p = 0.001$). There were additional increases in mean EMG from pre-fatigue to 1-minute post-fatigue (1.2% MVC; $p = 0.003$) and pre-fatigue to 3-minutes post-fatigue (1% MVC; $p = 0.017$).
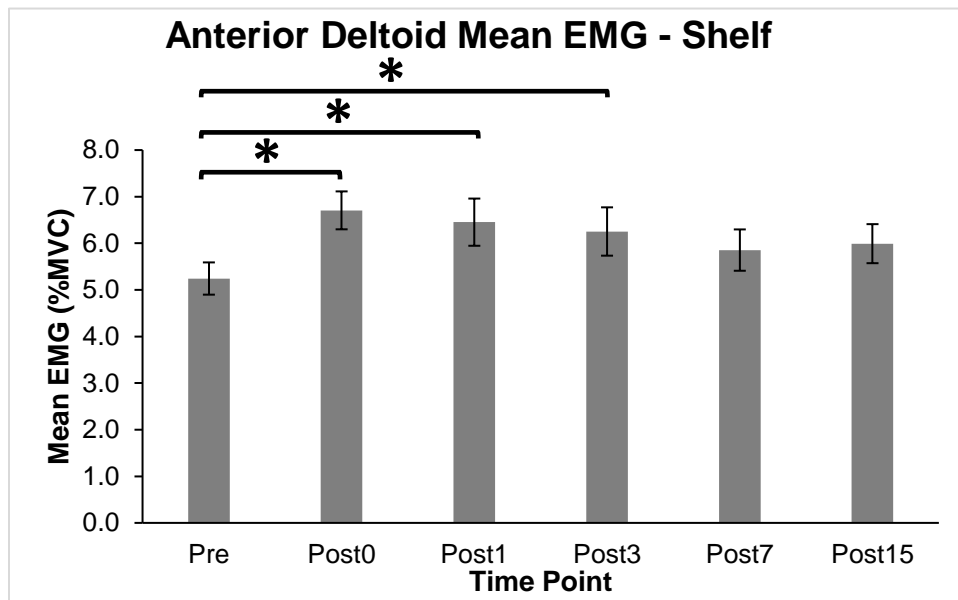
Figure 24. Anterior deltoid mean EMG amplitude for the Shelf ADL pre- and post-fatigue. Error bars indicate standard error. * indicates significance at $P < 0.05$.

5.0 Discussion

This thesis explored how fatigue state of the pectoralis major and its respective regions affect upper extremity movement patterns and surrounding shoulder musculature activation patterns. Comparisons were made pre-fatigue to post-fatigue time points. The results of this thesis indicate there may be minor compensations in muscular activity and kinematics associated with fatigue of the pectoralis major. The lack of many changes between pre- and post-fatigue surrounding shoulder muscle activity and upper extremity kinematics encourages the further study of compensatory mechanisms of a pectoralis major knock-out. This study also showed that future investigations of the pectoralis major may benefit from a focus on the abdominal region of the pectoralis major and the role it plays in shoulder and humeral movement, as well as shoulder muscle activity.

5.1 Key Findings

The objective of this study was to question how pectoralis major fatigue influences muscular activity and kinematics during activities of daily living as well as the presence of differential fatigue between regions of the pectoralis major. The main findings were: (1) The fatigue protocol produced differential fatigue across the regions of the pectoralis major, particularly in the abdominal region. (2) The fatigue protocol induced changes in range of motion at the thorax and humerus during post-fatigue measures for the three activities of daily living; and (3) The fatigue protocol induced changes in muscular activity during post-fatigue measures for the three activities of daily living, though small. These results suggest that fatiguing of the pectoralis major, particularly the clavicular and abdominal regions, may cause a change in surrounding muscular activity and upper extremity movement patterns.

70

5.2 Differential Fatigue

Hypothesis 3 stated the fatigue protocol would induce fatigue in the clavicular and sternocostal regions of the pectoralis major. This hypothesis is partially accepted, as fatigue occurred in both the clavicular and sternocostal regions of the pectoralis major, however, fatigue was most prevalent in the clavicular and abdominal regions of the muscle. This is compelling, as horizontal adduction and internal rotation tasks are actions commonly attributed to the clavicular and sternocostal regions of the muscle, but not of the abdominal region.

A number of factors may have influenced the differential fatigue recorded. First, fatigue in the clavicular and abdominal regions may not have produced any compensations in the ADLs studied, despite their selection due to their likelihood of demanding pectoralis contributions. The Curtain ADL required horizontal adduction, the Scratch ADL involved extension and horizontal adduction, and the Shelf ADL incorporated humeral flexion, all of which are mechanically favorable for both the clavicular and sternocostal regions. It is possible that due to the prevalence of fatigue in the clavicular and abdominal regions, that the ADLs in this thesis did not elicit any compensations because the ADLs did not involve some actions known to the abdominal region. Other actions of the abdominal pectoralis major outside of horizontal adduction and extension include humeral adduction (Brown et al., 2007; Paton & Brown, 1994). It is important to note that this thesis did not examine any overhead movements, which as stated previously, may have been a contributing factor in the lack of compensation from pre- to post-fatigue.

The definition of fatigue used for the purposes of this thesis was an increase in EMG amplitude coupled with a decrease in its frequency spectrum (Hagberg, 1981; Moritani et al., 1986). While both MdPF and MPF can be used as indicators of fatigue on their own, the

evaluation of fatigue using both amplitude and frequency measures is a stronger indication of fatigue.

5.3 Kinematics

Hypothesis 2a stated the fatigue protocol would cause an increase in trunk extension ROM and a decrease in thoracohumeral plane of elevation ROM during the Scratch ADL. This hypothesis was partially confirmed. There was an increase in thorax extension ROM post-fatigue with increases in extension continuing through 3-minutes post-fatigue. In addition to thorax extension, there was also an increase in right lateral bending ROM of the thorax following the fatigue protocol, with continued increases even 15-minutes post-fatigue. The hypothesis that there would be a decrease in thoracohumeral elevation ROM was not confirmed via statistical significance, however an increase in thoracohumeral extension was observed (~8°). Instead, horizontal adduction increased through 1-minute post-fatigue. Additionally, there was a decrease in elbow pronation ROM following the fatigue protocol, however the ROM was recovered, resulting in a greater ROM at 15-minutes. Looking at joint angle differences compared to pre-fatigue, the largest differences occurred at the elbow in flexion and pronation (~10-15° decrease) and in thoracohumeral flexion and horizontal adduction (~10° increase), though only the increase in thoracohumeral horizontal adduction was significant.

Hypothesis 2b stated the fatigue protocol would cause a decrease in thoracohumeral elevation ROM during the Curtain ADL. This hypothesis was partially confirmed, as there was a continued decrease in thoracohumeral flexion ROM following the fatigue protocol, although the magnitudes of the changes were not significant (~8° difference from pre-fatigue at 15-minutes post-fatigue). There was also an initial increase in right lateral bending ROM of the thorax, followed by a continued decrease in ROM through 15-mintues post-fatigue. The largest joint

72

angle differences in ROM compared to pre-fatigue joint angles were thoracohumeral flexion, horizontal adduction, and internal rotation, all decreasing in relation to pre-fatigue ROM (~8-12° decrease), however only the changes in horizontal adduction were significant (Figure 11).

Hypothesis 2c stated the fatigue protocol would cause an increase in trunk flexion ROM and a decrease in thoracohumeral elevation ROM during the Shelf ADL. This hypothesis was refuted. Instead of trunk flexion, there was an increase in right lateral bending ROM, though these increases were not significant. Instead of changes in thoracohumeral elevation ROM, there were decreases in both thoracohumeral horizontal adduction and internal rotation following the fatigue protocol, however only the decrease in internal rotation was significant. In addition to thorax and thoracohumeral changes, there was a continued increase in elbow pronation following the fatigue protocol. The largest joint angle differences in ROM occurred during elbow flexion (~5-7° increase) and thoracohumeral horizontal adduction and internal rotation (~5-12° decrease) (Figure 13).

After evaluating the maximum and minimum values of joint rotation for each ADL, the only changes occurred at the maximums of thorax extension during the Scratch ADL, which increased following the fatigue protocol. Interestingly, the minimums for this joint rotation did not increase with the maximum. Comparing the maximums to their respective joint angle ROMs (Figure 16 compared to Figures 19), they follow a similar pattern, although the joint angle maximums contained more significant interactions than the ROMs. This indicated high variability in the joint minimums, which is why there were no significant interactions.

The changes in joint angle rotation detected corresponded with the observed changes in muscular behavior, as a result of pectoralis major fatigue. Some of these alterations in movement during the ADLs are partially explained by the altered muscle activity. During the Scratch ADL,

there was an increase in anterior deltoid activity, though not significant, coupled with an increase in horizontal adduction ROM, although most of the horizontal adduction occurred behind the back. The increase in anterior deltoid activity could have been due to the stretching, as stretching of passive tissues can cause an increase in EMG of surrounding muscles (Solomonow, 2012). During the Shelf ADL, there was an increase in pronation and a decrease in internal rotation, coupled with an increase in infraspinatus activity. A decrease in internal rotation would indicate an increase in external rotation, which is an action of the infraspinatus. The increase in posterior deltoid activity coupled with a decrease in horizontal adduction indicated that there were changes in the second half of the movement, namely bringing the bottle back to the starting position. A decrease in horizontal adduction indicates an increase in horizontal abduction, which is an action of the posterior deltoid. These changes in both muscular activity and kinematics are supported by research in the lower extremity, as there has been abnormal hamstring activity coupled with a decrease in knee flexion following anterior cruciate ligament rupture treatment (Boerboom et al., 2001).

5.4 Muscular Activity

Hypothesis 1a stated the fatigue protocol would induce increases in muscular activity in the posterior deltoid, latissimus dorsi, and upper trapezius during the Scratch ADL. This was partially accepted, as there was an initial increase in latissimus dorsi activity, followed by a decrease past pre-fatigue activity for mean EMG. The same trend was observed in the posterior deltoid for mean EMG. However, changes seen in the posterior deltoid and latissimus dorsi were not significant. The involvement of the posterior deltoid and latissimus dorsi is logical, as the movement requires both extension and internal rotation, which are classic actions of each muscle, respectively (Ekholm et al., 1978; Gray, 1918).

74

Hypothesis 1b stated the fatigue protocol would induce increases in muscular activity of the anterior, middle, and posterior deltoids during the Curtain ADL. This hypothesis was not accepted. Unexpected changes occurred in sternocostal pectoralis major activity, as it continued to increase even 15-minutes post-fatigue, though not significant. While there was an expected increase in sternocostal pectoralis major activity following the fatigue protocol, the largest increase in activity existed from pre-fatigue to 15-minutes post-fatigue, indicating the muscle continued to be recruited even when the measurable presence of fatigue was dissipating. Additionally, the initial increase and subsequent decrease in upper trapezius activity was surprising, though this was not significant. This indicates participants may have been shrugging while completing the task immediately post-fatigue, but after about 3-minutes post-fatigue they began to recover, and this behavior did not continue.

Hypothesis 1c stated the fatigue protocol would induce increases in muscular activity in the anterior, middle, and upper trapezius during the Shelf ADL. This hypothesis is partially confirmed, as the anterior deltoid increased in mean EMG activity following the fatigue protocol. This is explained by the high amount of humeral flexion involved in raising the arm to the high shelf, especially with a weight.

Certain muscles may be compensating for pectoralis major fatigue, although there were sparse confirmatory significant results. Examining overall muscle contribution to each ADL suggests that the pectoralis major was not the prime mover in the Curtain, Scratch, and Shelf ADLs (Figures 21-23) which involve horizontal adduction, extension, internal rotation, and flexion. This may relate to the difficulty of achieving targeted muscle fatigue, as fatigue also manifested in surrounding musculature (Noguchi et al., 2013) (Appendix A). The effects of fatigue in surrounding musculature may be an issue in these results, as fatigue may have

continued to develop following the fatigue protocol (Tse et al., 2016). Muscles other than those collected may have also contributed to these movements and could have been influenced by pectoralis major fatigue. Glenohumeral muscles, such as suprapinatus, subscapularis, and teres major could have compensated in the presence of pectoralis major fatigue, as these muscles can perform some of the same movements as the pectoralis major (Gray, 1918; Rockwood Jr., 2009).

These ADLs were selected based on their clinical relevance to breast cancer survivors, as the pectoralis major is considered the most affected muscle as a result of treatment methods. Though not significant, there were changes in muscle activation across the three ADLs (Appendix E), which suggests small compensations, though not substantial. The lack of compensations identified (Figures 27-32) likely establish that a fatigue knock-out does not create the same level of change as a damaged muscle or a torn tendon (McCully et al., 2006) or that the ADLs selected were low-demand movements and resulted in low-level muscle activations, making identification of fatigue compensations problematic (0-10% MVC). However, this aligns with previous ADL research (Hagstrom, Shorter, & Marshall, 2017), which shows that the difference in EMG amplitude between affected and unaffected sides in breast cancer survivors is small (2-4% MVC). It is also possible that the lack of changes seen in other muscles as a result of pectoralis major fatigue comes from fatigue in the surrounding shoulder musculature in addition to the pectoralis major (Appendix A). Brookham et al. (2018b) found that there were greater overall activations of surrounding shoulder musculature in concordance with sternocostal pectoralis major dysfunction in breast cancer survivors, which led to more effort and faster fatigue in surrounding shoulder musculature. There may be some conceptual cross-over of this behavior in a fatigue-induced pectoralis dysfunction model as implemented in this thesis.

5.5 Implications

This thesis expands knowledge regarding the pectoralis major muscle and establishes a foundation for future research involving the muscle. The key findings suggest that pectoralis major's regions fatigue differently, and this fatigue modestly influences shoulder muscle activation patterns and kinematics. The presence of differential fatigue in the pectoralis major suggests further exploration could be informative, especially in the abdominal region. A reliable and valid MVC posture must be quantified for this region of the muscle, and further investigation of the actions of the abdominal region throughout postural ranges in order to evaluate how it contributes to humeral movement, especially if it fatigues as easily as observed.

This study showed that while fatigue was present in the pectoralis major, minimal changes accompanied the fatigue, suggesting a higher demanding movement or task may need to be incorporated. Thus, targeted muscle fatigue may not be powerful enough to impact task performance, as much as a nerve block or an injury would (McCully et al., 2006). Though the changes following fatigue are not as drastic as those reported following an Achilles tendon rupture (Boerboom et al., 2001; Suydam, Buchanan, Manal, & Gravare, 2015) or an ACL tear, differences existed. Further, while the ADLs in this thesis are clinically relevant to previous breast cancer research (Brookham et al., 2018b, 2018a; Maciukiewicz, 2017), the outcomes of thesis revealed the pectoralis major may not contribute to these movements as once was thought. As outlined in Suydam et al. (2013), is important to understand the connection between biomechanical changes with functional limitation, as it will guide interventions and help to find the root causes of the issues.

5.6 Limitations and Future Directions

5.6.1 Surface EMG

Limitations regarding surface EMG need to be taken into account when interpreting the results. First, the signals obtained from all muscles are susceptible to noise. Care was taken to minimize cable artifact by taping them out of the way and to minimize the sliding of electrodes over the muscle by securing the electrodes with tape. However, due to the nature of the ADL tasks (especially the Scratch task), there may have been cable sway. Cross talk and heart rate removal in the pectoralis major regions was also problematic, as the pectoralis minor lies right below the pectoralis major and heart rate is prevalent in this muscle. There is evidence that pectoralis minor activity may be distinguishable from pectoralis major activity through a diagonal humeral flexion task (Castelein, Cagnie, Parlevliet, Danneels, & Cools, 2015). Further, due to the location of the muscle, some participants may have had adipose tissue overlaying the pectoralis major and other muscles, which may have promoted cross talk in the EMG signals (Kuiken, Lowery, & Stoykov, 2003).

5.6.2 Data Reduction

The EMG data reduction protocol used for this thesis may have washed out some results, as the mean EMG was evaluated across the entirety of the task. Similarly, there may have also been a washout of kinematic results, as the ROM was taken across the entirety of the task. Both EMG and kinematic data were reduced to one number, which may have made it hard to discern differences pre- to post-fatigue. This could have been mitigated by parsing ADL into smaller events, however, then the specific event would no longer be a true activity of daily living and would instead be a small component of the activity.

The kinematic data may have also been subject to sampling error. Literature suggests that collection of multiple trials per participant for a given task can minimize inherent variability. To be specific, collecting 3-5 trials has been able to capture 88-95% of an individual's variability (Frost, Beach, Mcgill, & Callaghan, 2015). While the tasks in this thesis were relatively constrained, with targets to minimize variability, participants only performed one repetition of each ADL at each time point due to time constraints, especially for the first few post-fatigue measures (0-, 1-, and 3-minutes post-fatigue). Opting to only collect one repetition allows for variability in the data, however one repetition was still selected in the hopes that participants would perform as naturally as possible, rather than potentially producing a learning effect.

The fatigue data indicated that differential fatigue occurred between regions of the pectoralis major, however not all participants fatigued in the same way, with some participants fatiguing in one, two, or all three regions of the pectoralis major. This likely contributed to variability across participants in muscle activation and kinematic patterns.

This thesis used one-way repeated measures ANOVAs, which sought to determine the effects of fatigue on muscular activation strategies in addition to kinematic strategies, comparing tasks pre-fatigue to 5 different time points post-fatigue. The benefits of an ANOVA are that each participant is compared to themselves and that the sample population does not have to be very large. There were few statistically significant post-fatigue changes, which could have been due to variability in participants or selection of a sample population was too small to elicit a statistically significant response and thus underpowered. Additionally, all post-fatigue time points were assessed in the repeated measures ANOVA, which may not have picked up on any differences between pre-fatigue and post-fatigue. There is potential that if only pre- and 0-minutes post-fatigue were assessed, there might have been significant responses detected. However, the

differences from pre-fatigue to 0-minutes post-fatigue with regards to muscle activations were very small in magnitude and these differences may not persist if the ADLs were to be scaled up to more demanding tasks.

5.6.3 Task Selection and Specificity

The anatomical actions of the pectoralis major are known, as explored in the Literature Review, however limited information exists on how the pectoralis major contributes to shoulder movement as a whole. This thesis focuses on three activities of daily living, adapted from the findings of clinical research, with the assumption that the pectoralis major was highly involved. However, the experimental results suggest that the pectoralis major and its three regions were minimally involved, especially in the Shelf ADL. Further, no tasks were selected based on ergonomic relevance and it is possible that there are activities of daily living or workplace tasks that would involve the pectoralis major more than the three examined. Finally, the ADLs assessed in this thesis were submaximal tasks, resulting in low muscle activations, which may have made it difficult to discern changes post-fatigue.

5.6.4 Sex Differences

It has been established that there are sex differences in fatigue, with females more fatigue resistant and enduring longer in the same tasks (Chow et al., 2000; Enoka & Duchateau, 2008; Hicks et al., 2001). While the literature on myoelectric sex differences is small, there are studies to indicate that there are sex differences in muscle activation patterns, with males exhibiting greater overall muscle activity and strength (Alway, Grumbt, Gonyea, & Stray-Gundersen, 1989; Anders, Bretschneider, Bernsdorf, Erler, & Schneider, 2004). However, when corrected for age, mass, and lean body mass, differences in muscle activation and strength did not persist (Behm &

Sale, 1994; Heyward, Johannes-Ellis, & Romer, 1986; Ichinose, Kanehisa, Ito, Kawakami, & Fukunaga, 1998).

Females were not included in the study, as only the clavicular and superior regions of the sternocostal pectoralis major are typically available to collect in most women due to tissue filtering of breast tissue. As most of the fatigue seen in this study was either in the clavicular or abdominal regions, if females were included, fatigue would go undetected myoelectrically. While there is research to suggest that males and females are anatomically different when it comes to muscular structure in the lower extremity (Chow et al., 2000; Kubo et al., 2003), recent cadaveric evidence that there are no anatomical sex differences between males and females, although there are four main morphological variations in the pectoralis major (Haladaj, Wysiadecki, Clarke, Polguj, & Topol, 2019).

5.7 Future Directions

Important questions remain regarding the contributions of the pectoralis major to healthy and disrupted shoulder function. Considering additional ADLs and ergonomically relevant movements while increasing the number of muscles monitored would be constructive. Several deep muscles were not assessed in the current thesis, such as subscapularis, pectoralis minor, teres major, and supraspinatus. Additionally, it would be beneficial to investigate scapulothoracic kinematics, as there could be compensations occurring that were not assessed in this thesis, although the pectoralis major is not directly involved in scapolothoracic motion.

Unexpectedly, the abdominal pectoralis major fatigued, which likely influenced the results. It would be advantageous to investigate activation of this region more deliberately. Recent research reveals substantial abdominal region involvement in more humeral movement than was previously suspected. There are currently no guidelines for the MVCs that elicit the

greatest response from the muscle or a comprehensive understanding of the humeral movements this region is active in. Future research should aim to expand on the abdominal pectoralis major's involvement in humeral movement as well as how its fatigue potentially influences compensatory shoulder responses.

Although this study did not incorporate women and there is literature to suggest there are no anatomical differences in the pectoralis major (Haladaj et al., 2019), confirming male and female pectoralis major activation and fatigue patterns would be useful, in particular for pathological groups such as breast cancer survivors. However, it is unclear if sex differences in activation patterns exist. Future work in this area must be able to mitigate the tissue filtering problem when it comes to breast and adipose tissue that overlay this muscle.

With regards to data analysis, grouping participants based on their regional fatigue responses may help to differentiate compensatory mechanisms in muscular activity or kinematic patterns. Further, classification of participants based on their ability to perform the movement may be beneficial, as previous research has shown that in the presence of a disturbance, some participants are not able to perform the task in a similar manner to controls, while some participants are able to complete the movement in a way that is similar to the controls, but they do so with altered muscle activation patterns (Boerboom et al., 2001).

6.0 CONCLUSIONS

This thesis explored how pectoralis major fatigue affects muscle activation and kinematic strategies during common daily activities, while also characterizing whether differential fatigue in the pectoralis major occurred. It was novel in that it examined the pectoralis major's contributions to shoulder function using fatigue as a prospective knock-out for the muscle. The main outcome of this study was that the three regions of the pectoralis major experienced differential fatigue, previously an unexplored area of research with regards to this muscle. A secondary outcome of this thesis was that muscle activation and kinematic patterns changed as a result of pectoralis major fatigue, but these changes were nuanced. While the results of this thesis point to muscle contributions in ADLs commonly used to assess breast cancer survivors, these ADLs did not recruit the pectoralis major as much as has been previously thought. Literature suggests the pectoralis major is most affected from breast cancer treatment (Shamley et al., 2007; Stegnik-Jansen et al., 2011), however the difficulty in completing these movements may lie outside of pectoralis major dysfunction. Other muscles not collected likely also contributed to performing the ADLs and confounded the thesis results. In conclusion, more research needs to be done to continue to explore the pectoralis major's contributions to shoulder function in order to make confident statements about its role in modulating functional abilities in clinical populations, such as for breast cancer survivors.

REFERENCES

Aarimaa, V., Rantanen, J., Heikkila, J., Helttula, I., & Orava, S. (2004). Rupture of the pectoralis major muscle. *The American Journal of Sports Medicine*, *32*(5), 1256–1262.

Ackland, D. C., & Pandy, M. G. (2009). Lines of action and stabilizing potential of the shoulder musculature. *Journal of Anatomy*, *215*, 184–197. https://doi.org/10.1111/j.1469-7580.2009.01090.x

Al-Mulla, M. R., Sepulveda, F., & Colley, M. (2011). A review of non-invasive techniques to detect and predict localised muscle fatigue. *Sensors*, *11*, 3545–3594. https://doi.org/10.3390/s110403545

Alway, S. E., Grumbt, W. H., Gonyea, J., & Stray-Gundersen, J. (1989). Contrasts in muscle and myofibers of elite male and female bodybuilders. *Journal of Applied Physiology*, *67*(1), 24–31.

Anders, C., Bretschneider, S., Bernsdorf, A., Erler, K., & Schneider, W. (2004). Activation of shoulder muscles in healthy men and women under isometric conditions. *Journal of Electromyography and Kinesiology*, *14*(6), 699–707. https://doi.org/10.1016/j.jelekin.2004.04.003

Ashley, G. T. (1952). The manner of insertion of the pectoralis major muscle in man. *The Anatomical Record*, *113*(3), 301–307. https://doi.org/https://doi.org/10.1002/ar.1091130305

Barberini, F. (2014). The clavicular part of the pectoralis major: A true entity of the upper limb on anatomical, phylogenetic, ontogenetic, functional and clinical bases. Case report and review of the literature. *Italian Journal of Anatomy and Embryology*, *119*(1), 49–59. https://doi.org/10.13128/IJAE-14640

Barry, B. K., & Enoka, R. M. (2007). The neurobiology of muscle fatigue: 15 years later. *Integrative and Comparative Biology*, *47*(4), 465–473. https://doi.org/10.1093/icb/icm047

Behm, D. G., & Sale, D. G. (1994). Voluntary and evoked muscle contractile characteristics in active men and women. *Canadian Journal of Applied Physiology*, *19*(3), 253–265.

Boerboom, A. L., Hof, A. L., Halbertsma, J. P. K., van Raaij, J. J. A. M., Diercks, R. L., & van Horn, J. R. (2001). Atypical hamstrings electromyographic activity as a compensatory

mechanism in anterior cruciate ligament deficiency. *Knee Surgery, Sports Traumatology, Arthroscopy*, *9*, 211–216. https://doi.org/10.1007/s001670100196

Borg, G. (1990). Psychophysical scaling with applications in physical work and the perception of exertion. *Scandinavian Journal of Work, Environment and Health*, *16*(1), 55–58. https://doi.org/10.5271/sjweh.1815

Borstad, J. D., Szucs, K., & Navalgund, A. (2009). Scapula kinematic alterations following a modified push-up plus task. *Human Movement Science*, *28*(6), 738–751. https://doi.org/10.1016/j.humov.2009.05.002

Brookham, R. L., Cudlip, A. C., & Dickerson, C. R. (2018a). Examining upper limb kinematics and dysfunction of breast cancer survivors in functional dynamic tasks. *Clinical Biomechanics*, *55*, 86–93. https://doi.org/10.1016/j.clinbiomech.2018.04.010

Brookham, R. L., Cudlip, A. C., & Dickerson, C. R. (2018b). Quantification of upper limb electromyographic measures and dysfunction of breast cancer survivors during performance of functional dynamic tasks. *Clinical Biomechanics*, *52*, 7–13. https://doi.org/10.1016/j.clinbiomech.2017.12.011

Brookham, R. L., & Dickerson, C. R. (2016). Comparison of humeral rotation co-activation of breast cancer population and healthy shoulders. *Journal of Electromyography and Kinesiology*, *29*, 100–106. https://doi.org/10.1016/j.jelekin.2015.07.002

Brown, J. M. M., Wickham, J. B., McAndrew, D. J., & Huang, X. F. (2007). Muscles within muscles: Coordination of 19 muscle segments within three shoulder muscles during isometric motor tasks. *Journal of Electromyography and Kinesiology*, *17*, 57–73. https://doi.org/10.1016/j.jelekin.2005.10.007

Carrino, J. A., Chandnanni, V. P., Mitchell, D. B., Choi-Chinn, K., DeBerardino, T. M., & Miller, M. D. (2000). Pectoralis major muscle and tendon tears: Diagnosis and grading using magnetic resonance imaging. *Skeletal Radiology*, *29*, 305–313. https://doi.org/10.1007/s002560000199

Castelein, B., Cagnie, B., Parlevliet, T., Danneels, L., & Cools, A. (2015). Optimal normalization tests for muscle activation of the levator scapulae, pectoralis minor and rhomboid major: An electromyography study using maximum voluntary isometric contractions. *Archives of*

Physical Medicine and Rehabilitation, *96*, 1820–1827.
https://doi.org/10.1016/j.apmr.2015.06.004

Chaffin, D. B. (1974). Localized muscle fatigue - Definition and measurement. *Journal of Occupational Medicine*, *15*(4), 346–354. Retrieved from https://www.researchgate.net/publication/18816550

Chopp-Hurley, J. N., Brookham, R. L., & Dickerson, C. R. (2016). Identification of potential compensatory muscle strategies in a breast cancer survivor population: A combined computational and experimental approach. *Clinical Biomechanics*, *40*, 63–67. https://doi.org/10.1016/j.clinbiomech.2016.10.015

Chopp-Hurley, J. N., & Dickerson, C. R. (2015). The potential role of upper extremity muscle fatigue in the generation of extrinsic subacromial impingement syndrome: a kinematic perspective. *Physical Therapy Reviews*, *20*(3), 201–209. https://doi.org/10.1179/1743288X15Y.0000000009

Chopp-Hurley, J. N., Langenderfer, J. E., & Dickerson, C. R. (2016). A probabilistic orthopaedic population model to predict fatigue-related subacromial geometric variability. *Journal of Biomechanics*, *49*(4), 543–549. https://doi.org/10.1016/j.jbiomech.2015.12.049

Chopp, J. N., Fischer, S. L., & Dickerson, C. R. (2011). The specificity of fatiguing protocols affects scapular orientation: Implications for subacromial impingement. *Clinical Biomechanics*, *26*(1), 40–45. https://doi.org/10.1016/j.clinbiomech.2010.09.001

Chow, R. S., Medri, M. K., Martin, D. C., Leekam, R. N., Agur, A. M., & McKee, N. H. (2000). Sonographic studies of human soleus and gastrocnemius muscle architecture : gender variability. *European Journal of Applied Physiology*, *82*, 236–244.

Cifrek, M., Medved, V., Tonković, S., & Ostojić, S. (2009). Surface EMG based muscle fatigue evaluation in biomechanics. *Clinical Biomechanics*, *24*, 327–340. https://doi.org/10.1016/j.clinbiomech.2009.01.010

Clancy, E. A., Bertolina, M. V., Merletti, R., & Farina, D. (2008). Time- and frequency-domain monitoring of the myoelectric signal during a long-duration, cyclic, force-varying, fatiguing hand-grip task. *Journal of Electromyography and Kinesiology*, *15*, 256–265. https://doi.org/10.1016/j.jelekin.2007.02.007

Clark, B. C., Collier, S. R., Manini, T. M., & Ploutz-Snyder, L. L. (2005). Sex differences in muscle fatigability and activation patterns of the human quadriceps femoris. *European Journal of Applied Physiology*, *94*, 196–206. https://doi.org/10.1007/s00421-004-1293-0

Cools, A. M., Witvrouw, E. E., De Clercq, G. A., Danneels, L. A., Willems, T. M., Cambier, D. C., & Voight, M. L. (2002). Scapular Muscle Recruitment Pattern: Electromyographic Response of the Trapezius Muscle to Sudden Shoulder Movement Before and After a Fatiguing Exercise. *Journal of Orthopaedic & Sports Physical Therapy*, *32*(5), 221–229. https://doi.org/10.2519/jospt.2002.32.5.221

De Luca, C J. (1979). Physiology amd mathematics of myoelectric signals. *IEEE Transactions on Biomedical Engineering*, *26*(6), 313–325.

De Luca, Carlo J. (1997). The use of surface electromyography in biomechanics. *Journal of Applied Biomechanics*, *13*, 135–163.

De Luca, Carlo J., & Merletti, R. (1988). Surface myoelectric signal cross-talk among muscles of the leg. *Electroencephalography and Clinical Neurophysiology*, *69*(6), 568–575. https://doi.org/10.1016/0013-4694(88)90169-1

Dickerson, C. R., Meszaros, K. A., Cudlip, A. C., Chopp-Hurley, J. N., & Langenderfer, J. E. (2015). The influence of cycle time on shoulder fatigue responses for a fixed total overhead workload. *Journal of Biomechanics*, *48*(11), 2911–2918. https://doi.org/10.1016/j.jbiomech.2015.04.043

Dideriksen, J. L., Farina, D., & Enoka, R. M. (2010). Influence of fatigue on the simulated relation between the amplitude of the surface electromyogram and muscle force. *Philosophical Transactions of the Royal Society A: Mathematical, Physical and Engineering Sciences*, *368*, 2765–2781. https://doi.org/10.1098/rsta.2010.0094

Drake, J., & Callaghan, J. (2006). Elimination of electrocardiogram contamination from electromyogram signals: An evaluation of currently used removal techniques. *Journal of Electromyography and Kinesiology*, *16*(2), 175–187.

Ebaugh, D. D., McClure, P. W., & Karduna, A. R. (2006). Effects of shoulder muscle fatigue caused by repetitive overhead activities on scapulothoracic and glenohumeral kinematics. *Journal of Electromyography and Kinesiology*, *16*, 224–235.

https://doi.org/10.1016/j.jelekin.2005.06.015

Ekholm, J., Arborelius, U., Hillered, L., & Ortqvist, A. (1978). Shoulder muscle EMG and resisting moment during diagonal exercise movements resisted by weight-and-pulley-circuit. *Scandinavian Journal of Rehabilitation Medicine*, *10*(4), 179–185.

Enoka, R. M., & Stuart, D. G. (1992). Neurobiology of muscle fatigue. *Journal of Applied Physiology*, *72*(5), 1631–1648. https://doi.org/10.1152/jappl.1992.72.5.1631

Enoka, Roger M., & Duchateau, J. (2008). Muscle fatigue: What, why and how it influences muscle function. *Journal of Physiology*, *586*(1), 11–23. https://doi.org/10.1113/jphysiol.2007.139477

Farina, D. (2004). M-wave properties during progressive motor unit activation by transcutaneous stimulation. *Journal of Applied Physiology*, *97*, 545–555. https://doi.org/10.1152/japplphysiol.00064.2004

Frost, D. M., Beach, T. A. C., Mcgill, S. M., & Callaghan, J. P. (2015). A proposed method to detect kinematic differences between and within individuals. *Journal of Electromyography and Kinesiology*, *25*(3), 479–487. https://doi.org/10.1016/j.jelekin.2015.02.012

Fung, L., Wong, B., Ravichandiran, K., Agur, A., Rindlisbacher, T., & Elmaraghy, A. (2009). Three-dimensional study of pectoralis major muscle and tendon architecture. *Clinical Anatomy*, *22*(4), 500–508. https://doi.org/10.1002/ca.20784

Gandevia, S. C. (2001). Spinal and supraspinal factors in human muscle fatigue. *Physiological Reviews*, *81*(4), 1725–1789.

Gentil, P., Oliveira, E., De Araujo Rocha Junior, V., Do Carmo, J., & Bottaro, M. (2007). *Effects of exercise order on upper-body muscle activation and exercise performance*. *Journal of Strength and Conditioning Research* (Vol. 21).

Gould, D., Kelly, D., Goldstone, L., & Gammon, J. (2001). Examining the validity of pressure ulcer risk assessment scales: developing and using illustrated patient simulations to collect the data visual analogue scale. *Journal of Clinical Nursing*, *10*, 697–706.

Gray, H. (1918). *Anatomy of the Human Body*. (W. H. Lewis, Ed.) (20th ed.). Philadelphia: Lea & Febiger.

Guo, J.-Y., Zheng, Y.-P., Huang, Q.-H., & Chen, X. (2008). Dynamic monitoring of forearm muscles using one-dimensional sonomyography system. *The Journal of Rehabilitation Research and Development*, *45*(1), 187–196. https://doi.org/10.1682/JRRD.2007.02.0026

Hagberg, M. (1981). Work load and fatigue in repetitive arm elevations. *Ergonomics*, *24*(7), 543–555. https://doi.org/10.1080/00140138108924875

Hagstrom, A. D., Shorter, K. A., & Marshall, P. W. (2017). Changes in unilateral upper limb muscular strength and electromyographic activity after a 16-week strength training intervention in survivors of breast cancer. *Journal of Strength and Conditioning Research*, *33*(1), 225–233.

Haladaj, R., Wysiadecki, G., Clarke, E., Polguj, M., & Topol, M. (2019). Anatomical Variations of the pectoralis major muscle : Notes on their impact on pectoral nerve innervation patterns and discussion on their clinical relevance. *BioMed Research International*, *2019*, 1–15.

Hall, L. C., Middlebrook, E. E., & Dickerson, C. R. (2011). Analysis of the influence of rotator cuff impingements on upper limb kinematics in an elderly population during activities of daily living. *Clinical Biomechanics*, *26*(6), 579–584. https://doi.org/10.1016/j.clinbiomech.2011.02.006

Heyward, V. H., Johannes-Ellis, S. M., & Romer, J. F. (1986). Gender differences in strength. *Research Quarterly for Exercise and Sport*, *57*(2), 154–159.

Hicks, A. L., Kent-Braun, J., & Ditor, D. S. (2001). Sex Differences in Human Skeletal Muscle Fatigue. *Exercise and Sport Sciences Reviews*, *29*(3), 109–112. Retrieved from www.acsm-essr.org

Hodges, P. W., Pengel, L. H. M., Herbert, R. D., & Gandevia, S. C. (2003). Measurement of muscle contraction with ultrasound imaging. *Muscle and Nerve*, *27*, 682–692. https://doi.org/10.1002/mus.10375

Huang, Q. H., Zheng, Y. P., Chen, X., He, J. F., & Shi, J. (2007). *A System for the Synchronized Recording of Sonomyography, Electromy-ography and Joint Angle*. *The Open Biomedical Engineering Journal* (Vol. 1). Bentham Science Publishers Ltd. Retrieved from http://www.tups.org/

Huffenus, A. F., & Forestier, N. (2006). Effects of fatigue of elbow extensor muscles voluntarily

induced and induced by electromyostimulation on multi-joint movement organization. *Neuroscience Letters*, *403*, 109–113. https://doi.org/10.1016/j.neulet.2006.04.025

Hunter, S. K., Butler, J. E., Todd, G., Gandevia, S. C., & Taylor, J. L. (2006). Supraspinal fatigue does not explain the sex difference in muscle fatigue of maximal contractions. *Journal of Applied Physiology*, *101*, 1036–1044. https://doi.org/10.1152/japplphysiol.00103.2006

Ichinose, Y., Kanehisa, H., Ito, M., Kawakami, Y., & Fukunaga, T. (1998). Morphological and functional differences in the elbow extensor muscle between highly trained male and female athletes. *European Journal of Applied Physiology*, *78*, 109–114.

Inman, V., Saunders, D. M., & Abbott, L. C. (1944). Observations on the function of the shoulder joint. *The Journal of Bone and Joint Surgery*, *42*(1), 1–30.

Joshi, M., Thigpen, C. A., Bunn, K., Karas, S. G., & Padua, D. A. (2011). Shoulder external rotation fatigue and scapular muscle activation and kinematics in overhead athletes. *Journal of Athletic Training*, *2011*(4), 349–357. Retrieved from www.nata.org/jat

Koh, T. J., & Grabiner, M. D. (1992). Cross talk in surface electromyograms of human hamstring muscles. *Journal of Orthopaedic Research*, *10*(5), 701–709. https://doi.org/10.1002/jor.1100100512

Kubo, K., Kanehisa, H., Azuma, K., Ishizu, M., Okada, M., & Fukunaga, T. (2003). Muscle architectural characteristics in young and elderly men and women. *International Journal of Sports Medicine*, *24*, 125–130.

Kuiken, T. A., Lowery, M. M., & Stoykov, N. S. (2003). The effect of subcutaneous fat on myoelectric signal amplitude and cross-talk. *Prosthetics and Orthotics International*, *27*, 48–54.

Langenderfer, J., Jerabek, S. A., Thangamani, V. B., Kuhn, J. E., & Hughes, R. E. (2004). Musculoskeletal parameters of muscles crossing the shoulder and elbow and the effect of sarcomere length sample size on estimation of optimal muscle length. *Clinical Biomechanics*, *19*(7), 664–670. https://doi.org/10.1016/j.clinbiomech.2004.04.009

Leonardis, J. M., Desmet, D. M., & Lipps, D. B. (2017). Quantifying differences in the material properties of the fiber regions of the pectoralis major using ultrasound shear wave

elastography. *Journal of Biomechanics*, *63*, 41–46. https://doi.org/10.1016/j.jbiomech.2017.07.031

Lieber, R. L., & Fridén, J. (2000). Functional and clinical significance of skeletal muscle architecture. *Muscle & Nerve*, *23*, 1647–1666. https://doi.org/10.1002/1097-4598(200011)23:11<1647::AID-MUS1>3.3.CO;2-D

Lipps, D. B., Sachdev, S., & Strauss, J. B. (2017). Quantifying radiation dose delivered to individual shoulder muscles during breast radiotherapy. *Radiotherapy and Oncology*, *122*, 431–436. https://doi.org/10.1016/j.radonc.2016.12.032

Lopes, J. M., Aubier, M., Jardim, J., Aranda, J. V, Macklem, P. T., Aranda, J., & T Macklem, A. P. (1983). Effect of caffeine on skeletal muscle function before and after fatigue. *Journal of Applied Physiology*, *54*(5), 1303–1305. Retrieved from www.physiology.org/journal/jappl

Maciukiewicz, J. (2017). *Longitudinal assessment of functional upper limb abilities in a breast cancer survivor population*. The University of Waterloo.

Manktelow, R., McKee, N., & Vettese, T. (1980). An anatomical study of the pectoralis major muscle as related to functioning free muscle transplantation. *Plastic and Reconstructive Surgery*, *65*(5), 610–615.

Marmor, L., Bechtol, C. O., & Hall, C. B. (1961). Pectoralis major muscle: Function of sternal portion and mechanism of rupture of normal muscle: Case reports. *Journal of Bone and Joint Surgery*, *43*(1), 81–87.

McCully, S. P., Suprak, D. N., Kosek, P., & Karduna, A. R. (2006). Suprascapular nerve block disrupts the normal pattern of scapular kinematics. *Clinical Biomechanics*, *21*, 545–553. https://doi.org/10.1016/j.clinbiomech.2006.02.001

McCully, S. P., Suprak, D. N., Kosek, P., & Karduna, A. R. (2007). Suprascapular nerve block results in a compensatory increase in deltoid muscle activity. *Journal of Biomechanics*, *40*, 1839–1846. https://doi.org/10.1016/j.jbiomech.2006.07.010

McDonald, A. C. (2017). *Understanding the response of the shoulder complex to the demands of repetitive work*. McMaster University.

McDonald, A. C., Brenneman, E. C., Cudlip, A. C., & Dickerson, C. R. (2014). The spatial dependency of shoulder muscle demands for seated lateral hand force exertions. *Journal of*

Applied Biomechanics, *30*(1), 1–11. https://doi.org/10.1123/jab.2012-0221

McDonald, A., Picco, B. R., Belbeck, A. L., Chow, A. Y., & Dickerson, C. R. (2012). Spatial dependency of shoulder muscle demands in horizontal pushing and pulling. *Applied Ergonomics*, *43*(6), 971–978. https://doi.org/10.1016/j.apergo.2012.01.005

Mendez-Rebolledo, G., Gatica-Rojas, V., Guzman-Muñoz, E., Martinez-Valdes, E., Guzman-Venegas, R., & Berral de la Rosa, F. J. (2018). Influence of fatigue and velocity on the latency and recruitment order of scapular muscles. *Physical Therapy in Sport*, *32*, 80–86. https://doi.org/10.1016/j.ptsp.2018.04.015

Merletti, R, & Lo Conte, L. R. (1995). *Advances in processing of surface myoelectric signals: Part I. Biol. Eng. & Comput* (Vol. 33).

Merletti, Roberto, Knaflitz, M., & De Luca, C. J. (1990). *Myoelectric manifestations of fatigue in voluntary and electrically elicited contractions*. *Journal of Applied Physiology* (Vol. 69). Retrieved from www.physiology.org/journal/jappl

Micklewright, D., St Clair Gibson, A., Gladwell, V., & Al Salman, A. (2017). Development and validity of the rating-of-fatigue scale. *Sports Medicine*, *47*, 2375–2393. https://doi.org/10.1007/s40279-017-0711-5

Moritani, T., Muro, M., & Nagata, A. (1986). Intramuscular and surface electromyogram changes during muscle fatigue. *Journal of Applied Physiology*, *60*(4), 1179–1185. Retrieved from www.physiology.org/journal/jappl

Mulla, D. M., McDonald, A. C., & Keir, P. J. (2018). Upper body kinematic and muscular variability in response to targeted rotator cuff fatigue. *Human Movement Science*, *59*, 121–133. https://doi.org/10.1016/j.humov.2018.04.001

Nadon, A. L., Vidt, M. E., Chow, A. Y., & Dickerson, C. R. (2016). The spatial dependency of shoulder muscular demands during upward and downward exertions. *Ergonomics*, *59*(10), 1294–1306. https://doi.org/10.1080/00140139.2015.1136697

Noguchi, M., Chopp, J. N., Borgs, S. P., & Dickerson, C. R. (2013). Scapular orientation following repetitive prone rowing: Implications for potential subacromial impingement mechanisms. *Journal of Electromyography and Kinesiology*, *23*(6), 1356–1361. https://doi.org/10.1016/j.jelekin.2013.08.007

Öberg, T., Sandsjö, L., & Kadefors, R. (1990). Electromyogram mean power frequency in non-fatigued trapezius muscle. *European Journal of Applied Physiology and Occupational Physiology*, *61*, 362–369. https://doi.org/10.1007/BF00236054

Öberg, T., Sandsjö, L., & Roland Kadefors, &. (1994). Subjective and objective evaluation of shoulder muscle fatigue. *Ergonomics*, *37*(8), 1323–1333. https://doi.org/10.1080/00140139408964911org/10.1080/00140139408964911

Orizio, C., Gobbo, M., Diemont, B., Esposito, F., & Veicsteinas, A. (2003). The surface mechanomyogram as a tool to describe the influence of fatigue on biceps brachii motor unit activation strategy. Historical basis and novel evidence. *European Journal of Applied Physiology*, *90*, 326–336. https://doi.org/10.1007/s00421-003-0924-1

Paton, M. E., & Brown, J. M. M. (1994). An electromyographic analysis of functional differentiation in human pectoralis major muscle. *Journal of Electromyography and Kinesiology*, *4*(3), 161–169.

Petilon, J., Carr, D. R., Sekiya, J. K., & Unger, D. V. (2005). *Pectoralis major muscle injuries: Evaluation and management*. *J Am Acad Orthop Surg* (Vol. 13).

Phadke, V., Braman, J. P., LaPrade, R. F., & Ludewig, P. M. (2011). Comparison of glenohumeral motion using different rotation sequences. *Journal of Biomechanics*, *44*(4), 700–705. https://doi.org/10.1016/j.jbiomech.2010.10.042

Potvin, J. R., & Fuglevand, A. J. (2017). A motor unit-based model of muscle fatigue. *PLoS Computational Biology*, *13*(6), e1005581. https://doi.org/10.1371/journal.pcbi.1005581

Rockwood Jr., C. A. (2009). *The Shoulder - Volume 1*. (C. A. Rockwood Jr., F. A. Matsen III, M. A. Wirth, S. B. Lippitt, E. V Fehringer, & J. W. Sperling, Eds.) (Fourth). Philadelphia: Saunders Elsevier.

Sato, Y., & Takafuji, T. (1992). Abdominal part artery of axillary artery: Proposed term for the artery supplying the abdominal part of the musculus pectoralis major. *Cells Tissues Organs*, *145*(3), 220–228. https://doi.org/https://doi.org/10.1159/000147370

Schenkman, M., & Rugo De Cartaya, V. (1987). Kinesiology of the shoulder complex. *Journal of Orthopaedic & Sports Physical Therapy*, *8*(9), 438–450. Retrieved from www.jospt.org

Shamley, D. R., Srinanaganathan, R., Weatherall, R., Oskrochi, R., Watson, M., Ostlere, S., &

Sugden, E. (2007). Changes in shoulder muscle size and activity following treatment for breast cancer. *Breast Cancer Research and Treatment*, *106*, 19–27. https://doi.org/10.1007/s10549-006-9466-7

Shi, J., Chang, Q., & Zheng, Y.-P. (2010). Feasibility of controlling prosthetic hand using sonomyography signal in real time: Preliminary study. *The Journal of Rehabilitation Research and Development*, *47*(2), 87–98. https://doi.org/10.1682/JRRD.2009.03.0031

Solomonow, M. (2012). Neuromuscular manifestations of viscoelastic tissue degradation following high and low risk repetitive lumbar flexion. *Journal of Electromyography and Kinesiology*, *22*(2), 155–175. https://doi.org/10.1016/j.jelekin.2011.11.008

Solomonow, M., Baratta, R., Bernardi, M., Zhou, B., Lu, Y., Zhu, M., & Acierno, S. (1994). Surface and wire EMG crosstalk in neighbouring muscles. *Journal of Electromyography and Kinesiology*, *4*, 131–142. https://doi.org/10.1016/1050-6411(94)90014-0

Stegnik-Jansen, C. W., Buford Jr., W. L., Patterson, R. M., & Gould, L. J. (2011). Computer simulation of pectoralis major muscle strain to guide exercise protocols for patients after breast cancer surgery. *Journal of Orthopaedic & Sports Physical Therapy*, *41*(6), 417–426.

Suydam, S. M., Buchanan, T. S., Manal, K., & Gravare, K. (2015). Compensatory muscle activation caused by tendon lengthening post-Achilles tendon rupture. *Knee Surgery, Sports Traumatology, Arthroscopy*, *23*, 868–874. https://doi.org/10.1007/s00167-013-2512-1

Tarata, M. T. (2003). Mechanomyography versus electromyography, in monitoring the muscular fatigue. *BioMedical Engineering Online*, *2*(3). https://doi.org/10.1186/1475-925X-2-3

Taylor, S. A. F., Kedgley, A. E., Humphries, A., & Shaheen, A. F. (2018). Simulated activities of daily living do not replicate functional upper limb movement or reduce movement variability. *Journal of Biomechanics*, *76*, 119–128. https://doi.org/10.1016/j.jbiomech.2018.05.040

Tsai, N.-T., Mcclure, P. W., & Karduna, A. R. (2003). Effects of muscle fatigue on 3-dimensional scapular kinematics. *Archives of Physical Medicine and Rehabilitation*, *84*, 1000–1005. https://doi.org/10.1016/S0003-9993(03)00127-8

Tse, C. T. F., McDonald, A. C., & Keir, P. J. (2016). Adaptations to isolated shoulder fatigue during simulated repetitive work. Part I: Fatigue. *Journal of Electromyography and*

Kinesiology, *29*, 42–49. https://doi.org/10.1016/j.jelekin.2015.07.003

Tseng, B. Y., Gajewski, B. J., & Kluding, P. M. (2010). Reliability, responsiveness, and validity of the visual analog fatigue scale to measure exertion fatigue in people with chronic stroke: A preliminary study. *Stroke Research and Treatment*, *2010*, 10–13. https://doi.org/10.4061/2010/412964

Umehara, J., Kusano, K., Nakamura, M., Morishita, K., Nishishita, S., Tanaka, H., … Ichihashi, N. (2018). Scapular kinematic and shoulder muscle activity alterations after serratus anterior muscle fatigue. *Journal of Shoulder and Elbow Surgery*, *27*(7), 1205–1213. https://doi.org/10.1016/j.jse.2018.01.009

Vanderthommen, M., Duteil, S., Wary, C., Raynaud, J. S., Leroy-Willig, A., Crielaard, J. M., & Carlier, P. G. (2003). A comparison of voluntary and electrically induced contractions by interleaved 1 H- and 31 P-NMRS in humans. *Journal of Applied Physiology*, *94*(1012–1024). https://doi.org/10.1152/japplphysiol.00887.2001

Veeger, H. E. J., & van der Helm, F. C. T. (2007). Shoulder function: The perfect compromise between mobility and stability. *Journal of Biomechanics*, *40*, 2119–2129. https://doi.org/10.1016/j.jbiomech.2006.10.016

Vidt, M. E., Santago, A. C., Marsh, A. P., Hegedus, E. J., Tuohy, C. J., Poehling, G. G., … Saul, K. R. (2016). The effects of a rotator cuff tear on activities of daily living in older adults: A kinematic analysis. *Journal of Biomechanics*, *49*(4), 611–617. https://doi.org/10.1016/j.jbiomech.2016.01.029

Whittaker, R. (2017). *Upper extremity kinematic changes and shoulder muscle fatigue during a repetitive goal directed task*. University of Waterloo.

Whittaker, R. L., La Delfa, N. J., & Dickerson, C. R. (2018). Algorithmically detectable directional changes in upper extremity motion indicate substantial myoelectric shoulder muscle fatigue during a repetitive manual task. *Ergonomics*, *0*(0), 1–37. https://doi.org/10.1080/00140139.2018.1536808

Winter, D. A. (2009). *Biomechanics and Motor Control of Human Movement*. *Motor Control* (Fourth, Vol. 2nd). Hoboken: John Wiley & Sons. https://doi.org/10.1002/9780470549148

Wolfe, S. W., Wickiewicz, T. L., & Cavanaugh, J. T. (1992). Ruptures of the pectoralis major

muscle: An anatomic and clinical analysis. *The American Journal of Sports Medicine*, *20*(5), 587–593.

Wu, G., & Cavanaugh, P. R. (1995). ISB recommendations for standardization in the reporting of kinematic data. *Journal of Biomechanics*, *28*(10), 1257–1261.

Wu, G., Van Der Helm, F. C. T., Veeger, H. E. J., Makhsous, M., Van Roy, P., Anglin, C., … Buchholz, B. (2005). ISB recommendation on definitions of joint coordinate systems of various joints for the reporting of human joint motion - Part II: Shoulder, elbow, wrist and hand. *Journal of Biomechanics*, *38*(5), 981–992. https://doi.org/10.1016/j.jbiomech.2004.05.042

Wüst, R. C. I., Winwood, K., Wilks, D. C., Morse, C. I., Degens, H., & Rittweger, J. (2010). Effects of smoking on tibial and radial bone mass and strength may diminish with age. *Journal of Clinical Endocrinology and Metabolism*, *95*, 2763–2771. https://doi.org/10.1210/jc.2009-2462

Yoon, T., De-Lap, B. S., Griffith, E. E., & Hunter, S. K. (2008). Age-related muscle fatigue after a low-force fatiguing contraction is explained by central fatigue. *Muscle and Nerve*, *37*, 457–466. https://doi.org/10.1002/mus.20969

Yung, M., Mathiassen, S. E., & Wells, R. P. (2012). Variation of force amplitude and its effects on local fatigue. *European Journal of Applied Physiology*, *112*, 3865–3879. https://doi.org/10.1007/s00421-012-2375-z

Zheng, Y. P., Chan, M. M. F., Shi, J., Chen, X., & Huang, Q. H. (2006). Sonomyography: Monitoring morphological changes of forearm muscles in actions with the feasibility for the control of powered prosthesis. *Medical Engineering and Physics*, *28*(5), 405–415. https://doi.org/10.1016/j.medengphy.2005.07.012

Appendix A: Fatigue in Surrounding Shoulder Musculature

Table 14: Fatigue presence in surrounding shoulder musculature during the internal rotation reference contractions. 'X' indicates a MdPF decrease of 8% or greater. Grey shaded boxes indicate an increase in mean EMG amplitude. A grey shaded box with an 'X' indicates an increase in RMS amplitude and a decrease in MdPF, representative of fatigue in the muscle. '-' indicates a removal of data due to the EMG signal being greater than physiologically possible.

Participant	Anterior Deltoid	Middle Deltoid	Posterior Deltoid	Infraspinatus	Latissimus Dorsi	Upper Trapezius
1	X	X	-			X
2	X	X			X	X
3	X	X			X	X
4	-	-	-	-	-	-
5	-	-	-	-	-	-
6	X	X	X		X	X
7	X			X		X
8		X		X		X
9		X	X	X		X
10		X				X
11	X	X	X	X		
12				X	-	X
13		X	X			X
14				X		X
15			X			X
16		X				X
17	X	X	X	X		X
18		X	X	X		-
19		X	X	X		X
20	X	X				X
Total Participants Fatigued	**5**	**11**	**6**	**7**	**3**	**11**

Appendix B: Non-Significant Joint Angle ROMs

Curtain ADL
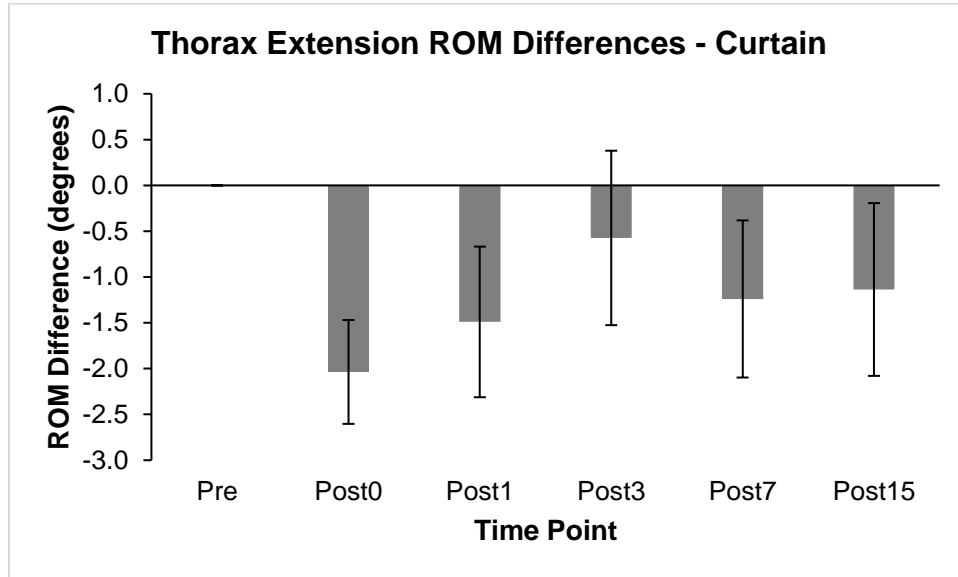
Figure 25. Thorax extension ROM differences for the Curtain ADL pre- and post-fatigue. Negative values indicate decrease in thorax extension post-fatigue. Error bars indicate standard error.
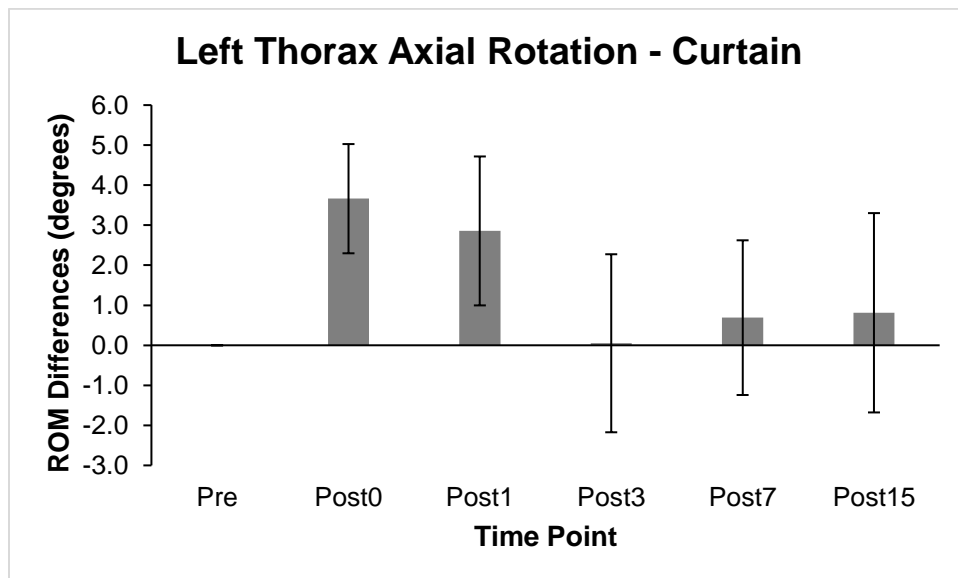
Figure 26. Left thorax axial rotation ROM differences for the Curtain ADL pre- and post-fatigue. Negative values indicate a decrease in left thorax axial rotation post-fatigue. Error bars indicate standard error.
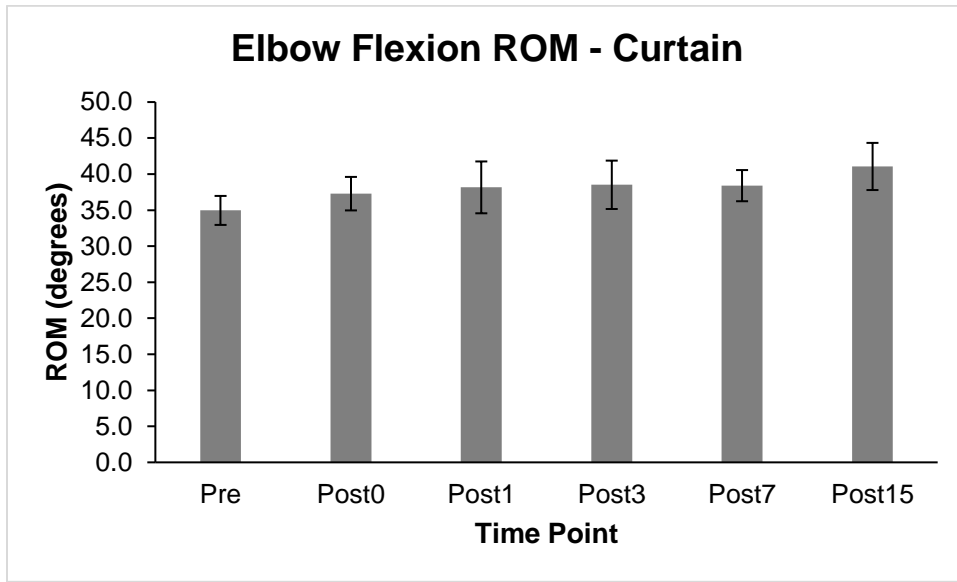
Figure 27. Elbow flexion ROM for the Curtain ADL pre- and post-fatigue. Error bars indicate standard error.
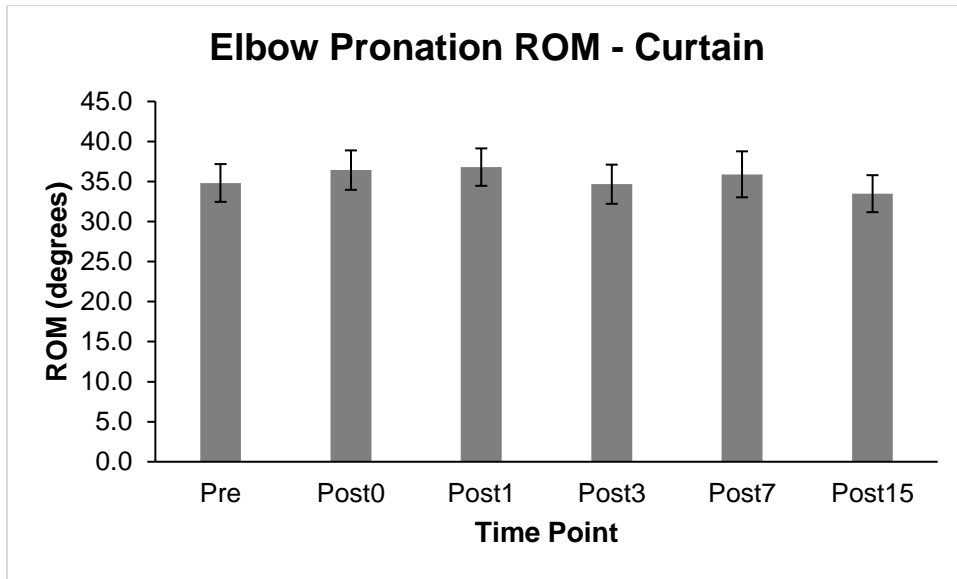
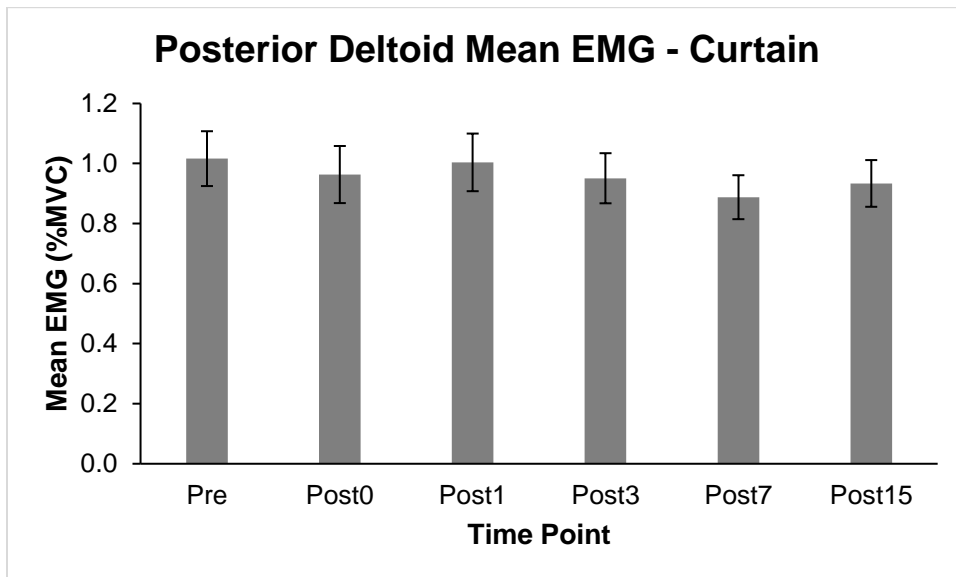**Figure 28.** Elbow pronation ROM for the Curtain ADL pre- and post-fatigue. Error bars indicate standard error.
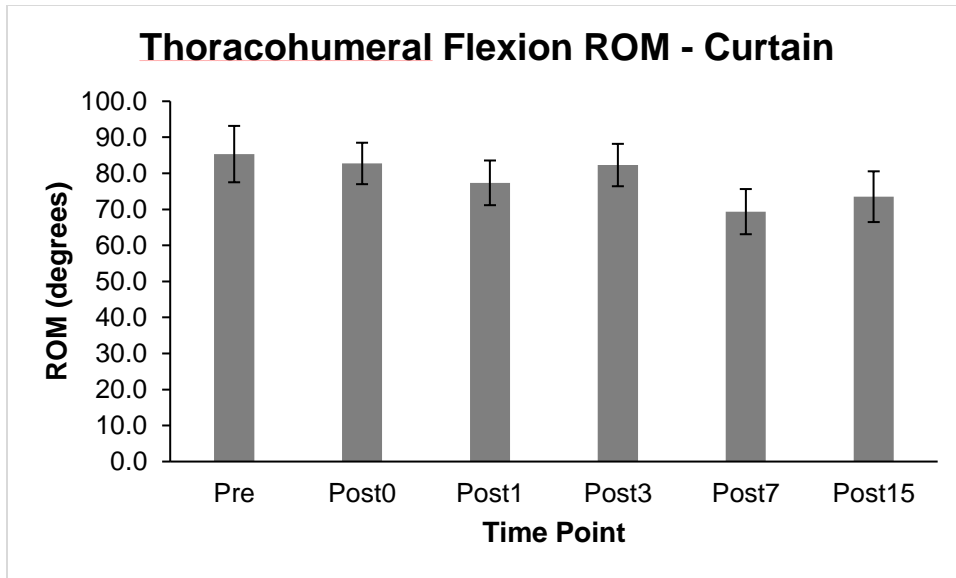
Figure 29. Thoracohumeral flexion ROM for the Curtain ADL pre- and post-fatigue. Error bars indicate standard error.
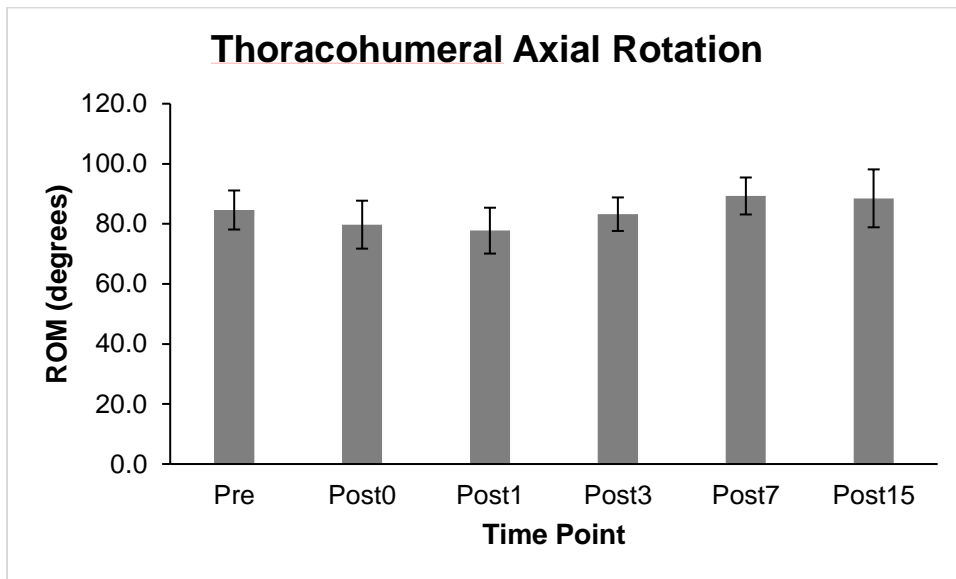
Figure 30. Thoracohumeral axial rotation ROM for the Curtain ADL pre- and post-fatigue. Error bars indicate standard error.

Scratch ADL
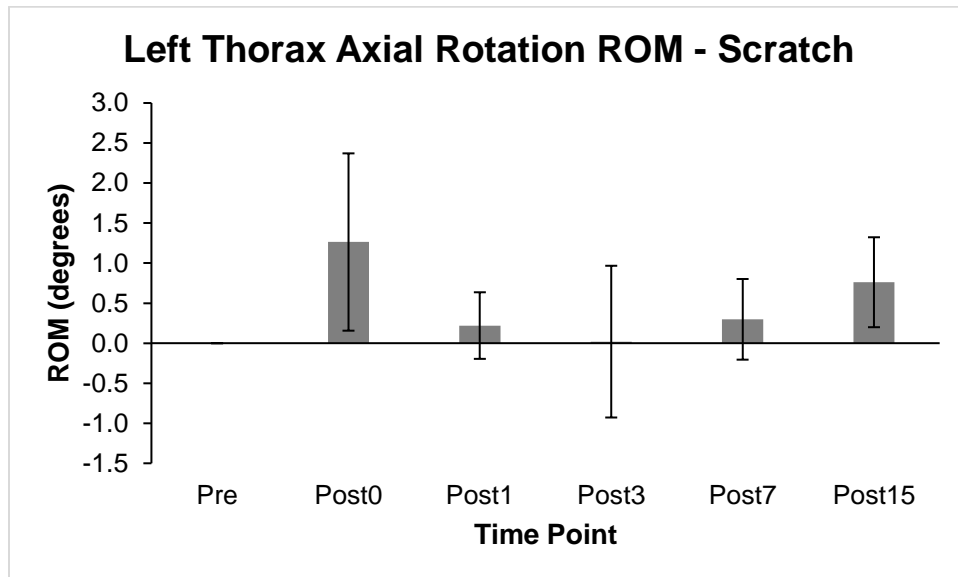
Figure 31. Left thorax axial rotation ROM differences for the Scratch ADL pre- and post-fatigue. Error bars indicate standard error.
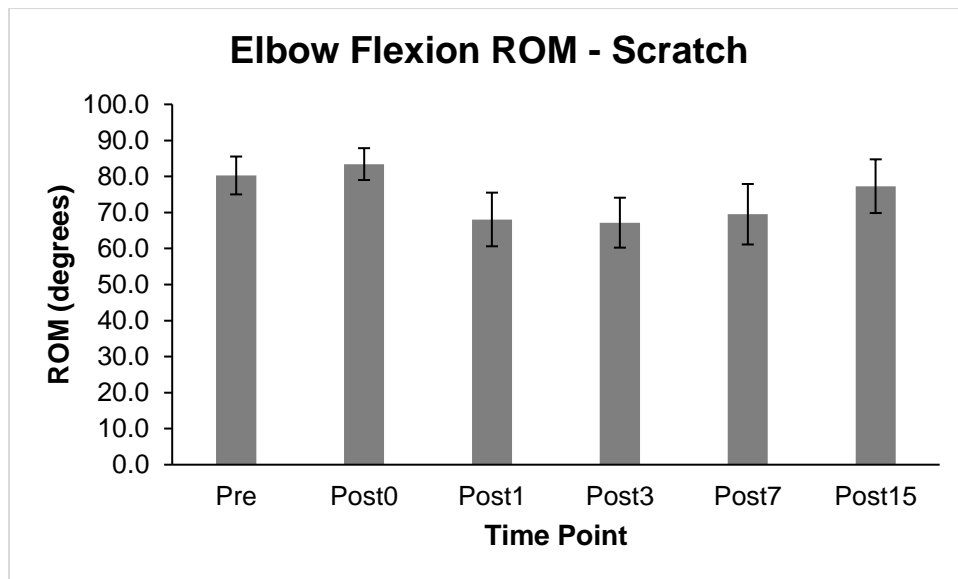
Figure 32. Elbow flexion ROM for the Scratch ADL pre- and post-fatigue. Error bars indicate standard error.
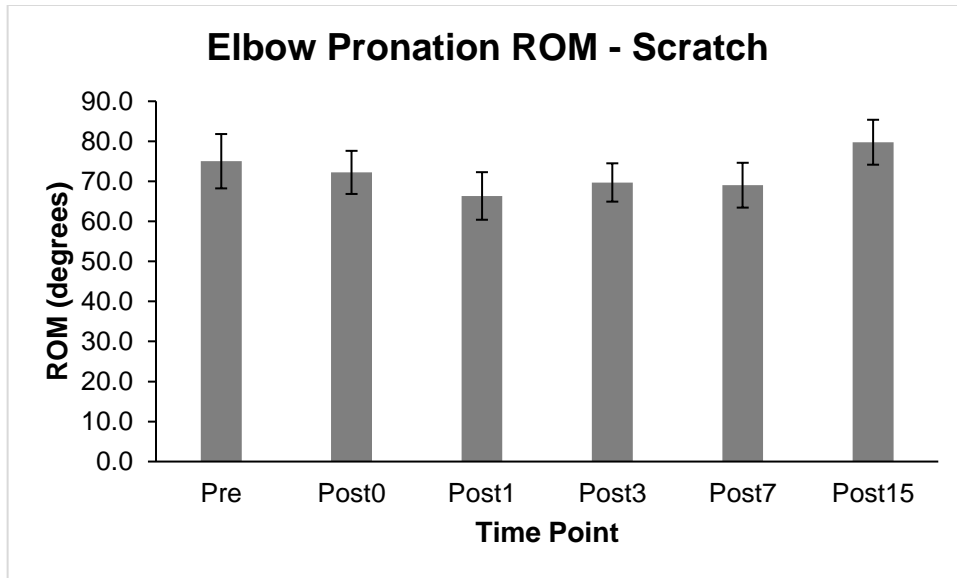
Figure 33. Elbow pronation for the Scratch ADL pre- and post-fatigue. Error bars indicate standard error.
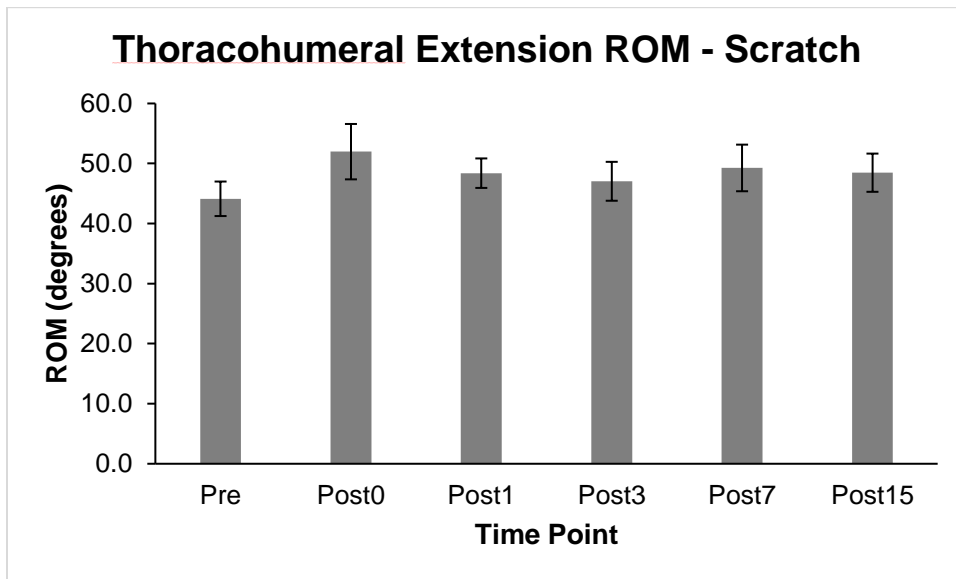
Figure 34. Thoracohumeral extension ROM differences for the Scratch ADL pre- and post-fatigue. Error bars indicate standard error.
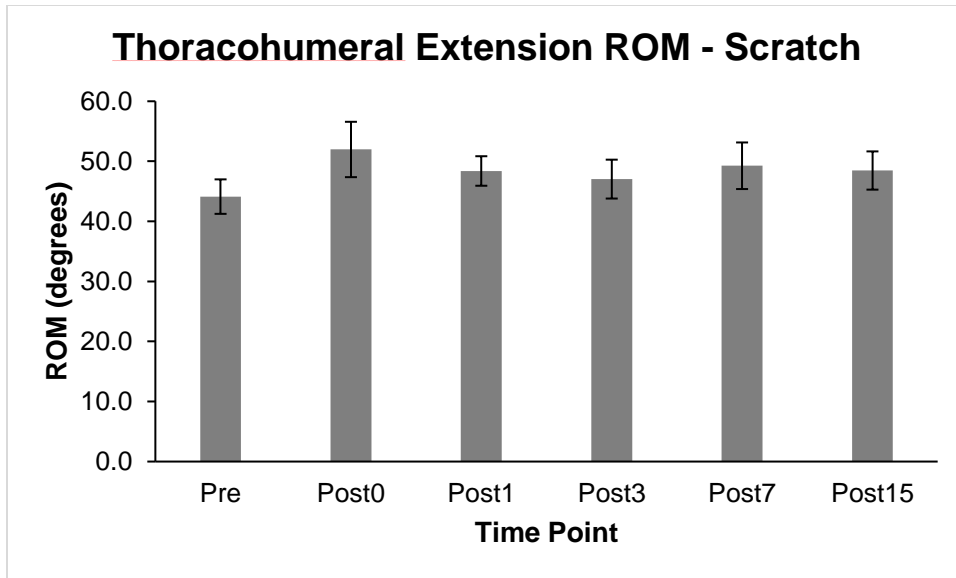
Figure 35. Thoracohumeral axial rotation ROM differences for the Scratch ADL pre- and post-fatigue. Error bars indicate standard error.

Shelf ADL
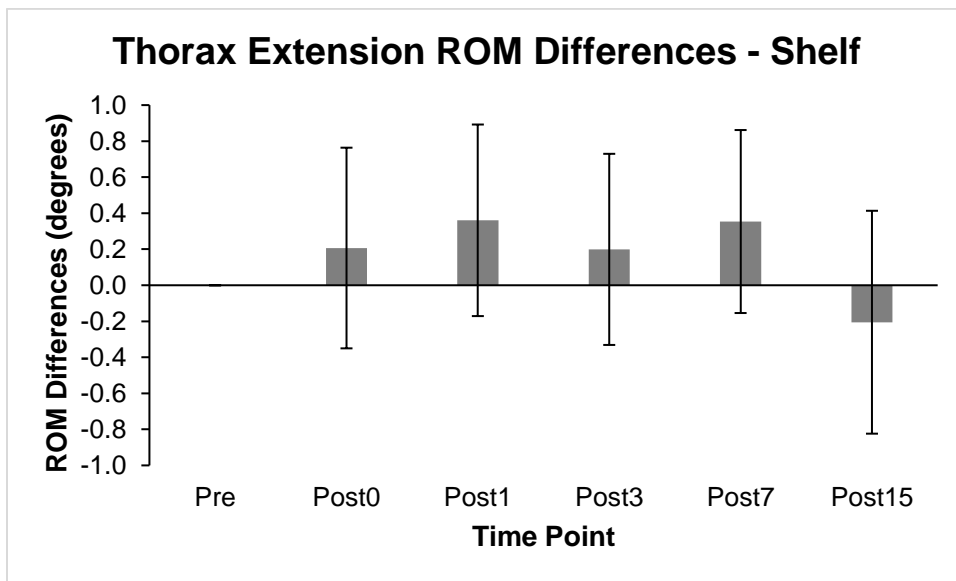
Figure 36. Thorax extension ROM differences for the Shelf ADL pre- and post-fatigue. Error bars indicate standard error.
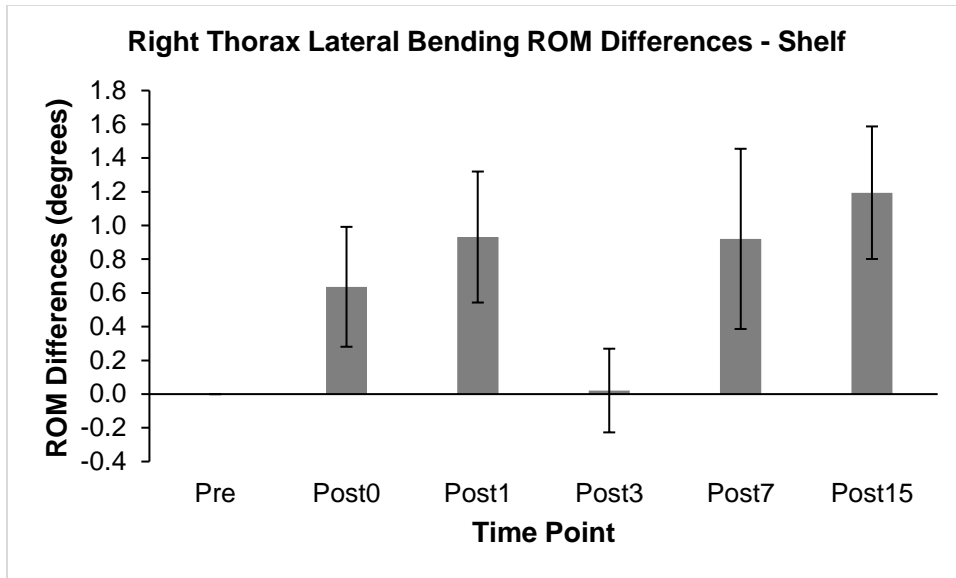
Figure 37. Right thorax lateral bending ROM differences for the Shelf ADL pre- and post-fatigue. Error bars indicate standard error.
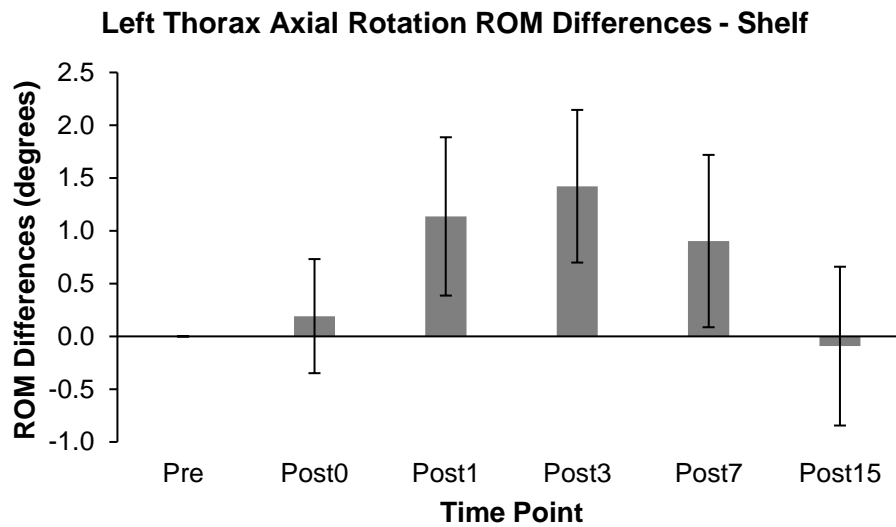
Figure 38. Left thorax axial rotation ROM differences for the Shelf ADL pre- and post-fatigue. Error bars indicate standard error.
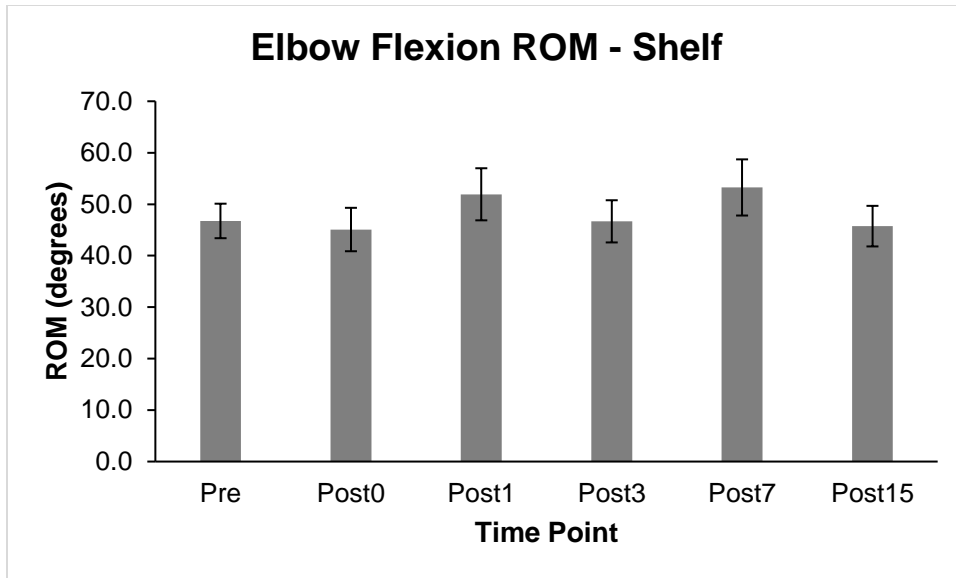
Figure 39. Elbow flexion ROM for the Shelf ADL pre- and post-fatigue. Error bars indicate standard error.
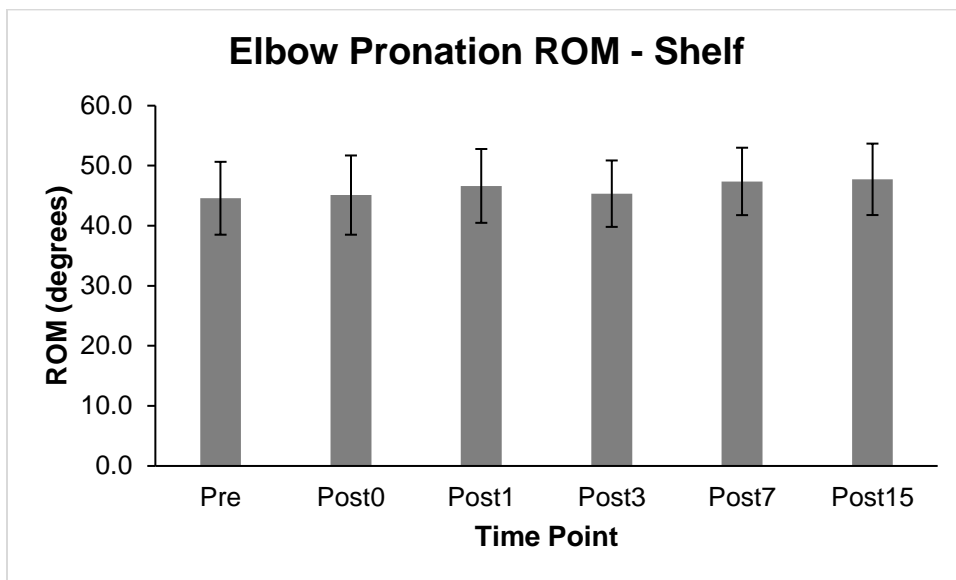
Figure 40. Elbow pronation ROM for the Shelf ADL pre- and post-fatigue. Error bars indicate standard error.
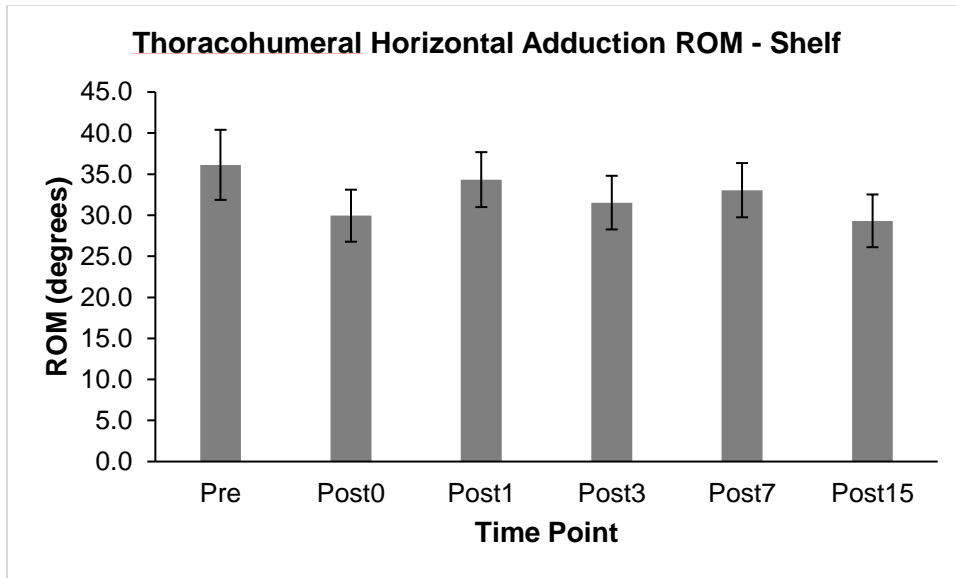
Figure 41. Thoracohumeral horizontal adduction ROM for the Shelf ADL pre- and post-fatigue. Error bars indicate standard error.
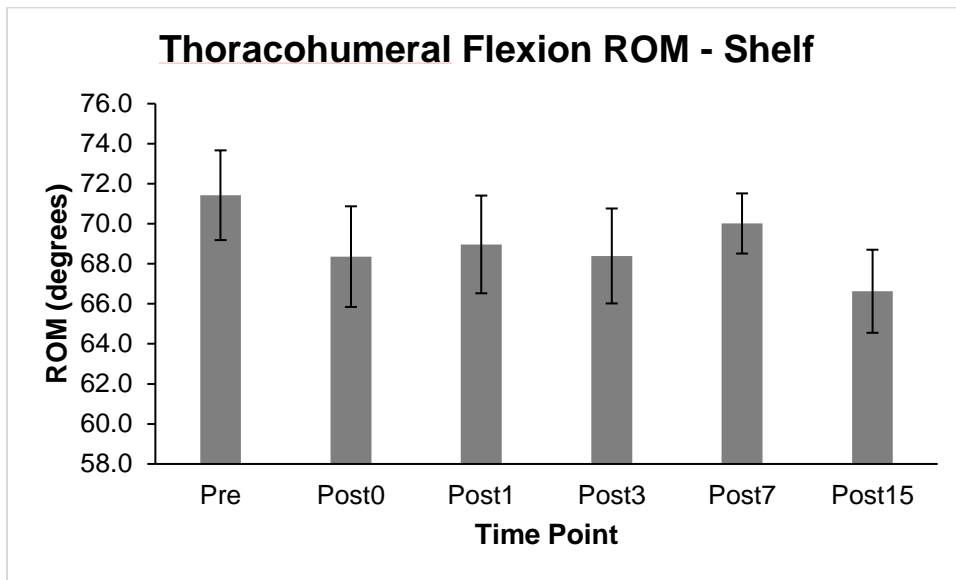
Figure 42. Thoracohumeral flexion ROM for the Shelf ADL pre- and post-fatigue. Error bars indicate standard error.

Appendix C: Non-Significant Mean and Median RMS

Mean EMG – Curtain ADL
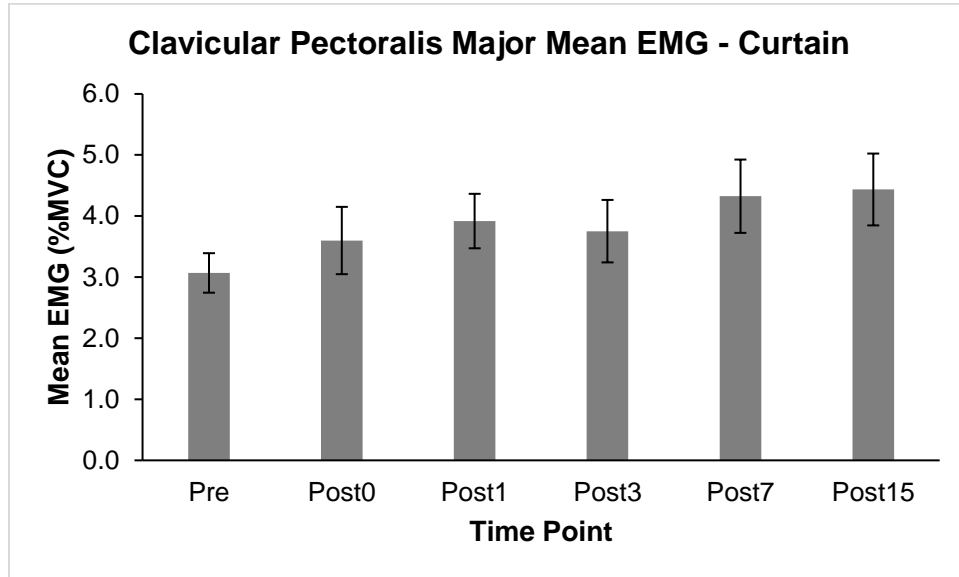
Figure 43. Clavicular pectoralis major mean EMG amplitude for the Curtain ADL pre- and post-fatigue. Error bars indicate standard error.
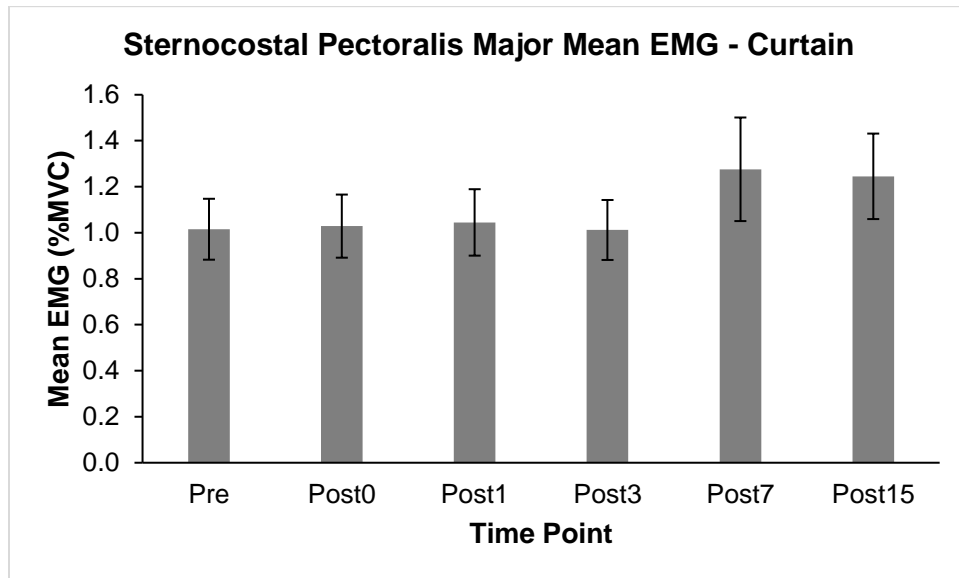
Figure 44. Sternocostal pectoralis major mean EMG amplitude for the Curtain ADL pre- and post-fatigue. Error bars indicate standard error.
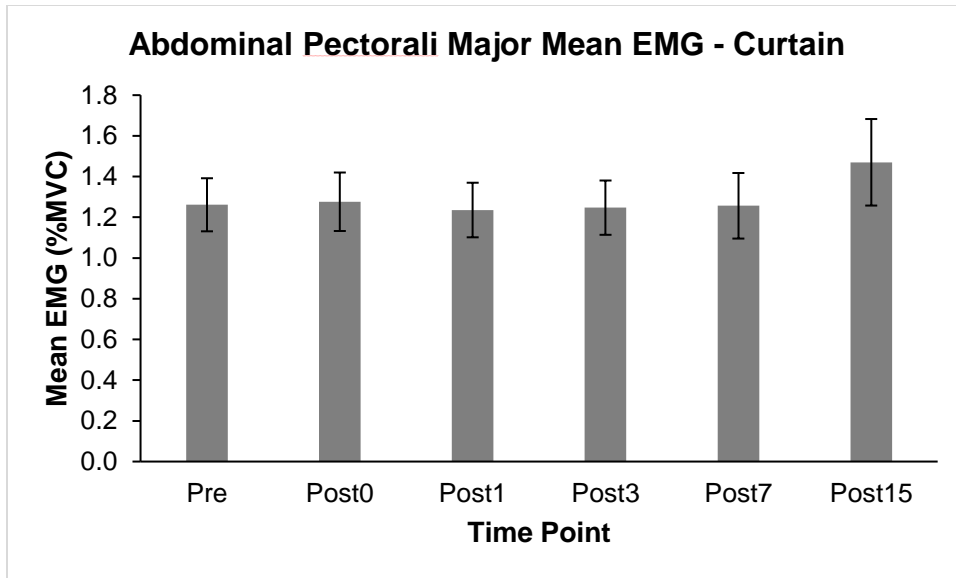
Figure 45. Abdominal pectoralis major mean EMG amplitude for the Curtain ADL pre- and post-fatigue. Error bars indicate standard error.
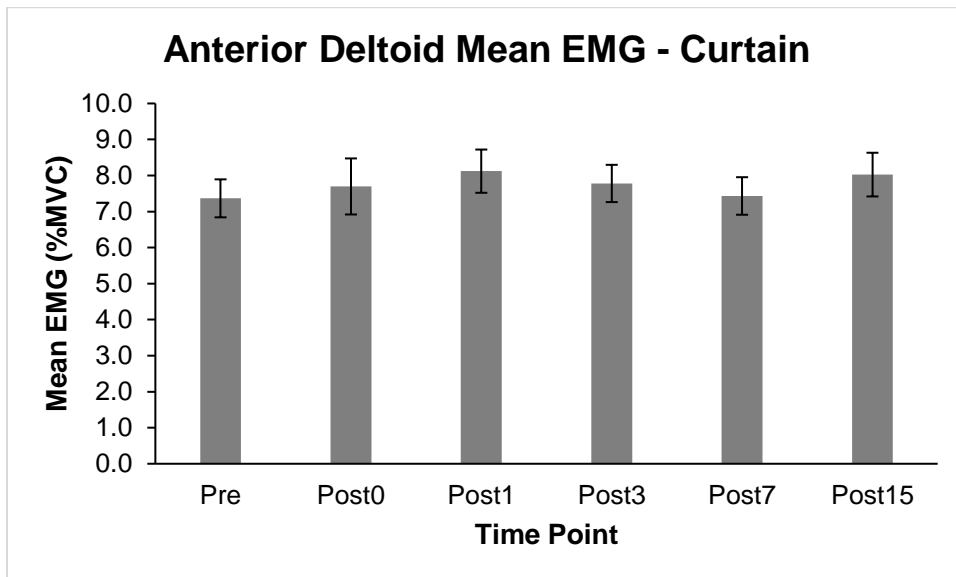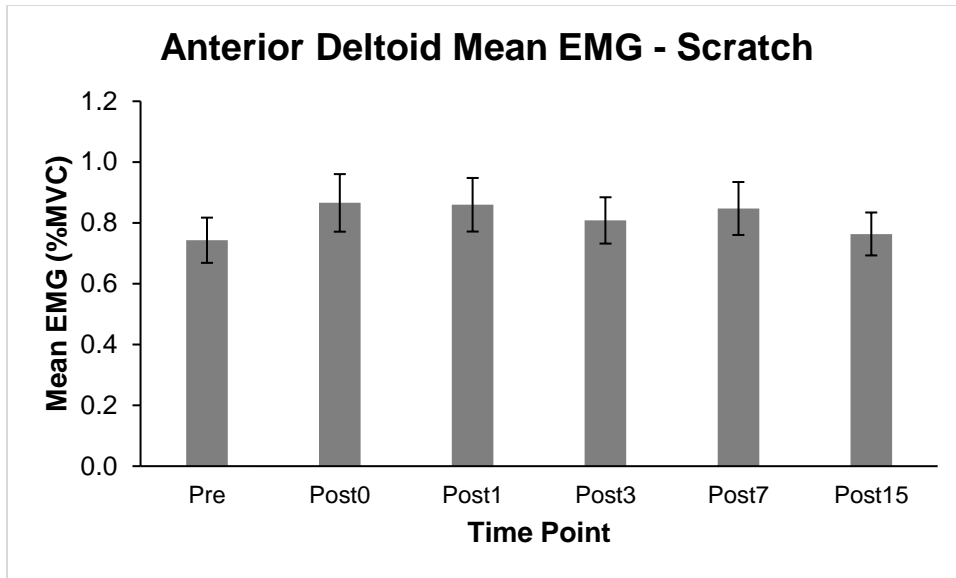

Figure 46. Anterior deltoid mean EMG amplitude for the Curtain ADL pre- and post-fatigue. Error bars indicate standard error.
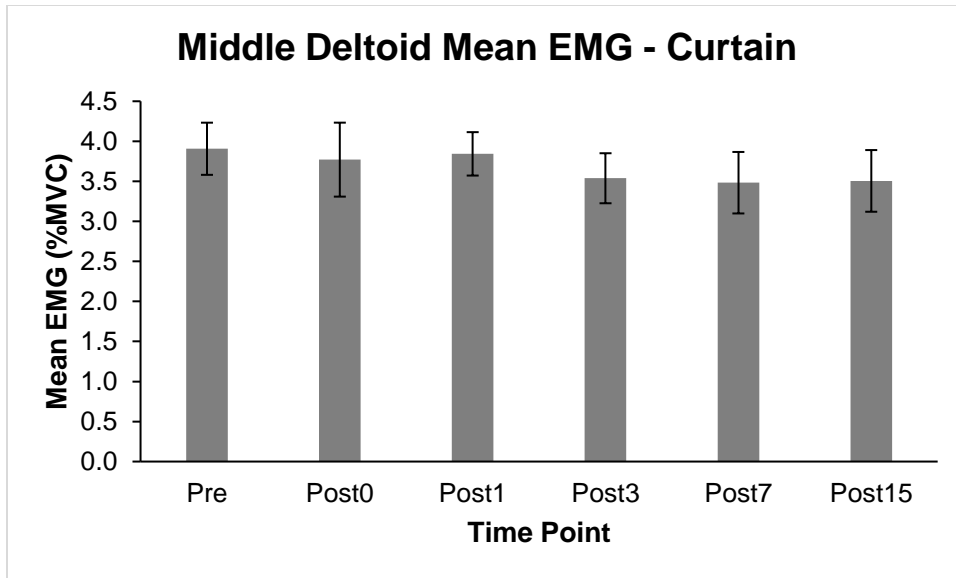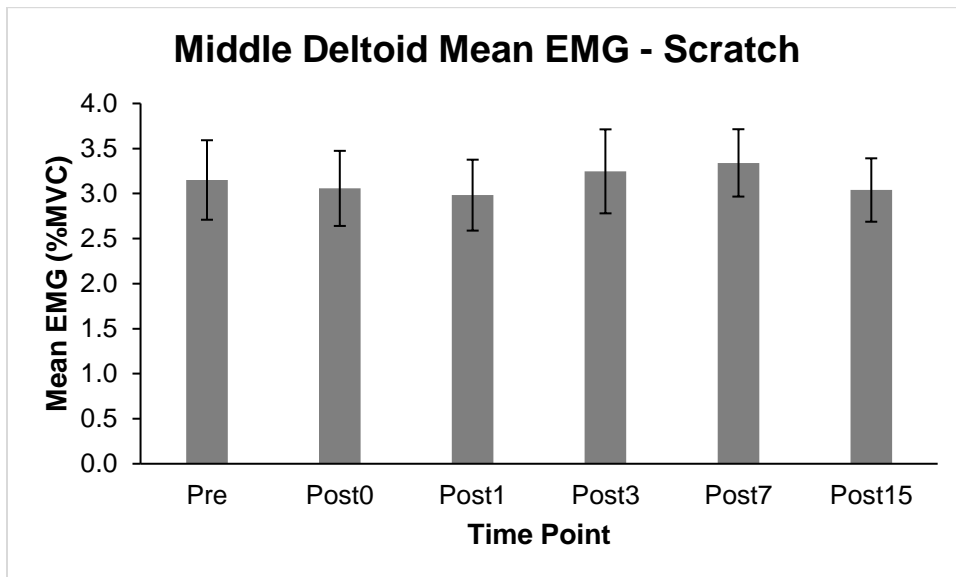
Figure 47. Middle deltoid mean EMG amplitude for the Curtain ADL pre- and post-fatigue. Error bars indicate standard error.
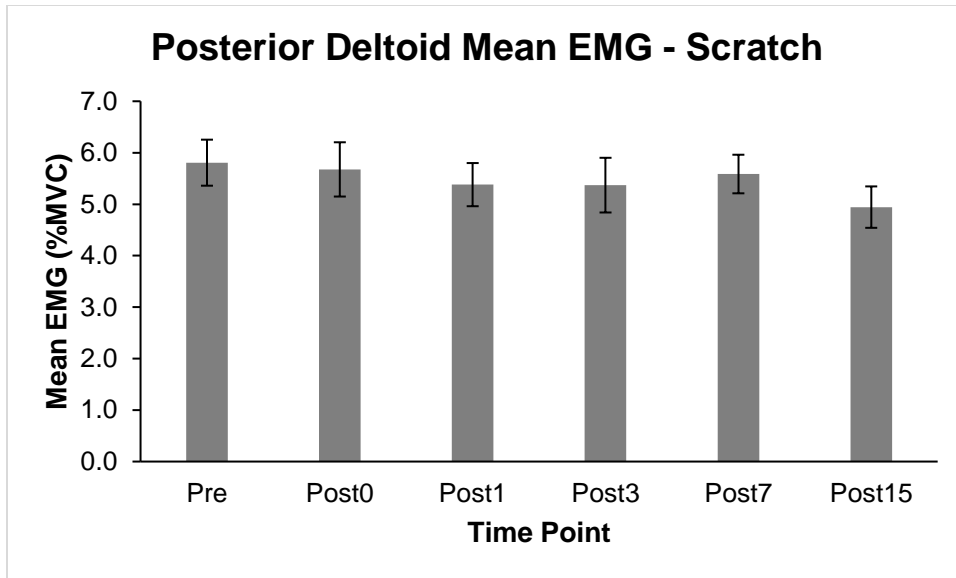

Figure 48. Posterior deltoid mean EMG amplitude for the Curtain ADL pre- and post-fatigue. Error bars indicate standard error.
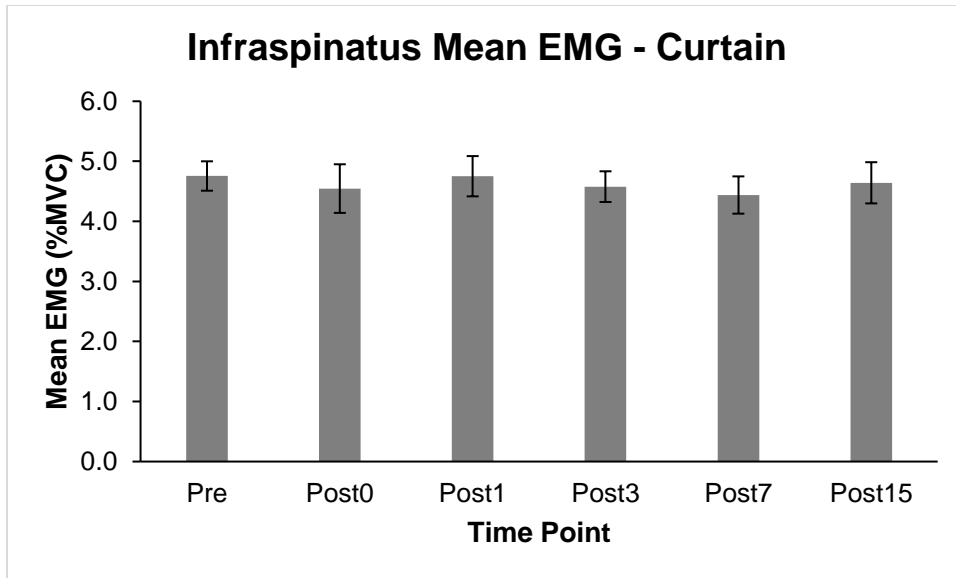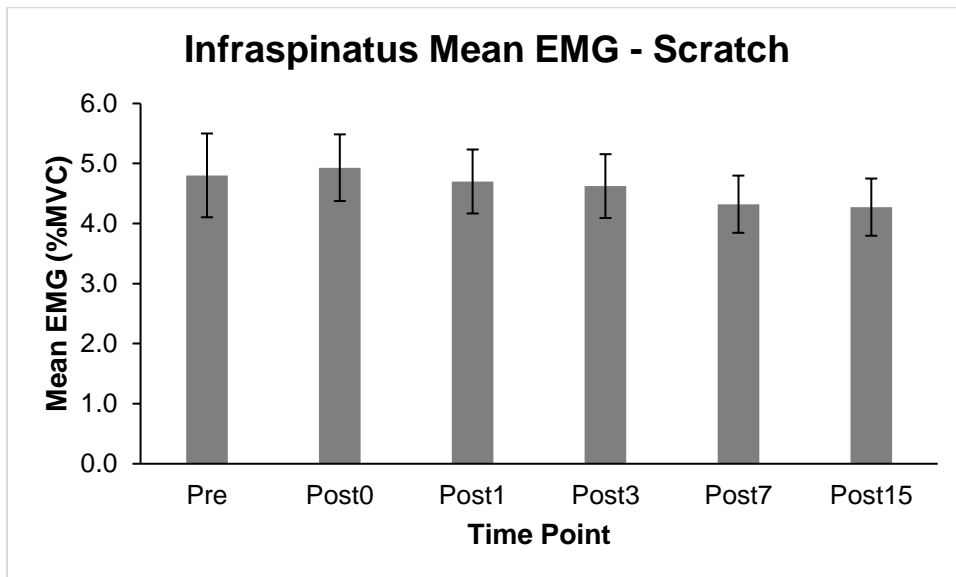
Figure 49. Infraspinatus mean EMG amplitude for the Curtain ADL pre- and post-fatigue. Error bars indicate standard error.
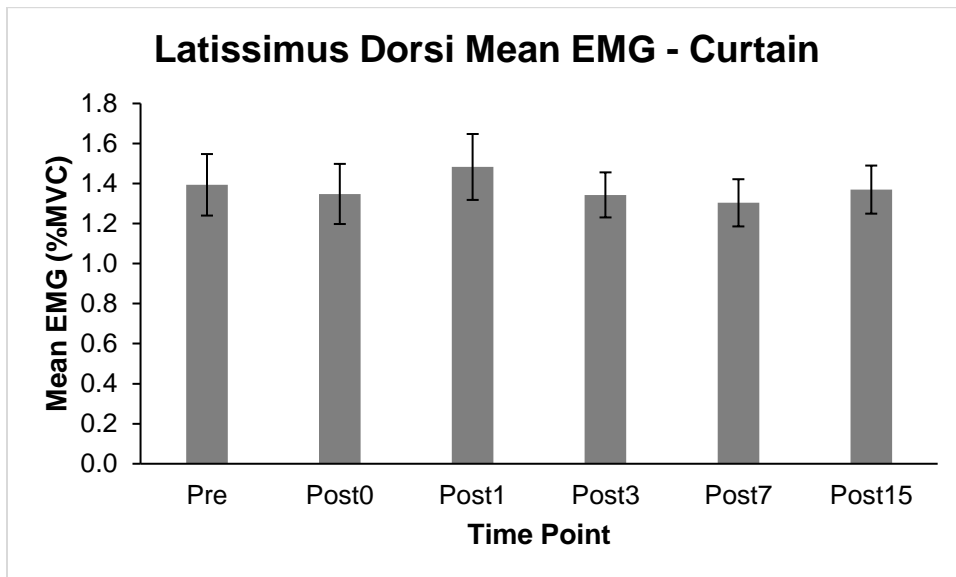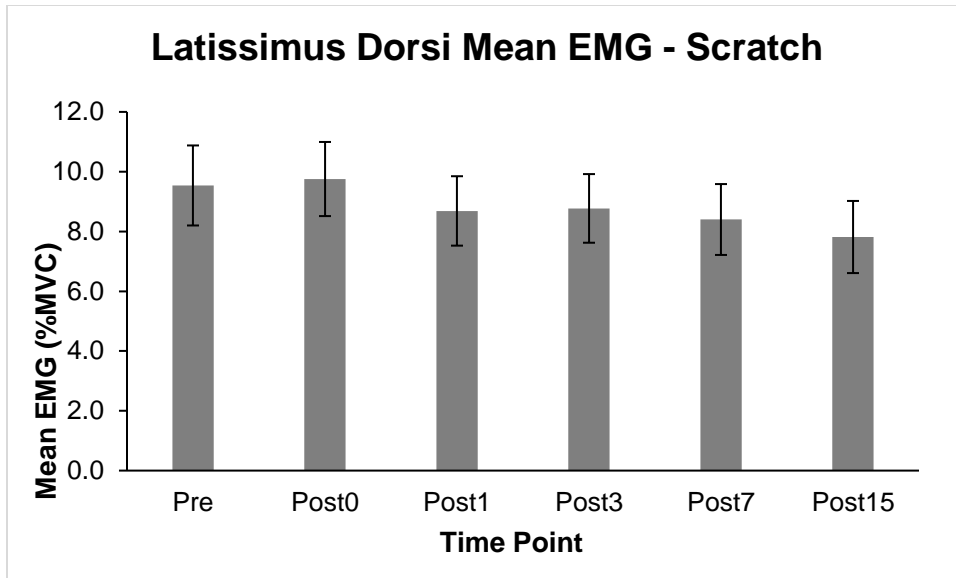

Figure 50. Latissimus dorsi mean EMG amplitude for the Curtain ADL pre- and post-fatigue. Error bars indicate standard error.
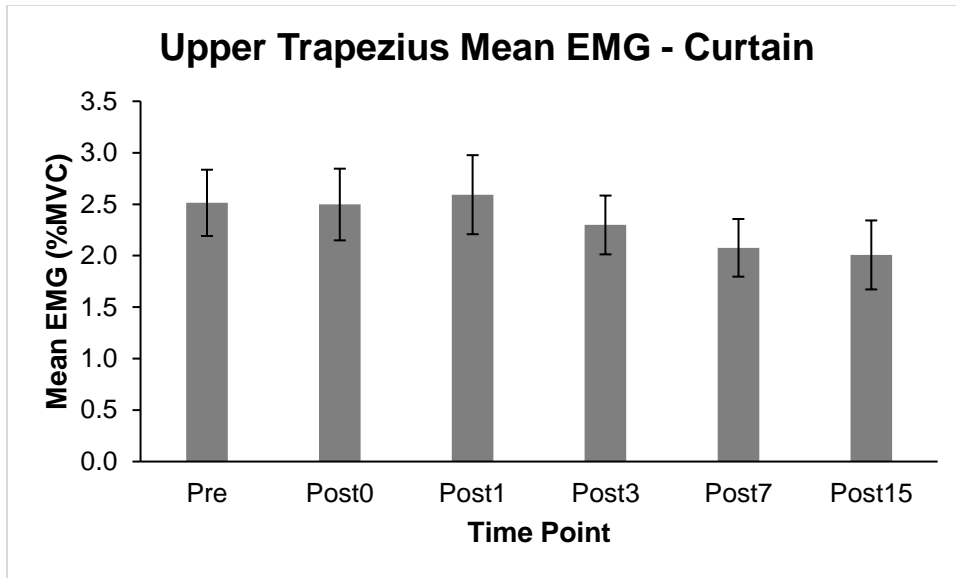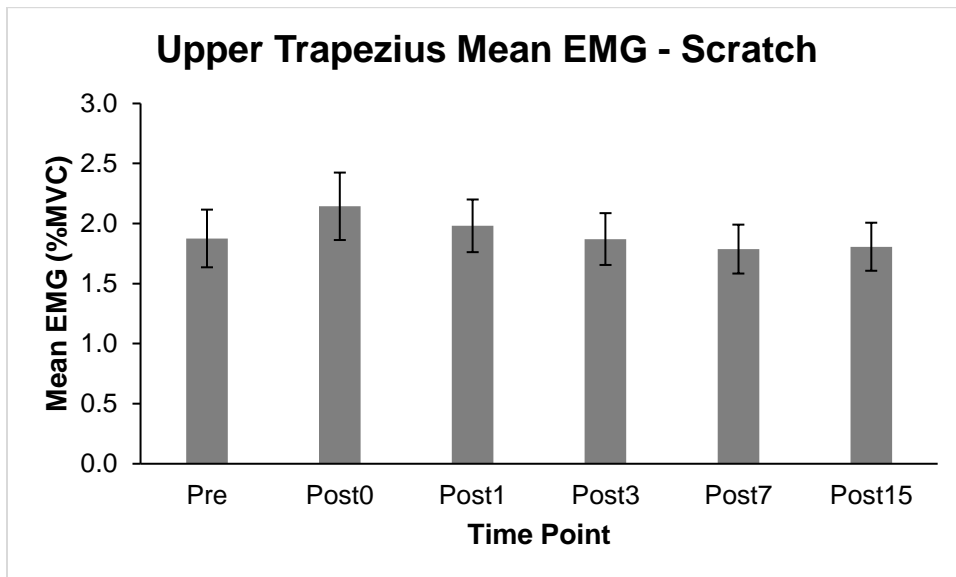
Figure 51. Upper trapezius mean EMG amplitude for the Curtain ADL pre- and post-fatigue. Error bars indicate standard error. This dataset violated sphercity and was subsequently Greenhouse-Geisser corrected so that the main effect was no longer significant ($p = 0.054$).
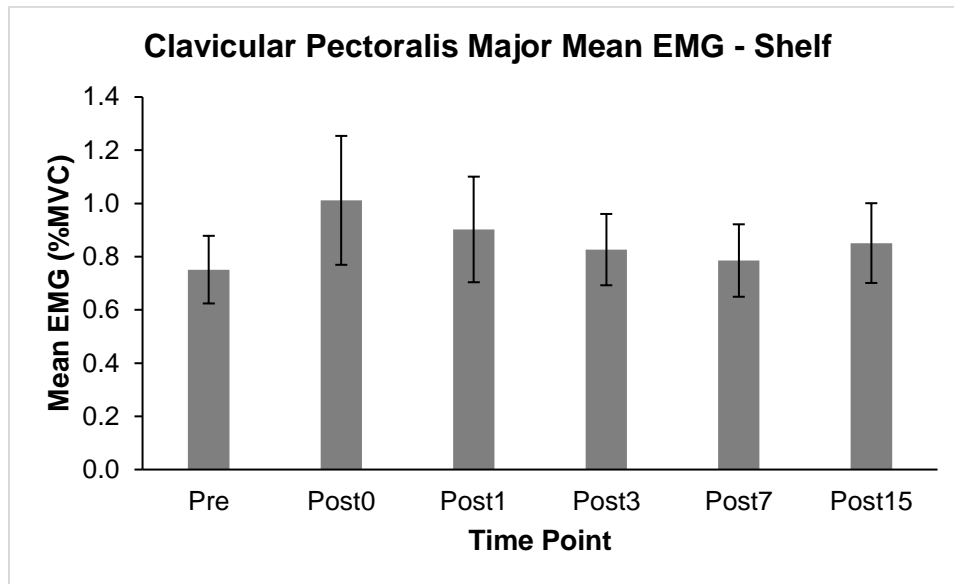
Mean EMG – Scratch ADL
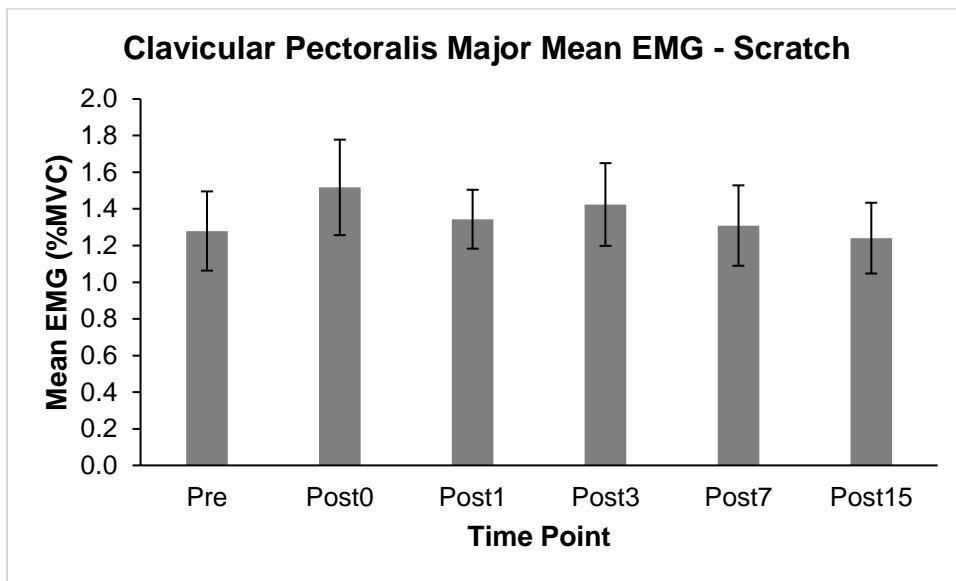
Figure 52. Clavicular pectoralis major mean EMG amplitude for the Scratch ADL pre- and post-fatigue. Error bars indicate standard error.
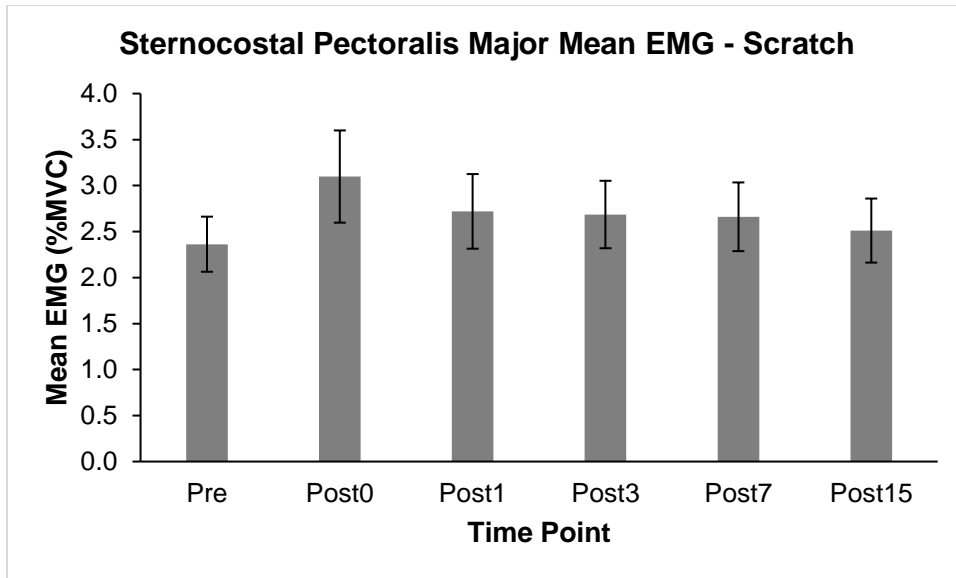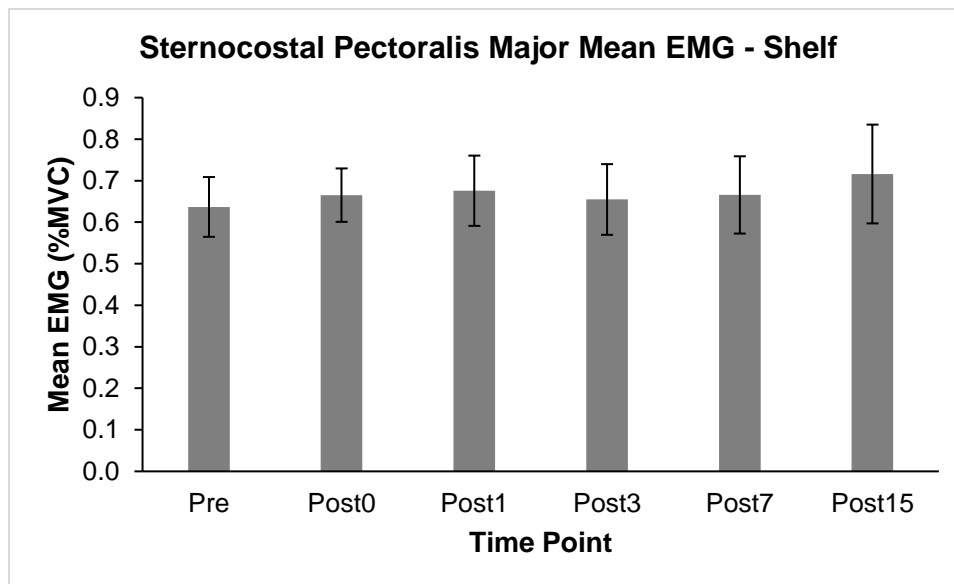
Figure 53. Sternocostal pectoralis major mean EMG amplitude for the Scratch ADL pre- and post-fatigue. Error bars indicate standard error.
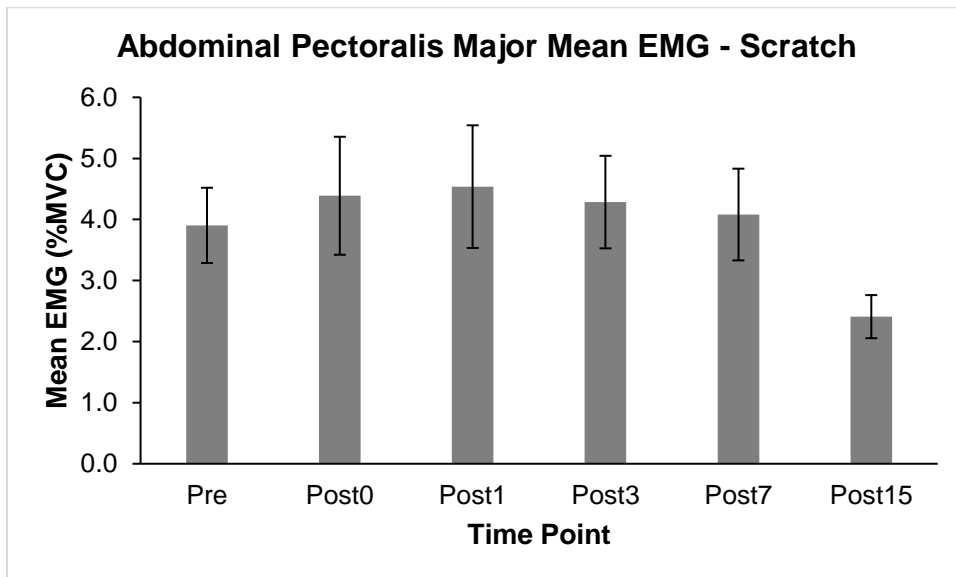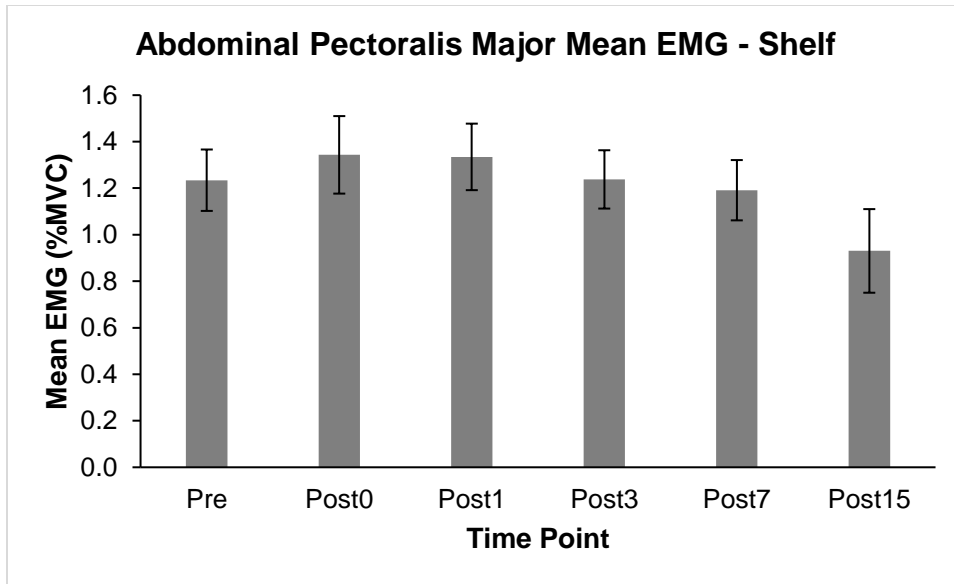

Figure 54. Abdominal pectoralis major mean EMG amplitude for the Scratch ADL pre- and post-fatigue. Error bars indicate standard error. This dataset violated sphercity and was subsequently Greenhouse-Geisser corrected so that the main effect was no longer significant ($p = 0.063$).

Figure 55. Anterior deltoid mean EMG amplitude for the Scratch ADL pre- and post-fatigue. Error bars indicate standard error.
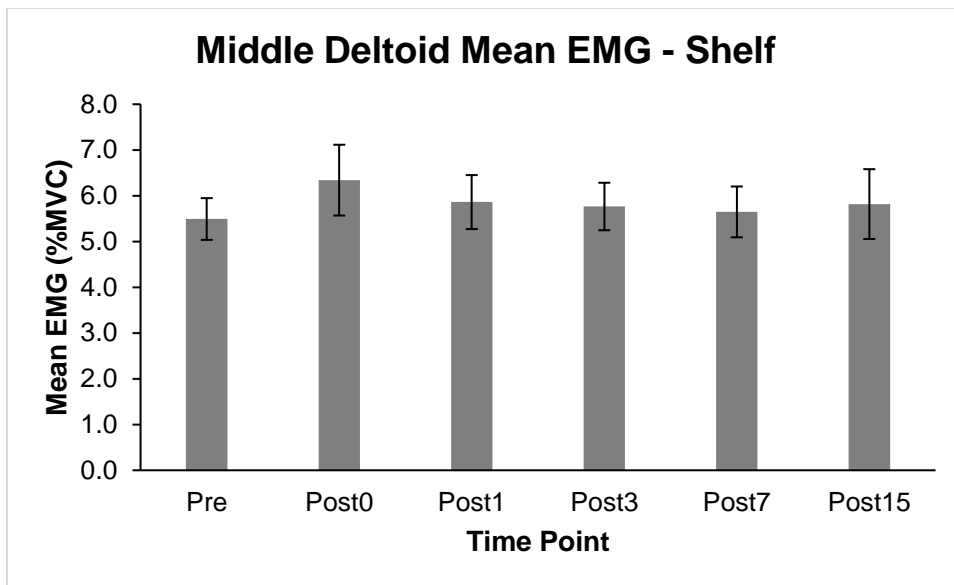

Figure 56. Middle deltoid mean EMG amplitude for the Scratch ADL pre- and post-fatigue. Error bars indicate standard error.

Figure 57. Posterior deltoid mean EMG amplitude for the Scratch ADL pre- and post-fatigue. Error bars indicate standard error.

Figure 58. Infraspinatus mean EMG amplitude for the Scratch ADL pre- and post-fatigue. Error bars indicate standard error.

Figure 59. Latissimus dorsi mean EMG amplitude for the Scratch ADL pre- and post-fatigue. Error bars indicate standard error.

Figure 60. Upper trapezius mean EMG amplitude for the Scratch ADL pre- and post-fatigue. Error bars indicate standard error.

Mean EMG – Shelf ADL

Figure 61. Clavicular pectoralis major mean EMG amplitude for the Shelf ADL pre- and post-fatigue. Error bars indicate standard error.

Figure 62. Sternocostal pectoralis major mean EMG amplitude for the Shelf ADL pre- and post-fatigue. Error bars indicate standard error.

Figure 63. Abdominal pectoralis major mean EMG amplitude for the Shelf ADL pre- and post-fatigue. Error bars indicate standard error. This dataset violated sphercity and was subsequently Greenhouse-Geisser corrected so that the main effect was no longer significant ($p = 0.060$).

Figure 64. Middle deltoid mean EMG amplitude for the Shelf ADL pre- and post-fatigue. Error bars indicate standard error.
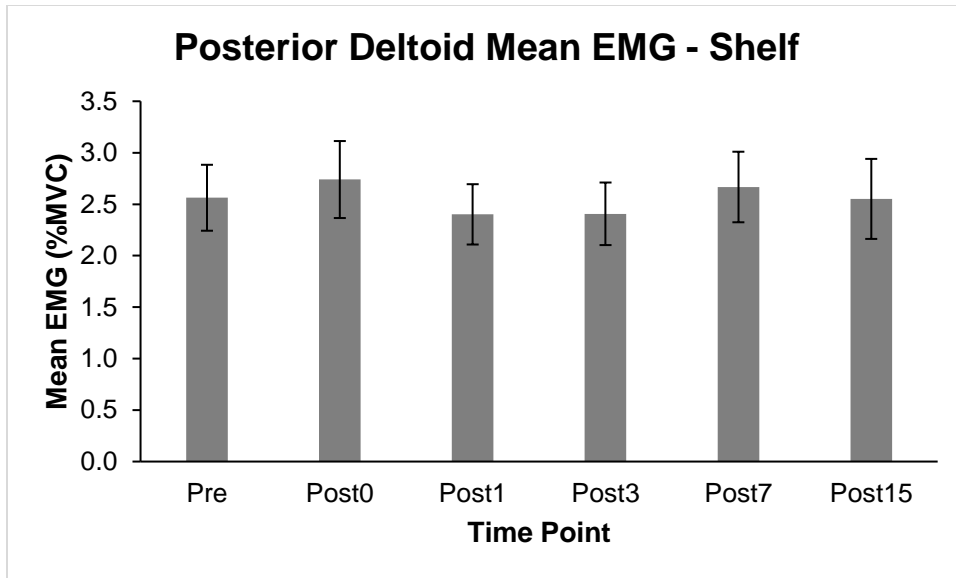
Figure 65. Posterior deltoid mean EMG amplitude for the Shelf ADL pre- and post-fatigue. Error bars indicate standard error.
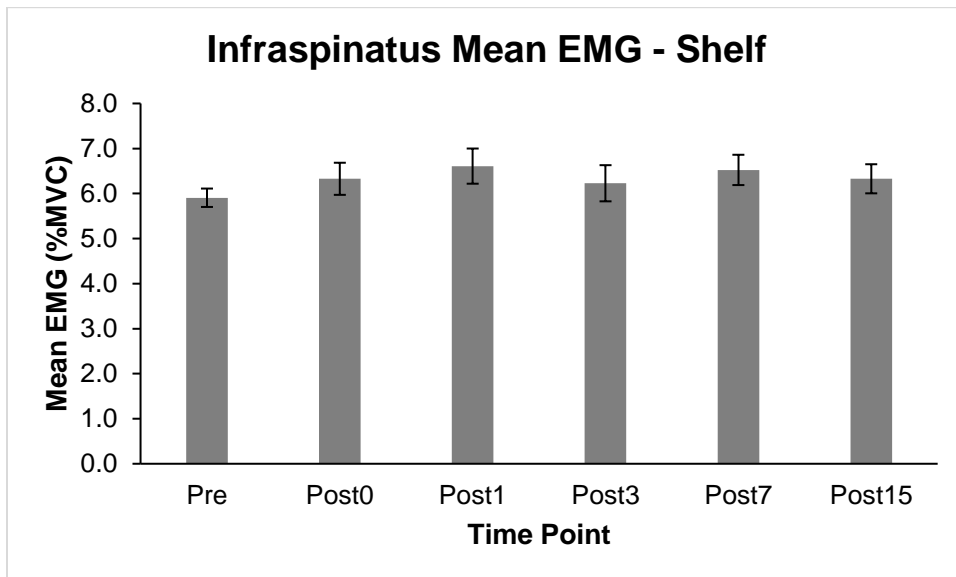

Figure 66. Infraspinatus mean EMG amplitude for the Shelf ADL pre- and post-fatigue. Error bars indicate standard error.
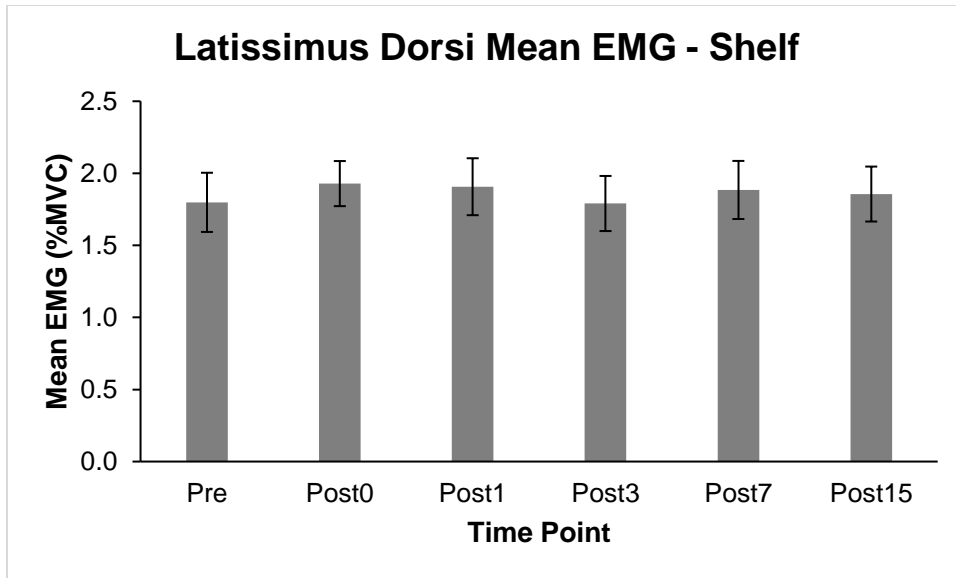
Figure 67. Latissimus dorsi mean EMG amplitude for the Shelf ADL pre- and post-fatigue. Error bars indicate standard error.
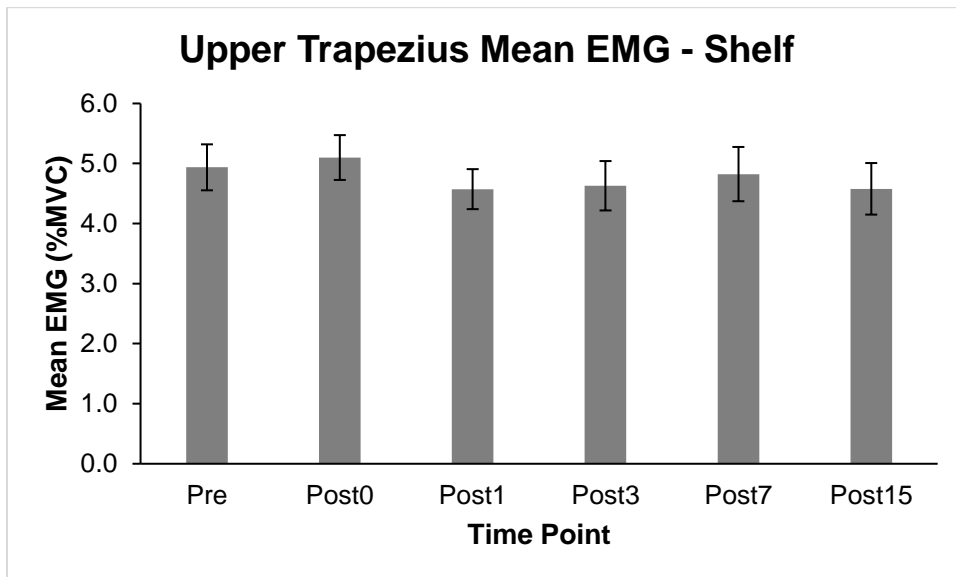

Figure 68. Upper trapezius mean EMG amplitude for the Shelf ADL pre- and post-fatigue. Error bars indicate standard error.